

**Vinylogous Michael Cascade Reactions Employing Silyl Glyoxylates
and Silyl Glyoximides**

Gregory Ronald Boyce

A dissertation submitted to the faculty of the University of North Carolina at Chapel Hill
in partial fulfillment of the requirements for the degree of Doctor of Philosophy in the
Department of Chemistry.

Chapel Hill
2011

Approved by:

Jeffrey S. Johnson

Maurice S. Brookhart

Malcolm Forbes

David A. Nicewicz

Marcey L. Waters

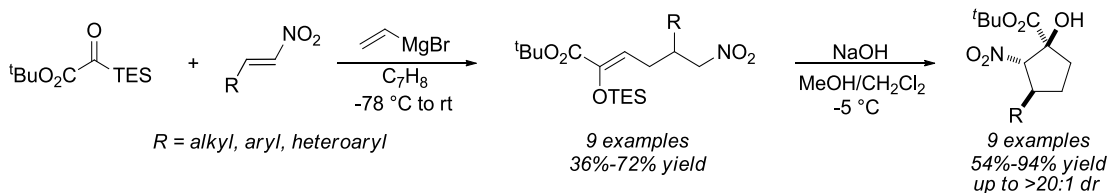
© 2011
Gregory Ronald Boyce
ALL RIGHTS RESERVED

ABSTRACT

GREGORY RONALD BOYCE: Vinylogous Michael Cascade Reactions Employing
Silyl Glyoxylates and Silyl Glyoximides
(Under the direction of Jeffrey S. Johnson)

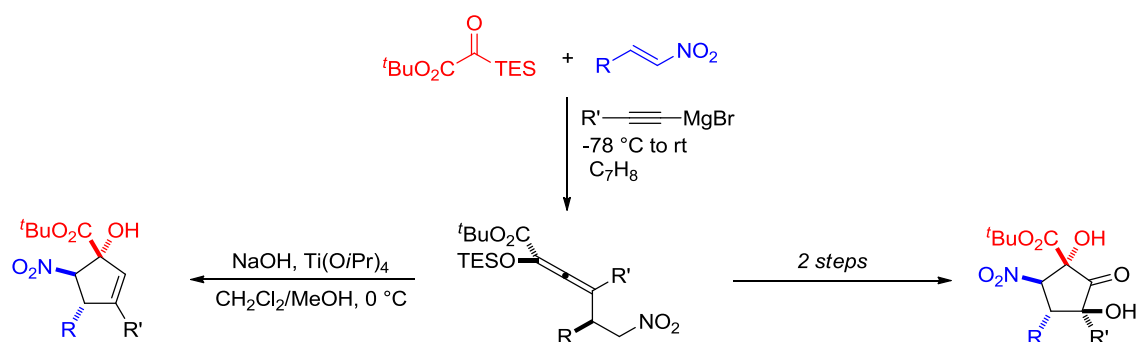
I. Vinylation-Initiated Vinylogous Michael Cascade of Silyl Glyoxylates and Elaboration to Nitrocyclopentanols

An investigation of the reaction parameters required to achieve a vinylation-initiated vinylogous Michael cascade of silyl glyoxylates and nitroalkenes was performed. The reaction achieved the (*Z*)-enol silane products with complete regio- and diastereoselectivity. A rationale for the high levels of selectivity is discussed. Discussion of how the probable mechanism of the three-component coupling was discerned (vinylogous Michael, [3,3] rearrangement, or Diels-Alder type pathway) is presented. This method provides an easily accessible synthetic equivalent to the unusual α -keto ester homoenolate. These (*Z*)-enol silane products were further elaborated to nitrocyclopentanols via a highly diastereoselective Henry cyclization. Rationale for the diastereoselectivity is presented as well as an analysis of this methodology's impact compared to other methods for highly substituted nitrocyclopentanols is also presented.



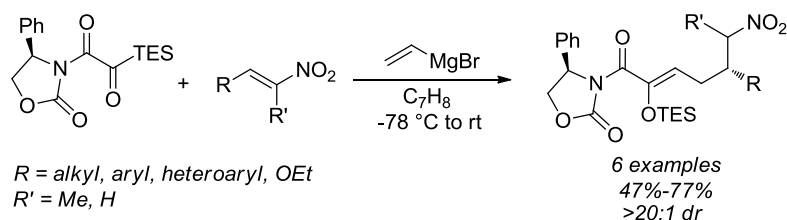
II. Alkynylation-Initiated Vinylogous Michael Reaction of Silyl Glyoxylates and Elaboration to Cyclopentanol Derivatives

An investigation of the reaction parameters necessary to accomplish an alkynylation-initiated Kuwajima-Reich/vinylogous Michael cascade of silyl glyoxylates and nitroalkenes is presented. The title three-component coupling provided tetrasubstituted silyloxyallenes with high levels of regio- and diastereoselectivity. The impressive selectivity of this transformation was investigated through a quantum mechanical study using the density functional theory approach at the level of B3LYP/6-311G(d). This study corroborated previous studies on the identity of the transient secondary nucleophile as the (Z)-glycolate enolate and provided a rationale for the excellent diastereoselectivity observed through nitro group coordination to the (Z)-glycolate enolate. A discussion of the additional empirical studies performed to confirm the proposed mechanism is also presented. The tetrasubstituted silyloxyallene products were then derivatized to cyclopentenols and cyclopentitols.



III. Silyl Glyoximides as Asymmetric Conjunctive Reagents through Long-Range Stereoinduction

The utility of silyl glyoximides as a new class of asymmetric conjunctive reagents in the vinylation-initiated vinylogous Michael cascade with vinyl Grignard and nitroalkenes is presented. The reaction affords the desired γ -adducts with excellent regio- and diastereoselectivity. A rationale for this long range stereochemical transmission is proposed. A discussion of the benefits of silyl glyoximides compared to silyl glyoxylates in terms of the current methodology is presented. Initial studies towards the various Henry cyclizations are also presented.



ACKNOWLEDGEMENTS

I am extremely grateful for all the support I have received over the course of my career at the University of North Carolina from my friends, family, and coworkers. First and foremost though, I need to thank my advisor, Professor Jeffrey S. Johnson, for his unrelenting support and instruction during my time in his group. Looking back on my tenure here, I am amazed at the level of engagement and personal interest Jeff maintains with his students. Despite Jeff's successes and his stature in the synthetic community, he remains surprisingly humble and down to earth. I am also extremely grateful for Jeff's "open-door" policy and for the level of autonomy he afforded me in my research. These qualities coupled with his seemingly infinite amount of patience made him a fantastic boss to work for. Jeff's commitment to his students is paramount and for all these reasons and more I know I could not have had a better advisor, or role model.

I would like to thank Professor Marcey L. Waters for serving as chair for my defense committee. I also would like to thank Professors Maurice S. Brookhart, Malcolm Forbes, and David A. Nicewicz for serving on this final defense committee and thank Professors Michel Gagné and Michael T. Crimmins for serving on my preliminary defense committee. Additional recognition is required for Professors Maurice S. Brookhart and Michael T. Crimmins who were kind enough to serve as references in my search for an academic position.

I also need to thank Professor Philip J. Parsons for his invaluable role in my academic development. Before I knew Professor Parsons, I did not have a serious interest

in pursuing organic chemistry as a career. After many meetings with him and taking his course in heterocyclic chemistry at the University of Sussex, I discovered a passion for organic synthesis. Phil gave me the confidence to pursue this degree; without his influence this achievement would not have been possible.

During my time at UNC, I have been extremely privileged to work with an excellent group of skilled coworkers. I would like to thank the members of the Johnson group, past and present, for engendering such a friendly and cooperative atmosphere in which to conduct research. I gratefully acknowledge the past group members who took me under their wing and not only taught me every lab technique I know, but also helped me prepare for my oral examinations, reviewed my manuscripts, and provided such an exceptional example to follow. Although I am indebted to each member of the Johnson group, Steve Greszler and Matt Campbell truly went above and beyond to make me the chemist I am today. I also would like to thank the members of the middle lab who made coming to work something to look forward to each day: Ashley Berman, Matt Campbell, Steve Greszler, Scott Krabbe, Justin Malinowski, Erika Malow and our particularly talented undergraduate Adam Gray. I have also been fortunate to be part of an excellent class of students whom accompanied me on this long journey to attain this degree. Whether studying for classes or simply going through the trials of graduate school together, I am grateful for the camaraderie of Dan Schmitt, Anne-Marie Schmitt, and Mike Slade, and Austin Smith.

I would also like to thank my family the infinite support and love I have received from them throughout my life. First, I would like to thank my Mom and Dad for their unending love and support. They have always been there for me, provided

encouragement, and expressed a deep and genuine pride in my accomplishments. I have not always made life easy on them; however, they continued to support me no matter what mistakes I've made and for that I cannot thank them enough. I would also like to express my deepest gratitude to my Grandma and Grandpap, who have been such an important part of my life and have shown such love and support for me in all that I do. I am also indebted to my godparents, Aunt Sheri and Uncle RJ, have always supported and encouraged me in all that I do and do their best to make sure that life is never dull. I also must thank them deeply for the high level of enthusiasm they have shown about me moving only an hour away from them which has made me feel so loved. Lastly, I would like to thank my Uncle Michael, Aunt Dena, Matthew, Mikey, Mary Elizabeth, Christopher and Daniel for always supporting me, expressing their pride in my accomplishments, and supporting my "potion-making."

I am also grateful for the love and support of Gary and Tina Silverstein, who have done so much for me. Although, my only relation to them is the distance from my home to theirs, they have treated me like their own and shown so much love and encouragement over the years. I will always appreciate the weekend trips to their place in the Blue Ridge Mountains for good hikes, good food, and most importantly, good company.

Graduate school is a unique experience to say the least, and I know I would not have been able to do it without the support of my friends. First, I would like to thank my closest friends, Kelly A. Bernardo, Victor B. DiGregorio, Jonathan Gitlen, Angelena Ledford, Eddie Tabishesky and Mike Vallone for always being there for me and helping me to laugh at all the ridiculous things that life brings. During my time in North Carolina,

I've had the privilege of getting to know some great people, especially Mario Piergallini and Joseph Hon who I am lucky to have in my life. I cannot forget to thank the Florida Posse who have kept me lighthearted and grounded since high school; Michelle Bernardo, Tammy Bernardo, Crissy Iglesias, Jackie Moeller, and Alexis Sopkiw.

For My Family
In Loving Memory of My Grandmother
Evelyn G. Koenig
(1929-2008)

TABLE OF CONTENTS

LIST OF TABLES	xvi
LIST OF FIGURES AND SCHEMES	xviii
LIST OF ABBREVIATIONS AND SYMBOLS.....	xxiii
 CHAPTER 1	 VINYLATION-INITIATED VINYLOGOUS MICHAEL REACTION OF SILYL GLYOXYLATES AND ELABORATION TO NITROCYCLOPENTANOLS.....
	1
1.1	Introduction.....
	1
1.2	Background.....
	2
1.2.1	Reactivity Umpolung.....
	2
1.2.2	The Utility of the [1,2]-Brook Rearrangement in Tandem C–C Bond Formation.....
	3
1.2.3	Conventional Silyl Glyoxylate Reactivity.....
	5
1.2.4	Vinylogous Michael Reaction.....
	9
1.2.5	Origin of the Title Reaction.....
	15
1.3	Results and Discussion.....
	16
1.3.1	Investigation of Reaction Parameters.....
	16
1.3.2	Justification of the Enolsilane Stereochemistry.....
	17
1.3.3	Optimization Studies.....
	18
1.3.4	Scope and Limitations.....
	23
1.3.5	Studies on the Reaction Mechanism.....
	26
1.4	Secondary Transformations.....
	28
1.4.1	Potential Piperidine Synthesis.....
	29

1.4.2	Henry Cyclization.....	33
1.4.3	Optimization.....	34
1.4.4	Determination of Relative Stereochemistry.....	35
1.4.5	Reaction Scope and Trends.....	36
1.4.6	Attempts at Aza-Henry Cyclization Variant.....	37
1.5	Conclusion.....	40
1.6	Experimental Details.....	40
1.7	References.....	63

CHAPTER 2	ACETYLIDE-INITIATED VINYLOGOUS MICHAEL CASCADE OF SILYL GLYOXYLATES AND ELABORATION TO CYCLOPENTANOL DERIVATIVES.....	66
2.1	Introduction.....	66
2.2	Background.....	67
2.2.1	Prevalence of Cyclopentitols in Nature.....	67
2.2.2	Prevalence of Cyclopentenols in Medicinally Relevant Molecules.....	67
2.2.3	Synthetic Approaches to Cyclopentanol Derivatives.....	69
2.2.4	Kuwajima-Reich Rearrangement.....	70
2.2.5	Utility of Silyloxyallenes.....	71
2.2.6	Spirodiepoxidation of Allenes.....	72
2.2.7	Origin of the Title Reaction.....	72
2.2.8	Comparison to Precedented Silyl Glyoxylate Coupling with Acetylide Nucleophiles.....	74
2.3	Results and Discussion.....	75
2.3.1	Optimization of Reaction Parameters.....	75
2.3.2	Reaction Scope.....	77
2.4	Computational Studies.....	82
2.4.1	Thermodynamics of the Secondary Nucleophile.....	82
2.4.2	DFT-Optimized Transition States.....	84
2.4.3	Implications on the Regio- and Diastereoselectivity.....	85
2.4.4	Additional Mechanistic Support for the Theoretical Studies from the Benzyldenemalononitrile-Terminated Three-Component Coupling.....	86

2.5	Secondary Transformations to Cyclopentanol Derivatives.....	87
2.5.1	Henry Cyclization of Silyloxyallenes.....	88
2.5.2	Optimization.....	89
2.5.3	Reaction Scope.....	90
2.5.4	Determination of Relative Stereochemistry.....	91
2.5.5	Cyclopentitol Synthesis from Spirodiepoxides.....	93
2.5.6	Optimization of Reaction Parameters.....	94
2.5.7	Alternative Synthesis of Cyclopentitols.....	95
2.6	Conclusion.....	97
2.7	Experimental Details.....	98
2.8	References.....	119

CHAPTER 3	SILYL GLYOXIMIDES AS ASYMMETRIC CONJUNCTIVE REAGENTS THROUGH LONG-RANGE STEREOINDUCTION.....	121
3.1	Introduction.....	121
3.2	Background.....	122
	3.2.1 Inducing Asymmetry in Silyl Glyoxylate Couplings.....	122
	3.2.2 1,7-Asymmetric Induction in the Vinylogous Mukaiyama Aldol Reaction.....	124
	3.2.3 Origin of the Title Reaction and Initial Experiments.....	126
3.3	Results and Discussion.....	129
	3.3.1 Synthesis of Silyl Glyoximide 9	129
	3.3.2 Optimization of the Reaction Parameters.....	129
	3.3.3 Solving the Stereochemistry of Enolsilane 10a	130
	3.3.4 Reaction Scope.....	131
	3.3.5 Proposed Transition State.....	133
3.4	Secondary Transformation to Asymmetric Cyclopentanol Derivatives.....	135
	3.4.1 Asymmetric Cyclopentanol Synthesis.....	137
3.5	Conclusion.....	139
3.6	Experimental Details.....	140
3.7	References.....	149

LIST OF TABLES

Table 1-1	Stoichiometry Optimization.....	19
Table 1-2	Silyl Group Screen.....	20
Table 1-3	Screen of Various Additives.....	21
Table 1-4	Temperature Screen.....	22
Table 1-5	Screen of Various Nucleophiles.....	23
Table 1-6	Substrate Scope for the Vinylation-Initiated Three-Component Coupling.....	26
Table 1-7	Conditions for the Chemoselective Reduction of the Nitro Group.....	27
Table 1-8	Screen of Conditions for the Mannich Cyclization to 36	33
Table 1-9	Optimization of the Henry Cyclization Cascade.....	34
Table 1-10	Effects of Dichloromethane as Cosolvent.....	35
Table 1-11	Substrate Scope for the Diastereoselective Henry Cyclization Cascade.....	37
Table 1-12	Attempted Aza-Henry Cyclization Conditions.....	39
Table 2-1	Stoichiometry Screen for the Acetylide-Initiated Cascade.....	76
Table 2-2	Nucleophile Variation.....	77
Table 2-3	Nitroalkene Substrate Scope for the Three-Component Coupling.....	78
Table 2-4	Screen of Conditions to Accommodate 2-Nitrovinyl Ether as a Secondary Electrophile.....	80

Table 2-5	Acetylide Substrate Scope for the Three-Component Coupling.....	81
Table 2-6	Screen of Conditions to Induce Henry Cyclization.....	89
Table 2-7	Substrate Scope for the Henry Cyclization.....	91
Table 2-8	Equivalence Screen for One-Pot Spirodiepoxidation/Henry Cyclization.....	95
Table 2-9	Substrate Scope for Ketohydroxylation.....	97
Table 3-1	Stoichiometry Screen for the Silyl Glyoximide Three-Component Coupling.....	130
Table 3-2	Nitroalkene Substrate for the Three-Component Coupling.....	132

LIST OF FIGURES AND SCHEMES

Figure 1-1	Seebach's Analysis of Classical and Unploughing Reactivity Patterns on a Carbon Chain.....	2
Figure 1-2	[1,2]-Brook Rearrangement.....	3
Figure 1-3	Cyanation/[1,2]-Brook Rearrangement/C-Acylation Reaction of Acyl Silanes.....	4
Figure 1-4	Product Diversity in Acylsilane vs. Silyl Glyoxylate Chemistry.....	5
Scheme 1-1	Synthesis of Silyl Glyoxylates.....	6
Scheme 1-2	Original Silyl Glyoxylate Three-Component Coupling.....	7
Scheme 1-3	Successful Three-Component Coupling Reactions of Silyl Glyoxylate.....	8
Figure 1-5	Natural Products Targeted with Silyl Glyoxylate Chemistry.....	9
Figure 1-6	Example of α,α -Dicyanoolefin Vinylogous Michael Reactivity..	10
Figure 1-7	Seminal Work in the Vinylogous Michael Reaction.....	11
Scheme 1-4	Di- γ -Addition of Nitroalkenes to α -Thio Butenolide Derivatives.....	12
Figure 1-8	Takeda's Vinylogous Reactivity Cascade.....	13
Figure 1-9	Regioselectivity Challenges Arising from the Cyclic Enone Methodology.....	14
Figure 1-10	An Ideal Vinylogous Michael Transformation.....	14
Scheme 1-5	Proposed Access to the α -Keto Ester Homoenolate Synthon.....	15
Scheme 1-6	Divergent Silyl Glyoxylate Reactivity.....	16
Scheme 1-7	Initial Three-Component Coupling Study.....	17
Figure 1-11	Analysis of the Enolsilane Geometry.....	17
Scheme 1-8	Conversion of the Enolsilane 22a to Silyloxyepoxide 23	18

Scheme 1-9	Precedented Allylmagnesium Bromide Three-Component Coupling.....	24
Scheme 1-10	Proposed Allylmagnesium Bromide Three-Component Coupling.....	25
Scheme 1-11	Products Arising From Three Plausible Mechanisms for the Three Component Coupling.....	27
Scheme 1-12	Benzylidene Malonate Terminated Three-Component Coupling.....	28
Figure 1-12	Proposed Subsequent Transformations of ϵ -Nitro Enolsilanes.....	28
Figure 1-13	Piperidine Containing Natural Products.....	29
Figure 1-14	Piperidine Containing Drug Targets.....	29
Figure 1-15	Strategy for the Synthesis of Piperidine Derivatives.....	30
Scheme 1-13	Formation of Imine 35	32
Figure 1-16	Representative nOe Correlations for 39	36
Figure 1-17	Proposed Synthesis of α,α -Disubstituted Amino Acids.....	38
Figure 1-18	Oroidin Alkaloid Natural Products.....	38
Figure 2-1	Representative Examples of Aminocyclitol Natural Products.....	67
Figure 2-2	Representative Examples of Cyclopentenol Natural Products.....	68
Figure 2-3	Representative Examples of Medicinally Relevant Carbanucleosides.....	68
Figure 2-4	Ring-Closing Metathesis as a General Method for the Synthesis of Cyclopentenols.....	69
Figure 2-5	Examples of Other Common Synthetic Routes to Cyclopentane Derivatives.....	70
Figure 2-6	The Kuwajima-Reich Rearrangement.....	71

Scheme 2-1	Enantioselective Kuwajima-Reich Rearrangement.....	71
Figure 2-7	Utility of Silyloxyallenes as Various Synthons.....	72
Scheme 2-2	Synthesis and Reactivity of Spirodiepoxides.....	72
Scheme 2-3	Three-Component Coupling Leading to Silyloxyallene 13a	73
Figure 2-9	Proposed Mechanism for the Formation of the Silyloxyallene 13a	74
Scheme 2-4	Precedented Silyl Glyoxylate Three-Component Coupling with Acetylide Nucleophiles.....	75
Scheme 2-5	Synthesis of 2-Nitrovinyl Ether.....	79
Figure 2-10	Relative Energies of the Potential Identities of the Secondary Nucleophilic Species.....	83
Figure 2-11	DFT-Optimized Transition States for TS1 Leading to the Observed Diastereomer and TS2 Which Would Lead to the Unobserved Diastereomer.....	84
Figure 2-12	Comparison of TS1 and TS2 with the Non-Reactive Rotamer TS1' and TS2'	86
Scheme 2-6	α,α -Dicyanoolefin Three-Component Coupling Employing Benzyldenemalononitrile.....	87
Scheme 2-7	Comparison of Silyloxyallene Cyclization Potential vs. Enolsilanes.....	88
Figure 2-13	Proposed Henry Cyclization Sequence.....	88
Figure 2-14	Representative nOe Correlations for 22b	92
Figure 2-15	Illustration of the Crystal Structure of 22b Solved by Dr. Peter White.....	93
Scheme 2-8	Proposed Cascade for the Synthesis of Fully Substituted Cyclopentitols.....	94
Figure 2-18	Representative nOe Correlations for 26b	96
Scheme 3-1	Asymmetric Induction in the Alkynylation Silyl Glyoxylates Cascade.....	122

Scheme 3-2	Successful Implementation of Diastereoselectivity in Silyl Glyoxylate Chemistry.....	124
Scheme 3-3	Vinylogous Mukaiyama Aldol Reaction with Vinylketene Silyl <i>N,O</i> -Acetal.....	125
Figure 3-1	Proposed Transition State for the 1,7-Remote Asymmetric Induction of Silyl <i>N,O</i> -Acetals.....	125
Scheme 3-4	Conceptual Framework for Asymmetry in the Vinylogous Michael Cascade.....	126
Scheme 3-5	Shibasaki's Synthesis of Allylic Alcohols and Attempted Application in the Silyl Glyoxylate Three-Component Coupling.....	127
Scheme 3-6	Initial Silyl Glyoximide Three-Component Coupling.....	128
Scheme 3-7	Application of Imido Acyl Silane 9 to the Three-Component Manifold.....	128
Scheme 3-8	Optimized Synthesis of Silyl Glyoximide 9	129
Scheme 3-9	Ozonolysis of 10a	131
Scheme 3-10	Reductive Ozonolysis of 10a	132
Scheme 3-11	Silyl Glyoximide Coupling Employing 1-Propynylmagnesium Bromide.....	133
Figure 3-2	Proposed <i>trans</i> Decalin-Like Transition State for the Silyl Glyoximide Coupling.....	134
Scheme 3-12	Comparison of the Reported Henry Cyclization to the Proposed Cyclization.....	136
Figure 3-3	Strategy for the Synthesis of Cyclopentenols from Enolsilanes.....	137
Figure 3-4	Structural Similarities between Cyclopentenol 19 and the Core Structure of (+)-Trehazolin.....	138
Scheme 3-13	Iodination of Enolsilane 10a	138

Scheme 3-14	Synthesis of Cyclopentenol 23 Utilizing Organoselenium Chemistry.....	139
-------------	---	------------

LIST OF ABBREVIATIONS AND SYMBOLS

2D-NMR	two-dimensional nuclear magnetic resonance
<i>p</i> -ABSA	<i>para</i> -acetamidobenzenesulfonyl azide
Ac	acetate
Ar	aryl
aq	aqueous
atm	atmospheres
Bn	benzyl
br	broad
br s	broad singlet
<i>n</i> Bu	<i>normal</i> -butyl
<i>t</i> Bu	<i>tert</i> -butyl
CAN	ceric ammonium nitrate
¹³ C	NMR carbon nuclear magnetic resonance spectroscopy
C–C	carbon-carbon bond
cat	catalytic amount or catalyst
conv	conversion
COSY	correlated spectroscopy
<i>m</i> CPBA	<i>meta</i> -chloroperoxybenzoic acid
d	doublet or days
DBU	1,8-diazabicyclo[5.4.0]undec-7-ene
DCC	<i>N,N'</i> -dicyclohexylcarbodiimide
dd	doublet of doublet
ddt	doublet of doublet of triplets

DIEA	ethyldiisopropylamine
dq	doublet of quartet
DMAP	4- <i>N,N</i> -dimethylaminopyridine
DMSO	dimethyl sulfoxide
dr	diastereomeric ratio
dt	doublet of triplet
<i>E</i>	<i>entgegen</i>
E ⁺ or E _I	electrophile
<i>endo</i>	endocyclic
eq	equation
equiv	equivalents
er	enantiomeric ratio
ESI	electrospray ionization
Et	ethyl
Et ₂ O	diethyl ether
EtOAc	ethyl acetate
EWG	electron withdrawing group
<i>exo</i>	exocyclic
FID	flame ionization detector
GI	Grubbs' first generation catalyst
GII	Grubbs' second generation catalyst
h	hour
¹ H NMR	proton nuclear magnetic resonance spectroscopy

<i>n</i> -hexanal	<i>normal</i> -hexanal
HOAc	acetic acid
HMBC	heteronuclear multiple bond correlation
HMQC	heteronuclear multiple quantum coherence
HPLC	high performance liquid chromatography
HRMS	high resolution mass spectroscopy
Hz	hertz
IR	infrared spectroscopy
<i>J</i>	coupling constant
L or Ln	ligand
LA	Lewis acid
LAH	lithium aluminum hydride
LRMS	low resolution mass spectroscopy
M	metal or molarity
m	multiplet
Me	methyl
MeCN	acetonitrile
Menth	menthyl
MeOH	methanol
mg	milligram
MHz	megahertz
min	minutes
mL	milliliter

mmol	millimole
mp	melting point
<i>n</i>	number of atoms or counterions
NBS	<i>N</i> -bromosuccinimide
NIS	<i>N</i> -iodosuccinimide
ND	not determined
NMO	<i>N</i> -methylmorpholine- <i>N</i> -oxide
nOe	nuclear Overhauser enhancement
NOESY	nuclear Overhauser enhancement spectroscopy
nr	no reaction
Nu	nucleophile
PG	protecting group
Ph	phenyl
ppm	parts per million
<i>i</i> Pr	<i>iso</i> -propyl
q	quartet
R	substituent
<i>R_f</i>	retention factor
<i>rac</i>	racemic
RCHO	aldehyde
RCM	ring-closing metathesis
rt	room temperature
s	singlet
S _N 2	bimolecular nucleophilic substitution

T	temperature
t	triplet
$t_{1/2}$	half-life
t_r	retention time
TBAF	tetrabutylammonium fluoride
TBS	<i>tert</i> -butyldimethylsilyl
TBSOTf	<i>tert</i> -butyldimethylsilyl trifluoromethanesulfonate
TEA	triethylamine
TES	triethylsilyl
Tf	trifluoromethanesulfonyl
THF	tetrahydrofuran
TLC	thin-layer chromatography
TMS	trimethylsilyl
triflate	trifluoromethanesulfonate
UV	ultraviolet
X	anionic ligand, halide, substituent, or number
X _c *	chiral auxiliary
Z	<i>zusammen</i>
Å	Ångstrom
[α]	optical rotation
δ	chemical shift or partial charge
μL	microliter

CHAPTER ONE

VINYLATION-INITIATED VINYLOGOUS MICHAEL CASCADE OF SILYL GLYOXYLATES*

1.1. Introduction

Vinylogous reactivity, the ability to transmit the electronic effects of nucleophilic or electrophilic character of a functional group through a π -system, has seen a resurgence of interest in the past decade. Although originally discovered by Claisen in 1926, this unique type of reactivity remained underutilized due to a dearth of methods for regiocontrol (α vs. γ) and long range stereochemical control. Various prefunctionalized motifs such as α,α -dicyanoolefins and butenolide derivatives have been developed to provide the desired reactivity, however, accessing vinylogous reactivity directly from simple metallodienolates remains challenging. In this Chapter, the three-component coupling reaction of silyl glyoxylates, vinyl magnesium bromide and nitroalkenes is disclosed. The combination of these reagents provides (*Z*)-silyl enol ether products through a unique direct vinylogous Michael cascade. The success of this coupling resides in the ability of silyl glyoxylate and vinyl magnesium bromide to function as the synthetic equivalent of the unusual α -keto ester homoenolate synthon and react in a

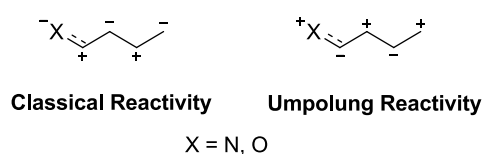
highly regio- and stereoselective manner in the presence of nitroalkenes as the secondary electrophile. The (Z)-enolsilanes accessed through this methodology were utilized in a second-stage Henry cyclization for the expeditious, diastereoselective synthesis of functionalized nitrocyclopentanols.

1.2 Background

1.2.1 Reactivity Umpolung

Reactivity umpolung,¹ or the reversal of the polarity of a functional group, has been a topic of extensive study for decades due to its ability to deliver structural motifs and bond forming events not possible with classical polarity chemistry. Heteroatoms impose an alternating acceptor and donor reactivity pattern on a carbon skeleton as illustrated by Seebach's analysis of classical and umpolung latent reactivity depicted in Figure 1.2.1.¹ This figure illustrates the differences between normal reactivity and umpolung reactivity. When normal reactivity is employed there is an odd number of carbons between the functional groups (1,3 and 1,5 structural motifs) in contrast to umpolung reactivity which provides an even number of carbons between the functional groups (1,2 and 1,4 structural motifs).¹ To access umpolung reactivity, the normal polarity of a functional group must be overridden. This is typically accomplished by utilization of synthetically equivalent groups such as acyl silanes and 1,3-dithianes.

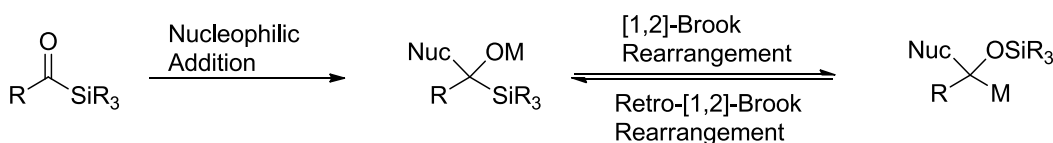
Figure 1-1. Seebach's Analysis of Classical and Umpolung Reactivity Patterns on a Carbon Chain



1.2.2. The Utility of the [1,2]-Brook Rearrangement in Tandem C–C Bond Formation

Originally studied by A. G. Brook in the mid-1900's, the 1,2-anionic migration of a silyl group from a carbon atom to oxygen to provide a silyloxy carbanion has received significant attention as a general method for accessing umpolung reactivity.² This migration, more commonly referred to as the [1,2]-Brook rearrangement, is illustrated in Figure 1-2. The driving force for this rearrangement is the strength of the Si–O bond which is > 30 kcal/mol more stable than a typical C–Si bond, however if the carbanion formed is not sufficiently stabilized the retro-[1,2]-Brook rearrangement can revert the carbanion back to the oxyanion species.³ The [1,2]-Brook rearrangement has found extensive use in tandem bond formations from acyl silane starting materials. When an acyl silane is attacked by a nucleophilic species with sufficient electron withdrawing character, the [1,2]-Brook rearrangement occurs forming the silyloxy carbanion which is then free to engage a secondary electrophile.

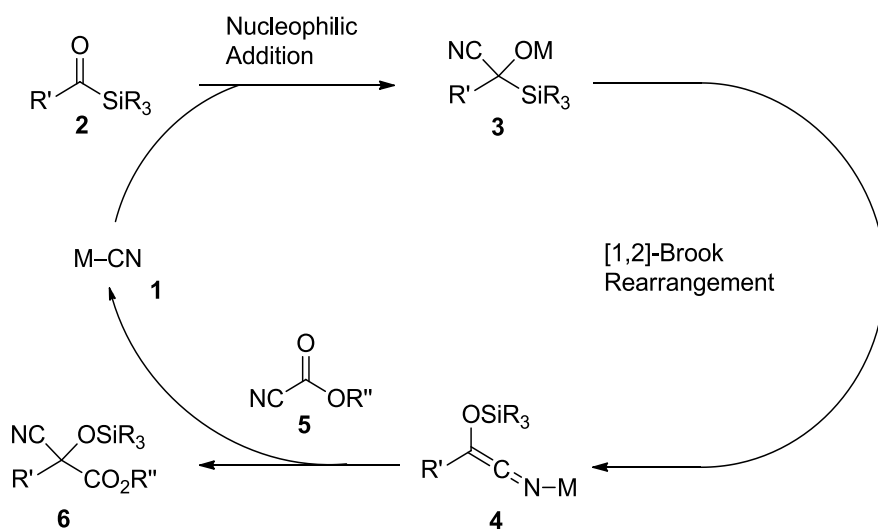
Figure 1-2. [1,2]-Brook Rearrangement



An illustrative example of the use of [1,2]-Brook rearrangement in a multicomponent coupling reaction of acyl silanes is depicted in Figure 1-3. The work disclosed by Linghu and coworkers provides access to α -cyano α -hydroxy esters from the reaction of acyl silanes and cyanofomate esters in the presence of a catalytic cyanide source. The tandem reaction initiates with nucleophilic addition of the metal cyanide **1** to

acyl silane **2** which generates the tetrahedral intermediate **3** which is poised to undergo the [1,2]-Brook rearrangement to the nitrile enolate **4**. Once formed, the nitrile enolate **4** can provide C-acylation by engaging the cyanoformate ester **5** to provide the α -cyano α -hydroxy ester **6** as the final product.

Figure 1-3. Cyanation/[1,2]-Brook Rearrangement/C-Acylation Reaction of Acyl Silanes

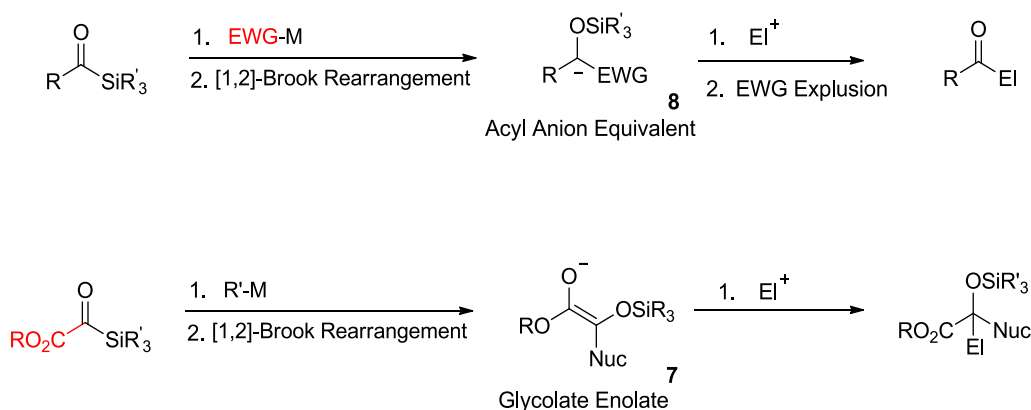


Although acyl silanes found significant utility as umpolung pronucleophiles² in various domino reactions, the requirement of the nucleophilic partner to be electron withdrawing to stabilize the nascent anion substantially hinders the scope of amenable substrates. Additionally, since the [1,2]-Brook rearrangement is reversible, substrates without sufficient anion stabilization will not possess ample driving force to undergo the [1,2]-Brook rearrangement or will lead to an incomplete reaction.

To address these shortcomings, silyl glyoxylates, acyl silanes with an embedded ester functionality, have been developed as a special class of umpolung pronucleophiles.⁵ The strongly electron withdrawing ester functionality in their core structure makes the [1,2]-Brook rearrangement highly favorable. This enables the expansion of the scope of

potential partners to non-electron withdrawing nucleophiles, such as Grignard reagents and hydrides as illustrated in Figure 1-4. Moreover, since non-stabilized nucleophiles are accommodated by this special class of umpolung reagents, the original nucleophilic partner is not expelled as a leaving group as is common in acyl silane chemistry. This distinguishing trait has enabled silyl glyoxylates to find substantial utility as geminal dipolar synthons **7** instead of acyl anion equivalents **8**.

Figure 1-4. Product Diversity in Acyl Silane vs. Silyl Glyoxylate Chemistry

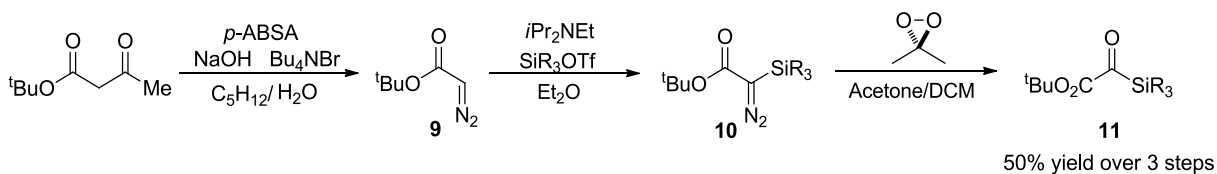


1.2.3. Conventional Silyl Glyoxylate Reactivity

Silyl glyoxylates have emerged as a reliable class of conjunctive reagents for the union of nucleophilic and electrophilic partners. The unique reactivity imparted to silyl glyoxylates in terms of the structural potential of the products is further illustrated in Figure 1-4. Conveniently, silyl glyoxylate reagents can be accessed from readily available starting materials on a large scale (>20 g) in a 50% yield over three steps as illustrated in Scheme 1-1.⁶ Performing a diazo transfer reaction on *tert*-butyl acetoacetate under phase transfer conditions provides α -diazo ester **9**. Silylation of **9** occurs with TESOTf and Hünig's base to provide the triethylsilyl diazo species **10**. Lastly, the

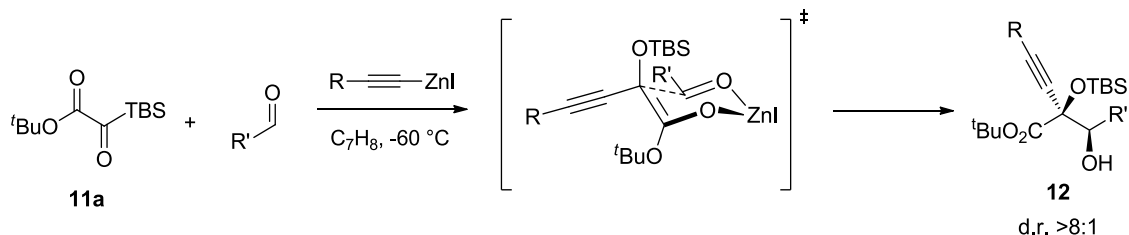
silyldiazoacetate **10** is taken on crude to a DMDO oxidation to provide the desired silyl glyoxylate **11**. The three step synthesis only requires one purification step after the oxidation of **10** to provide the desired silyl glyoxylate as a brilliant yellow oil. Moreover, the strategy is amenable to the synthesis of a variety of silyl glyoxylates by simply changing the silyl triflate employed in the second step. Using this synthetic pathway, TMS, TES, TBS and TIPS silyl glyoxylates have been created in our laboratory.

Scheme 1-1. Synthesis of Silyl Glyoxylates



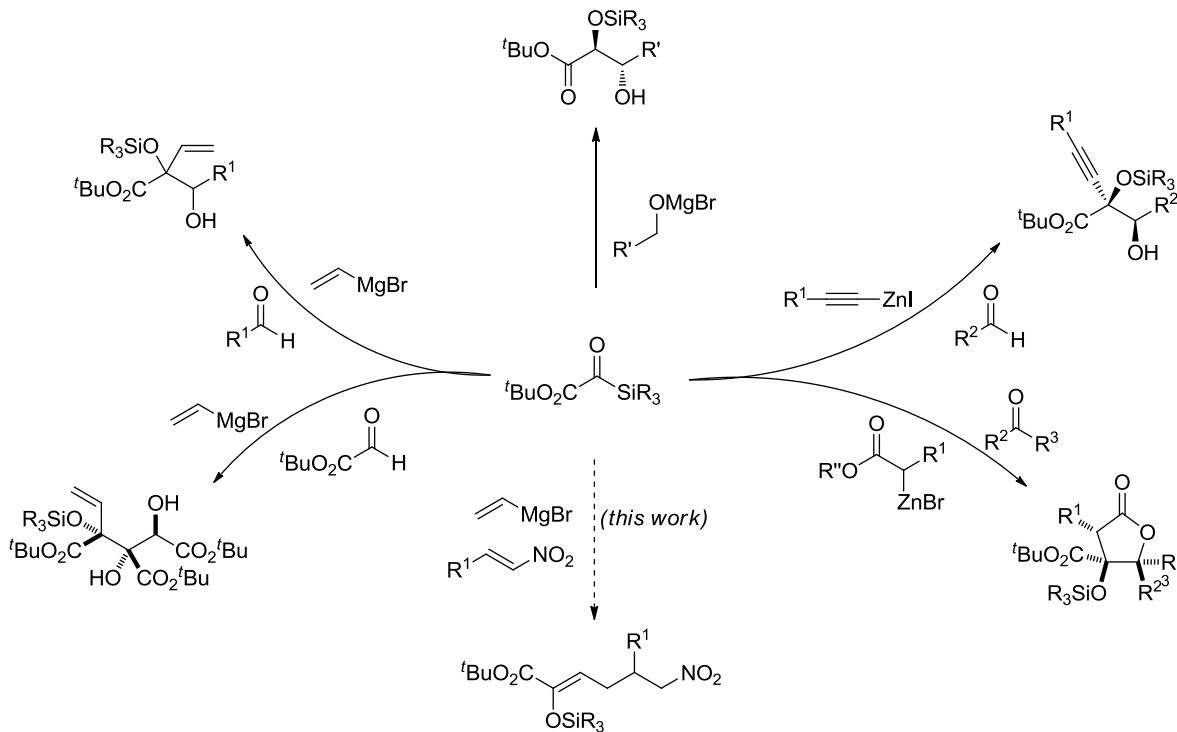
Initial studies on silyl glyoxylates performed by Nicewicz and Johnson demonstrated that these novel reagents were effective in three-component coupling reactions with a nucleophile and secondary electrophile.⁵ In this instance, illustrated in Scheme 1-2, alkynylzinc reagents were shown to function as capable nucleophilic initiators by chemoselectively engaging the silyl glyoxylate **11a** over the aldehyde secondary electrophile. Nucleophilic addition to the silyl glyoxylate results in an alkoxide which undergoes facile [1,2]-Brook rearrangement to form the glycolate enolate which can then combine with the aldehyde to provide glycolate aldol products **12**. In addition to the impressive chemoselectivity in the tandem alkynylation/[1,2]-Brook rearrangement/glycolate aldol reaction, the diol products **12** were obtained with good diastereoselectivity.

Scheme 1-2. Original Silyl Glyoxylate Three-Component Coupling



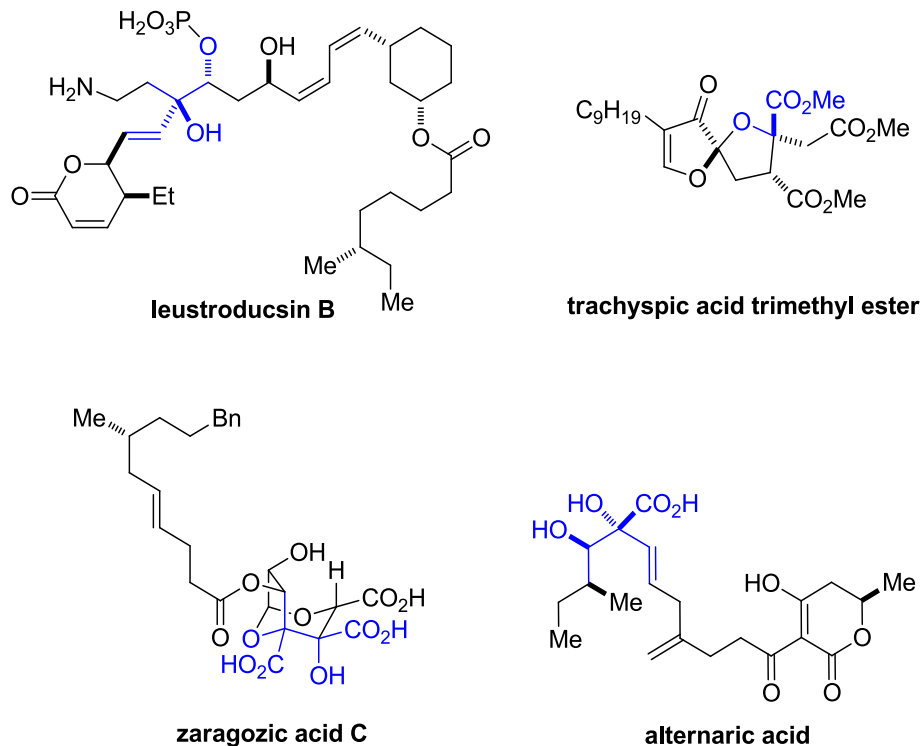
Since the original report in 2005, silyl glyoxylates have been shown to be amenable to a variety of reactions conditions with an extensive range of coupling partners as illustrated in Scheme 1-3. In terms of nucleophiles, hydrides (accessed via Meerwein/Ponndorf/Verley reduction),^{7a} Reformatsky reagents,^{7b} allyl and propargyl zinc reagents,⁵ methylmagnesium bromide,^{7c} and sulfonylimidates^{7d} have been demonstrated to successfully initiate various three-component coupling reactions. With respect to compatible electrophiles, aldehydes,⁵ ketones,^{7b} *N*-*tert*-butanesulfinyl aldimines,^{7d} β -lactones,^{7e} and silyl glyoxylates (dimerization)^{7f} have all been shown to be competent secondary electrophiles in silyl glyoxylate tandem reactions. Prior to the disclosed methodology, secondary electrophiles have been limited to carbonyls with no examples of Michael acceptors presented.

Scheme 1-3. Successful Three-Component Coupling Reactions of Silyl Glyoxylates



The complex and diverse molecular scaffolds obtained from the variety of multicomponent couplings of silyl glyoxylates have found extensive utilization in total synthesis of biologically active natural products. The glycolic acid subunit accessed in silyl glyoxylate chemistry is ubiquitous in natural products and these silyl glyoxylate adducts have provided efficient access to various advanced intermediates in the synthesis of natural products. To date, the total synthesis of leustroducsin B,⁸ trachyspic acid trimethyl ester,⁹ and zaragozic acid C^{7f} have been accomplished employing silyl glyoxylates. Alternaric acid has also been targeted due to the glycolic acid subunit present in the core structure of the natural product. Each natural product depicted in Figure 1-5 has the subunit accessed by silyl glyoxylate chemistry highlighted in blue.

Figure 1-5. Natural Products Targeted with Silyl Glyoxylate Chemistry

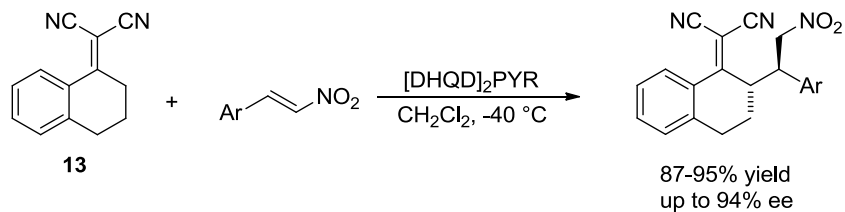


1.2.4. Vinylogous Michael Reaction

While the concept of vinylogy has been extensively applied in vinylogous aldols and related reactions such as the Mannich reaction; the vinylogous Michael reaction is rarely reported in the literature. The most common method to access this elusive reactivity employs the highly specialized α,α -dicyanoolefin moiety. α,α -Dicyanoolefins **13** are very effective as vinylogous Michael pronucleophiles since α,α -dicyanoolefins are highly acidic at the γ -position due to the stabilization of the electron withdrawing cyano groups coupled with their lack of α -protons. Once deprotonated, the α,α -dicyanoolefins provide the desired vinylogous reactivity as illustrated in the work of Deng and coworkers as depicted in Figure 1-6. The strong preference for the α,α -dicyanoolefins to

react in a vinylogous fashion instead of at the α -center is likely a combination of the γ -position being less sterically hindered as well as the additional stability imparted by the olefin being in conjugation with the electron withdrawing cyano groups.

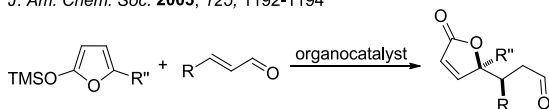
Figure 1-6. Example of α,α -Dicyanoolefin Vinylogous Michael Reactivity



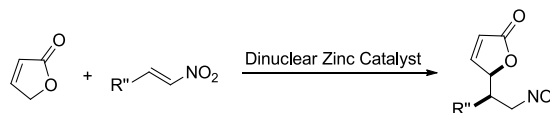
Although α,α -dicyanoolefins are useful due to their reactivity profile, the α,α -dicyanoolefin scaffold is not present in natural products or in medicinal compounds. This lack of relevance in the field of organic and medicinal chemistry requires that the moiety be removed after the desired vinylogous Michael reaction. This results in low atom economy as well as an undesirable inefficiency in step count which confines the applicability of these compounds to the academic. Outside the realm of α,α -dicyanoolefins, vinylogous Michael reactivity is considered a rarity. A testament to the difficulty of this transformation is that most of the examples of vinylogous Michael reactivity have occurred in the past two years and still require specialized starting materials to enable the desired reactivity. A summary of these methodologies is presented in Figure 1-7.

Figure 1-7. Seminal Work in the Vinylogous Michael Reaction

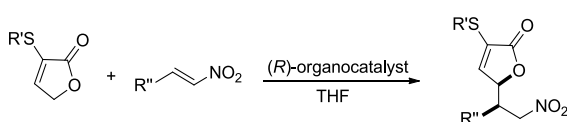
J. Am. Chem. Soc. **2003**, 125, 1192-1194



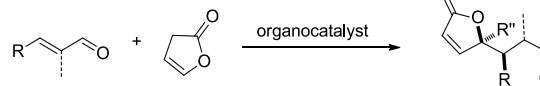
J. Am. Chem. Soc. **2009**, 131, 4572-4573



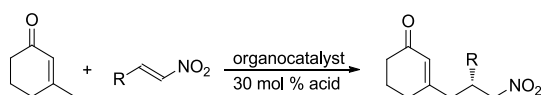
Org. Lett. **2011**, 13, 2026-2029



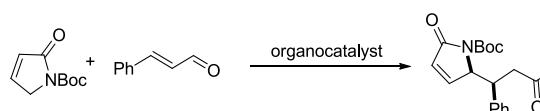
Org. Lett. **2011**, 13, 1540-1543



PNAS **2010**, 107, 20642-20647:



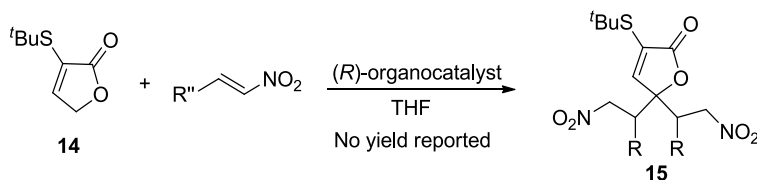
Angew. Chem. Int. Ed. **2011**, 50, 3232-3235



In 2003, MacMillan and coworkers disclosed the enantioselective vinylogous Michael reaction of 2-silyloxyfurans and enals by organocatalysis.¹¹ This seminal work provided much needed exposure to this underutilized reactivity and proved that high regioselectivity is possible. Besides the implications methodologically, these γ -butenolides possess a high application value since they are present in over 13,000 natural products.¹¹ The next hallmark work in the applicability of the vinylogous Michael nucleophilicity of butenolide derivatives was disclosed in 2009, where the Trost group utilized a dinuclear zinc catalyst to access the desired reactivity to nitroalkenes directly from 2(5H)-furanone.¹² This methodology chronicles the first direct asymmetric vinylogous Michael reaction from butenolide derivatives. It is worth noting, that since 1,2-addition to the nitro group of nitroalkenes does not product a stable adduct, the regioselectivity is rigged in this instance unlike in the MacMillan example. In 2011, two additional examples of direct vinylogous Michael reactivity of γ -butenolide derivatives

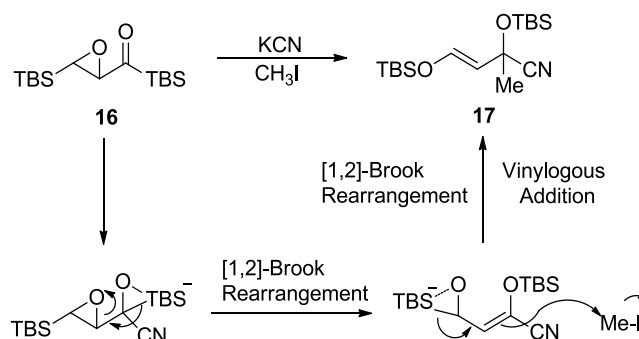
were disclosed. First, Alexakis and coworkers demonstrated that deconjugated butenolides can add to enals in a highly selective manner in the presence of an organocatalysis.¹³ The final work on the topic of vinylogous Michael reactivity of butenolides functionalized with α -thio substituents **14** by the Terada group.¹⁴ The specific importance of this work resides in the demonstration that a bulky α -substituent can enable di- γ -substitution **15** as illustrated in Scheme 1-5. This is an impressive result since α -addition is typically anticipated if both the α and γ positions are equally substituted.¹⁵ Similar methodologies have been reported with γ -butyrolactam substrates to imines¹⁶ and enals.¹⁷

Scheme 1-4. Di- γ -Addition of Nitroalkenes to α -Thio Butenolide Derivatives



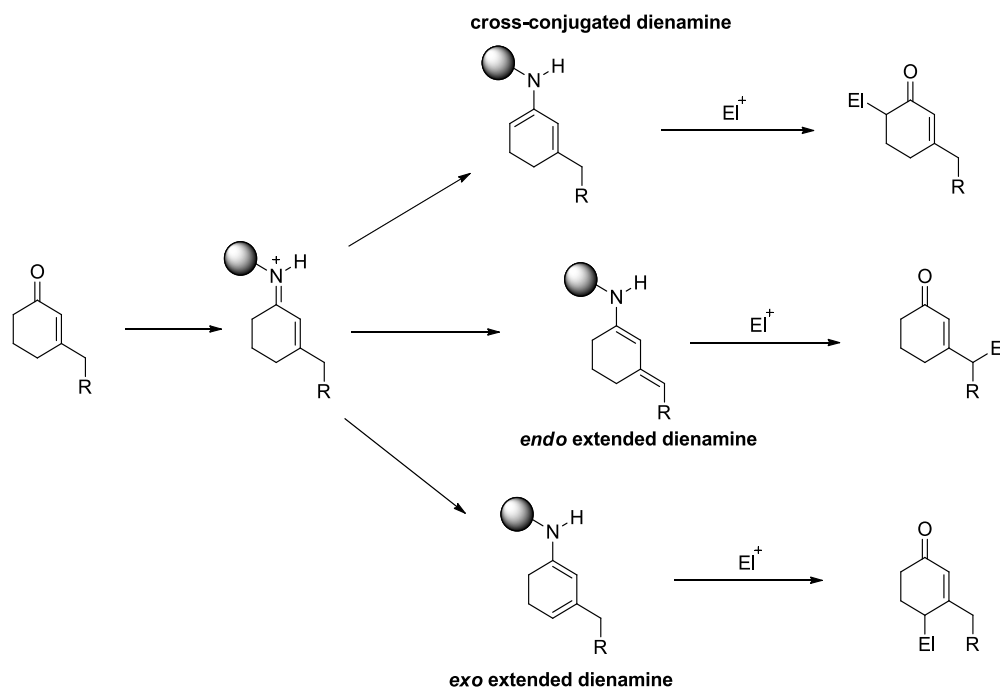
Two seminal works that provide vinylogous adducts without the use of α,α -dicyanoolefins or butenolide derivatives were reported by the Takeda group and the Melchiorre group. The first methodology reported in 2004 accessed vinylogous reactivity from an acyclic substrate via a [1,2]-Brook rearrangement. As illustrated in Figure 1-8, the Takeda group found that reacting the epoxy-acyl silane **16** with potassium cyanide in the presence of a secondary electrophile such as methyl iodide provides dienol products **17** via a [1,2]-Brook rearrangement/[1,2]-Brook rearrangement/vinylogous alkylation cascade.¹⁸ Although mechanistically unique, the methodology holds limited applicability due to the low yields and the highly specialized starting materials.

Figure 1-8. Takeda's Vinylogous Reactivity Cascade



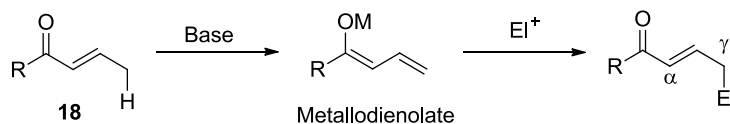
The second work disclosed the first asymmetric vinylogous Michael reaction of cyclic enones to nitroalkenes.¹⁹ Besides providing excellent yields, regioselectivity, and stereoselectivity the highlighted research is a vital contribution to the field since it allows for non-heterocyclic enones to be utilized for the first time. In this instance, the excellent regioselectivity for the γ -addition over α -addition is likely a function of the bulky amine catalyst blocking the α -site once condensed on the ketone. The impressive regioselectivity of this work is further highlighted by the potential challenges illustrated in Figure 1-9.

Figure 1-9. Regioselectivity Challenges Arising from the Cyclic Enone Methodology



The several vinylogous Michael methodologies described above highlight the infancy of this field with most of the significant achievements accomplished in the past two years as well as highlight the significant challenges that this reactivity still faces. More specifically, cyclic systems are always required for excellent selectivity, and these systems are almost exclusively heterocyclic compounds. The weakness of this field lay in the inability to access reliable vinylogous Michael reactivity directly from acyclic, simple starting materials such as **18** as illustrated in Figure 1-10.²⁰

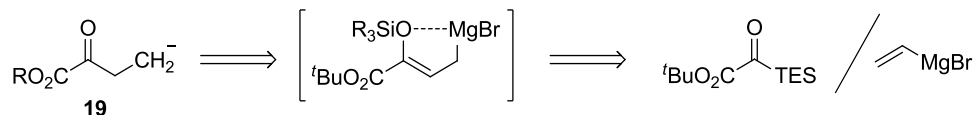
Figure 1-10. An Ideal Vinylogous Michael Transformation



1.2.5. Origin of the Title Reaction

The disclosed methodology arose from a desire to expand the utility of silyl glyoxylate chemistry to include Michael acceptors as the secondary electrophile. Nitroalkenes were chosen due to their highly electrophilic character and the synthetic utility of the nitro functionality.²¹ Since all previous silyl glyoxylate couplings provided α -addition from the requisite metallodienolate intermediates with high regioselectivity; an open question at the outset of this research was whether α - or γ -addition would predominate when the carbonyl secondary electrophile was replaced with a Michael acceptor. Since α/γ selectivity has been found to be highly substrate dependent,¹⁵ the variation of the secondary electrophile may exert preference for γ -addition. If the vinylogous pathway did predominate, then the combination of vinylmagnesium bromide and silyl glyoxylate would be shown to function as the unusual α -keto ester homoenolate synthon **19** as depicted in Scheme 1-5.

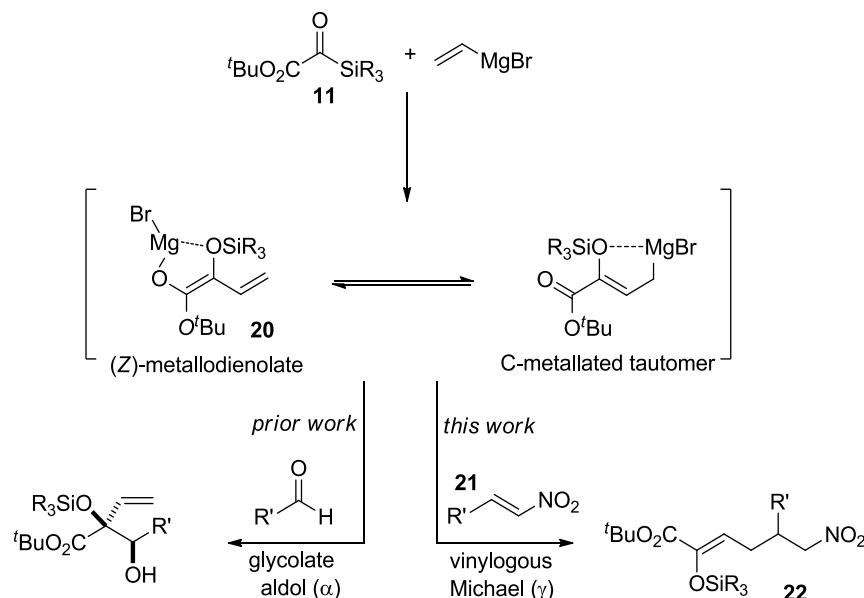
Scheme 1-5. Proposed Access to the α -Keto Ester Homoenolate Synthon



If the vinylogous Michael pathway does predominate, the proposed transformation would occur as outlined in Scheme 1-6. The cascade would initiate by vinylmagnesium bromide attacking silyl glyoxylate **11**, which will provide the (*Z*)-metallodienolate **20** after [1,2]-Brook rearrangement. This (*Z*)-metallodienolate species **20** could then act as a transient nucleophile and engage the nitroalkene **21** as the

secondary electrophile in a vinylogous Michael fashion to provide enolsilane **22** as the product of the cascade.

Scheme 1-6. Divergent Silyl Glyoxylate Reactivity



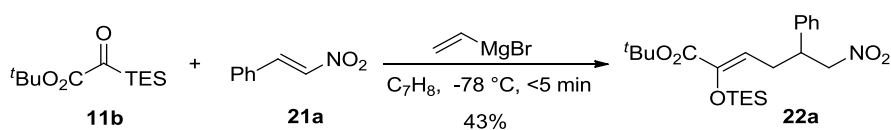
1.3 Results and Discussion

1.3.1 Investigation of Reaction Parameters

Due to the known nucleophile-initiated oligomerization of silyl glyoxylates in the absence of a secondary electrophile,^{5,7f} the reaction parameters would require the presence of the nitroalkene in the same pot as the silyl glyoxylate. This stipulation requires that the vinylmagnesium bromide act as a highly chemoselective nucleophile in favor of the silyl glyoxylate for the reaction to be plausible. Initial experiments with triethylsilyl (TES) glyoxylate, β -nitrostyrene and vinylmagnesium bromide at -78°C provided the desired vinylogous Michael reactivity as illustrated in Scheme 1-7. Product **22a** was obtained as a single stereo- and regioisomer of the enolsilane albeit in an unsatisfactory yield of 43% with silyl glyoxylate oligomers as the major byproducts.

Since the vinylation of the nitroalkene was not observed in the crude reaction mixture, vinylmagnesium bromide must act as a highly discriminating nucleophile with a strong preference for silyl glyoxylate over the nitroalkene. Since nitroalkenes are highly activated electrophiles themselves,²¹ the high level of chemoselectivity in favor of silyl glyoxylates is a testament to their highly electrophilic character.

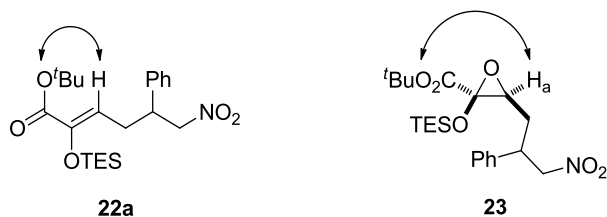
Scheme 1-7. Initial Three-Component Coupling Study



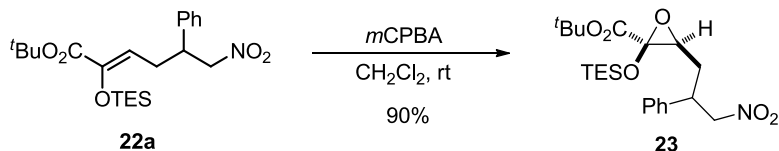
1.3.2. Justification of the Enolsilane Stereochemistry

The stereochemistry of the olefin of the enolsilane was determined by NOESY analysis as illustrated in Figure 1-11. A strong nOe correlation between the *tert*-butyl group of the ester and the vinyl proton strongly suggest a *syn* relationship. To confirm the identity of the enolsilane product **22a**, the silyl enol ether was converted to the silyloxyepoxide **23** using *m*CPBA as illustrated in Scheme 1-8. NOESY analysis of the corresponding silyloxyepoxide **23** verified the original finding with the presence of a nOe correlation between the *tert*-butyl group of the ester and the H_a while no nOe was observed between the TES group and H_a .

Figure 1-11. Analysis of the Enolsilane Geometry



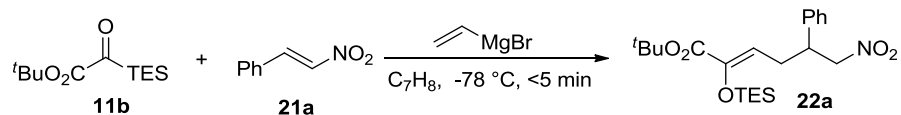
Scheme 1-8. Conversion of the Enolsilane **22a** to Silyloxyepoxide **23**



1.3.3. Optimization Studies

Optimization trials began with varying the stoichiometry of each reagent in the hopes of minimizing byproduct formation with the results summarized in Table 1-1. Initial studies using an equivalent ratio of each reagent resulted in significant silyl glyoxylate oligomerization. To compensate for this oligomerization, the equivalents of nitroalkene **21a** and vinylmagnesium bromide were increased (entry 2) which provided a significant improvement in yield to 60%. Flooding the system with 10 equivalents of nitroalkene **21a** provided further improvement in the yield to 70% (entry 3); however this method was abandoned due to the waste created. Lastly, increasing the equivalents of silyl glyoxylate **11b** to 50% excess adequately compensated for the silyl glyoxylate oligomerization pathway (entry 4) providing a 74% yield of the desired vinylogous adduct **22a**.

Table 1-1 Stoichiometry Optimization

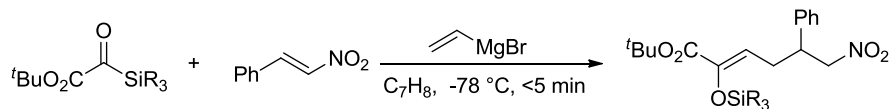


entry	silyl glyoxylate	β -nitrostyrene	vinyl Grignard	yield (%) ^b
1	1.0	1.0	1.0	43
2	1.0	2.0	1.5	60
3	1.0	10.0	5.0	70
4	1.5	1.0	1.5	74

^aAll reactions were conducted [**21a**]₀ = 0.1 M with the reaction warmed to room temperature immediately after the addition was complete. ^bIsolated Yield. See section 1.6 for additional experimental details.

With the optimized stoichiometry in hand, a screen of various silyl glyoxylates was accomplished since the size of the silyl group affects the rate of the [1,2]-Brook rearrangement; the results are summarized in Table 1-2. The silyl screen demonstrated that the TES and TBS groups functioned similarly in the reaction manifold. The much smaller TMS silyl glyoxylate **11c** performed poorest in the reaction providing only a 30% yield. The particularly poor performance of the TMS group is likely due to a very rapid [1,2]-Brook rearrangement that leads to substantial oligomerization. The largest silyl group, the TIPS silyl glyoxylate **11d** provided a 54% yield. Based on these findings, the triethylsilyl glyoxylate **11b** was chosen for further study since it provided the highest yield and is more easily deprotected and functionalized than the TBS silyl enol ether product.

Table 1-2. Silyl Group Screen

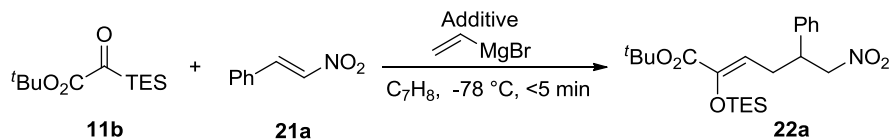


entry	silyl glyoxylate	SiR ₃	yield (%) ^b
1	11c	TMS	30
2	11b	TES	74
3	11a	TBS	72
4	11d	TIPS	54

^aAll reactions were conducted [**21a**]₀ = 0.1 M with the reaction warmed to room temperature immediately after the addition was complete. ^bIsolated Yield. See section 1.6 for additional experimental details.

In the hopes of further augmenting the yield by decreasing the reactivity of the (Z)-metallodienolate **20**, a series of additives were also screened with the results summarized in Table 1-3. The addition of lithium chloride (entry 1) halted desired reactivity providing silyl glyoxylate oligomerization as the only product. This predominance of the oligomerization pathway is likely due to lithium being an α -directing counterion. When α -addition is favored the harder electrophile,¹⁵ which is the unreacted silyl glyoxylate **11b** in this case, is preferred. Titanium (IV) tetrachloride was also employed (entry 2), but the Lewis acid had no beneficial effect on the yield. Lastly, trimethylsilyl chloride was added in an attempt to form the silyl ketene acetal and halt the (Z)-metallodienolate's nucleophilicity until the silyl glyoxylate is fully consumed. Regrettably, the addition of the silyl Lewis acid had negligible effect on the reaction.

Table 1-3. Screen of Various Additives

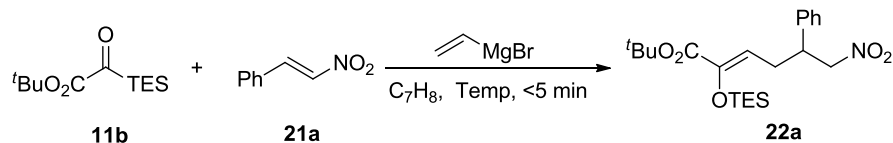


entry	additive	yield (%) ^b
1	LiCl	0
2	TiCl ₄	72
3	TMSCl	70

^aAll reactions were conducted $[\mathbf{21a}]_0 = 0.1\text{ M}$ with the reaction warmed to room temperature immediately after the addition was complete. ^bIsolated Yield. See section 1.6 for additional experimental details.

The temperature dependence of the reaction was then examined with the findings disclosed in Table 1-4. Raising the temperature to $-40\text{ }^\circ\text{C}$ (entry 1) provided significantly more oligomerization in comparison to the $-78\text{ }^\circ\text{C}$ trial (entry 2). This decrease in selectivity is congruent with the fact that the [1,2]-Brook rearrangement slows with decreasing temperature. Decreasing the temperature to $-90\text{ }^\circ\text{C}$ was also detrimental to the yield providing 53% of the desired vinylogous adduct (entry 3). In this instance, the [1,2]-Brook rearrangement appeared to proceed as quickly as at $-78\text{ }^\circ\text{C}$ based on the color change in the reaction. The decrease in yield in this trial is due to the formation of new, unidentified byproducts. The temperature was decreased to $-100\text{ }^\circ\text{C}$ (entry 4) the [1,2]-Brook rearrangement remained facile and the results mirrored those of entry 3.

Table 1-4. Temperature Screen



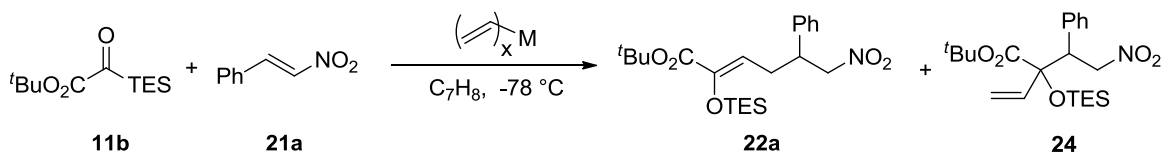
entry	temperature	solvent	yield (%) ^b
1	-40 °C	C ₇ H ₈	17
2	-78 °C	C ₇ H ₈	74
3	-90 °C	C ₇ H ₈	53
4	-100 °C	THF	53

^aAll reactions were conducted [**21a**]₀ = 0.1 M with the reaction warmed to room temperature immediately after the addition was complete. ^bIsolated Yield. See section 1.6 for additional experimental details.

With the parameters of the reaction extensively studied, the type of nucleophile was investigated in a final attempt to overcome the oligomerization pathway with the results summarized in Table 1-5. We speculated that varying the nucleophile may enable access to the α -addition adduct as well. As previously mentioned, our control nucleophile, vinylmagnesium bromide provided a 74% yield under the designated reaction parameters (entry 1). Switching to vinyl lithium provided trace amount of the α -adduct (entry 2); however, the majority of the crude mixture was silyl glyoxylate oligomerization. This result echoes the observations from the lithium chloride additive trial. Zinc (II) was then examined as the counterion on the vinyl nucleophile. Vinylzinc bromide was found to be unreactive in the reaction parameters up to 50 °C (entry 3). To increase the reactivity, divinylzinc was employed in the reaction manifold (entry 4). This nucleophile provided the desired product albeit in a diminished yield ranging from 30-45%. Exposing trivinylmagnesium zincate to the reaction conditions provided the desired reactivity, however, in a lower yield of 13-30% (entry 5). Based on these trials it is

reasonable to conclude that the lithium and zinc counterions promote α -addition which leads to silyl glyoxylate oligomerization as the major product over the α - or γ -coupling adduct.

Table 1-5. Screen of Various Nucleophiles



entry	nucleophile	yield (%) of 22a ^b
1	Vinylmagnesium Bromide	74
2	Vinyl Lithium	Trace 24
3	Vinylzinc bromide	Unreactive up to 50 °C
4	Divinylzinc	30-45
5	Trivinylzincate Species	13-30

^aAll reactions were conducted [**21a**]₀ = 0.1 M with the reaction warmed to room temperature immediately after the addition was complete. ^bIsolated Yield. See section 1.6 for additional experimental details.

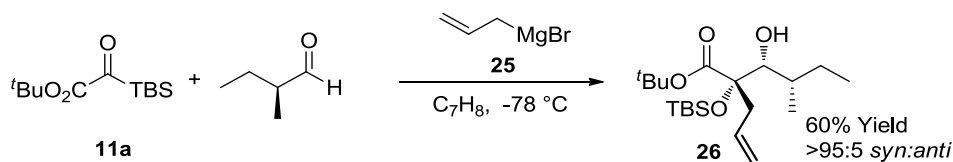
1.3.4. Scope and Limitations

With the optimized conditions in hand for the vinylation-initiated three-component coupling, the scope of amenable nucleophilic and electrophilic partners was investigated. Using β -nitrostyrene as the electrophilic control, isopropenylmagnesium bromide and β -styrylmagnesium bromide were employed to gauge whether substituted vinyl nucleophiles were competent cascade initiators. The isopropenyl trial provided predominantly silyl glyoxylate oligomerization with a 14% yield of the α -adduct. Likewise the β -styrylmagnesium bromide provided silyl glyoxylate oligomerization as the major product with trace α -adduct present in the crude mixture by ¹H NMR analysis.

Based on these trials, it appears that the added steric effects of the substituents at both the α - and β -positions caused the α -addition pathway to predominate which, in turn, favors oligomerization.

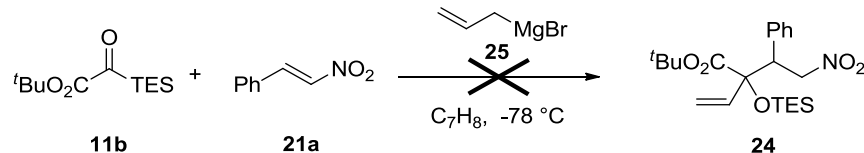
We then investigated allylmagnesium bromide as a non-conjugated unsaturated nucleophile to see whether the α -adduct would predominate. Based on previous studies by a former group member, allylmagnesium bromide **25** is a competent nucleophilic partner in the three-component coupling of silyl glyoxylates and aldehydes to provide α -adduct **26** as illustrated in Scheme 1-9.²²

Scheme 1-9. Precedented Allylmagnesium Bromide Three-Component Coupling



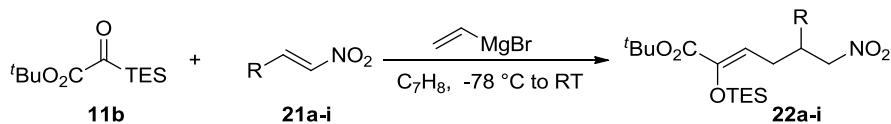
Applying the allylmagnesium bromide nucleophile in the nitroalkene three-component coupling reaction provided no desired α -adduct as illustrated in Scheme 1-10. The only observable product was silyl glyoxylate oligomerization which corroborates the hypothesis above that oligomerization is more favorable for the α -addition pathway than is Michael addition. At the point it is reasonable to conclude that the α vs. γ selectivity of a proposed silyl glyoxylate coupling depends heavily on the type of secondary electrophile employed.

Scheme 1-10. Proposed Allylmagnesium Bromide Three-Component Coupling



Acknowledging that vinylmagnesium bromide was the only nucleophilic partner compatible with the reaction conditions, the scope of the electrophilic partner was investigated. An examination of various alkyl, alkenyl, aryl, and heteroaryl nitroalkenes was conducted with the results summarized in Table 1-6. The yields ranged from 36-74% with aryl, heteroaryl and alkenyl nitroalkenes outperforming the alkyl substrates. Nitroethylene was also amenable to the reaction condition and provided a 57% yield of the unsubstituted (*Z*)-enolsilane (entry 6). The efficiency of the reaction tended to decrease with increasing steric hindrance from α -branching on the R group of the alkyl-substituted nitroalkenes. In example, (*E*)-1-nitrohept-1-ene (entry 7) providing a 58% yield which outperformed (*E*)-3-methyl-1-nitrobut-1-ene (entry 8) by 5%. The most sterically encumbered (*E*)-3,3-dimethyl-1-nitrobut-1-ene (entry 9) provided the poorest yield of the scope with a 36% yield.

Table 1-6. Substrate Scope for the Vinylation-Initiated Three-Component Coupling



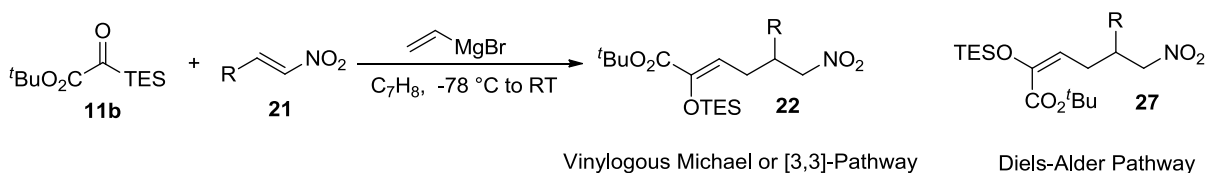
entry	product	R	yield (%) ^b
1	22a	Ph	72
2	22b	4-Cl-C ₆ H ₄	70
3	22c	2-thienyl	65
4	22d	2-furyl	64
5	22e	(<i>E</i>)-styryl	66
6	22f	H	57
7	22g	<i>n</i> -pentyl	58
8	22h	<i>i</i> Pr	53
9	22i	<i>t</i> Bu	36

^aAll reactions were conducted [**21**]₀ = 0.1 M with the reaction warmed to room temperature immediately after the addition was complete. ^bIsolated yield. See section 1.6 for additional experimental details.

1.3.5. Studies on the Reaction Mechanism

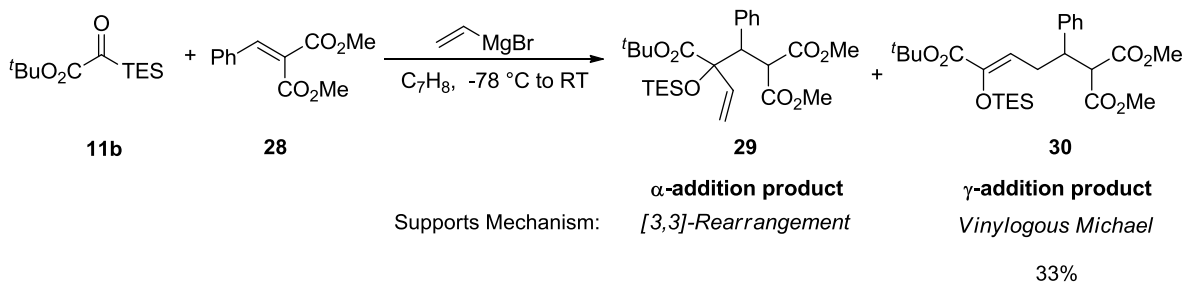
Based on the enolsilane products observed, there are three possible mechanisms by which these products could form: the vinylogous Michael cascade which we have thus far assumed, a α -addition to the $\pi_{N=O}$ of the nitro group followed by [3,3]-rearrangement,²³ and finally a Diels-Alder type pathway. As illustrated in Scheme 1-11, the Diels-Alder pathway would result in a (*E*)-enolsilane **27** thereby eliminating this pathway from the list of possible mechanisms, leaving the vinylogous Michael cascade and the [3,3]-cascade.

Scheme 1-11. Products Arising From Three Plausible Mechanisms for the Three-Component Coupling



The observed (*Z*)-selectivity for the silyl enol ether **22** is consistent with the Kuwajima-type (*Z*)-metallodienolate intermediate **20** which supports the vinylogous Michael cascade.²⁴ However, selectively forming the (*Z*)-silyl enol ether is also possible via the [3,3]-rearrangement cascade as well. To differentiate between the two possible mechanisms, benzylidene malonate **28** was exposed to the reaction conditions. Since benzylidene malonate will not undergo a 1,2-addition at the ester, this example should serve to discern the operative mechanism as illustrated in Scheme 1-12. If α -addition **29** is observed for this substrate, then the [3,3]-cascade is likely the functioning mechanism; if the γ -adduct **30** is isolated then the vinylogous Michael cascade case is supported. Subjecting benzylidene malonate to the reaction conditions provided a 33% yield of the γ -addition product **30** which eliminates the [3,3]-rearrangement as the likely mechanism. Based on this analysis, it is reasonable to conclude that a highly regio- and stereoselective vinylogous Michael cascade is the operative in the three-component coupling.

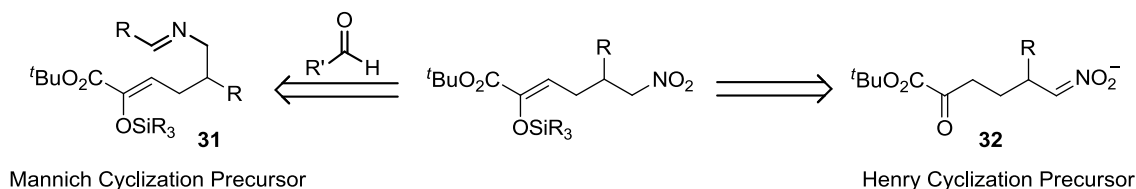
Scheme 1-12. Benzylidene Malonate Terminated Three-Component Coupling



1.4. Secondary Transformations

Due to the diversity of functionalization inherent to these heretofore unknown ε -nitro esters, we hypothesized that these compounds would be poised to undergo unique subsequent transformations. Specifically, we envisioned the synthesis of densely functionalized piperidines arising from a Mannich strategy and cyclopentanols arising from a Henry cyclization²⁵ of these substrates as illustrated in Figure 1-12. These two proposed transformations take advantage of very different aspects of the enolsilane functionality. For the Mannich cyclization, the nucleophilicity of the silyl enol ether functionality is utilized to attack the electrophilic imine which is formed from the pendant nitro functionality as seen in Mannich cyclization precursor **31**. In contrast, the Henry cyclization utilizes the nucleophilicity of the nitro group and exploits the silyl enol ether as a masking group for the electrophilic α -keto ester **32**.

Figure 1-12. Proposed Subsequent Transformations of ε -Nitro Enolsilanes



1.4.1. Potential Piperidine Synthesis

Piperidines are a common building block in alkaloid natural products as illustrated in Figure 1-13 as well as extensively utilized in medicinal chemistry as drugs as depicted in Figure 1-14. While there are a variety of methods to synthesize 2,6-disubstituted piperidines, the synthesis of multifunctional piperidines remains to be a challenge for synthetic chemists.²⁶ Some common methodologies for the synthesis of multisubstituted piperidines include cyclization of linear precursors via a nucleophilic substitution of an amine, ring-closing metathesis, aza Diels-Alder reactions, and reduction of pyridines.²⁶ The efforts to synthesize trisubstituted piperidine derivatives from these enolsilanes is herein recounted.

Figure 1-13. Piperidine Containing Natural Products

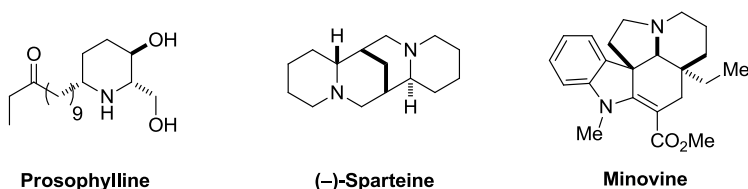
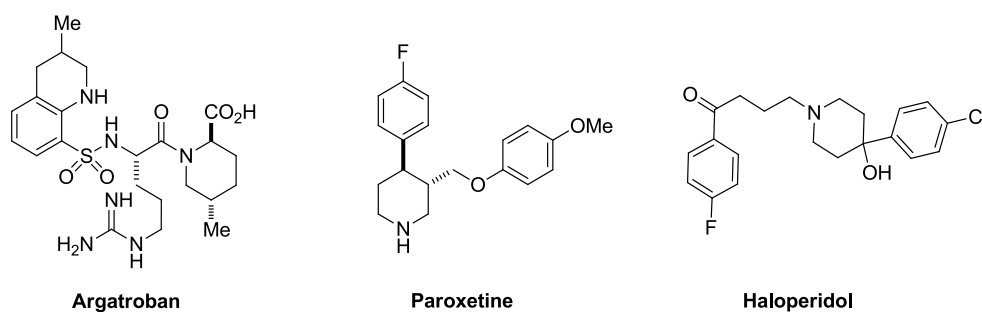


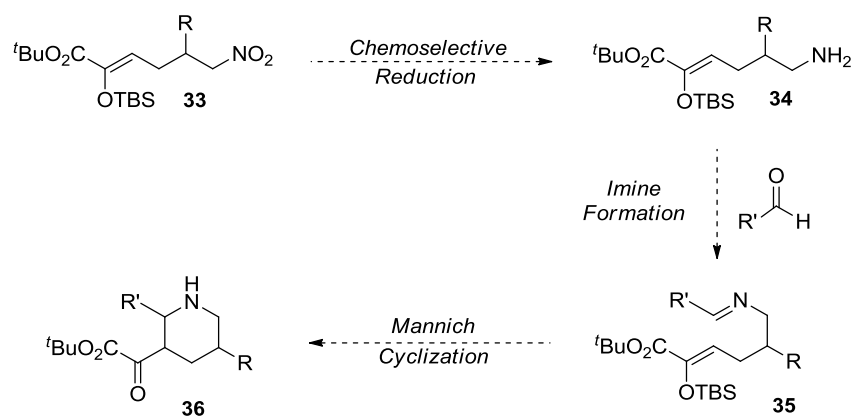
Figure 1-14. Piperidine Containing Drug Targets



Our strategy for the synthesis of piperidine derivatives is illustrated in Figure 1-15. An initial chemoselective reduction of the nitro group that preserves the silyl enol

ether functionality is required to provide amine **34**. Imine formation on **34** should fashion intermediate **35** which can provide the desired 2,3,5-trisubstituted piperidines **36** via an intramolecular Mannich reaction. The TBS silyl enol ether **33** formed from the TBS silyl glyoxylate was utilized in these studies since the TBS silyl enol ether is more stable which should aid in preserving the moiety during the reduction step.

Figure 1-15. Strategy for the Synthesis of Piperidine Derivatives



Studies towards the chemoselective reduction of the nitro group were conducted with the results summarized in Table 1-7. The most common conditions for nitro reduction resulted in either over-reduction or decomposition with no desired product obtained (entries 1-3). Nickel boride/hydrazine hydrate is known for reducing aliphatic nitro groups in the presence of alkenes;²⁷ however this trial (entry 4) provided no desired product. More exotic nitro reductions including Et₃SiH (entry 5), SmI₂ (entry 6), and TiCl₃ (entry 7) also provided no desired product. Gratifyingly, using an iron powder reduction (entry 8) provided the desired unsaturated amine product **34** in yields ranging from 80-90%.²⁸ The success of this method is a testament to the stability of TBS silyl

enol ethers since the reduction takes place in 1 M HCl and refluxing ethanol. Attempting this chemoselective reduction on the TES enolsilane **22a** provided only decomposition.

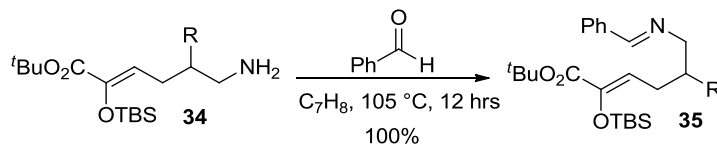
Table 1-7. Conditions for the Chemoselective Reduction of the Nitro Group

entry	conditions	result ^a
1	Zn ⁽⁰⁾ dust, AcOH, 70 °C	Decomposition
2	HCO ₂ NH ₄ , Pd/C, MeOH	Over-reduction
3	Lindlar's Catalyst	Decomposition
4	Ni ₂ B, N ₂ H ₄ ·H ₂ O, <i>i</i> PrOH	Decomposition
5	Et ₃ SiH, Pd(OAc) ₂ , THF/H ₂ O	Recovered S.M.
6	SmI ₂ , THF/MeOH	Decomposition
7	TiCl ₃ , H ₂ O, Dioxane	Decomposition
8	Fe ⁽⁰⁾ powder, 1M HCl/EtOH, 65 °C	80-90%

^aIsolated Yield. See section 1.6 for additional experimental details.

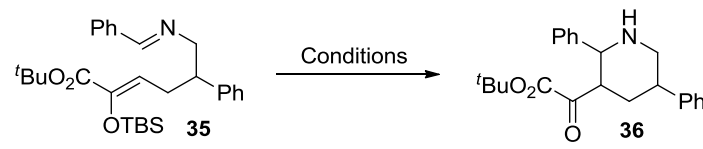
With conditions in hand for the selective reduction of the nitro group, efforts to access the imine **35** were undertaken. A variety of conditions for imine formation were attempted at room temperature with benzaldehyde employed as the control aldehyde; however, only recovered starting material was recovered in each instance. Heating the amine and aldehyde in refluxing toluene provided the desired transformation in quantitative yield as depicted in Scheme 1-13. At this point, the Mannich cyclization precursor has been attained in >80% yield over two steps.

Scheme 1-13. Formation of Imine **35**



Conditions to enable the desired Mannich reaction were conducted with the instructive results summarized in Table 1-8. Since the Lewis acid-induced Mannich reaction is well documented we began with a screen of known Lewis acid conditions (entries 1-5). Each of the screened Lewis acid conditions either provided either decomposition or recovered starting material. Employing trifluoroacetic anhydride (entry 6) to activate the imine provided the desired cyclization to **36**, however, the product was never obtained in a yield greater than 15% on a small scale. Deeming the Lewis acid route as untenable, a silyl enol ether deprotection-initiated cyclization was attempted by using TBAF at -20 °C (entry 7). While this method also provided the desired cyclization, but the yield was never higher than 8%, making it an unviable transformation. Lastly, heating imine **35** in refluxing toluene for three days (entry 8) provided only recovered starting material. The final entry proves that this imine species is highly stable even under extreme conditions which led us to abandon this piperidine synthesis strategy.

Table 1-8. Screen of Conditions for the Mannich Cyclization to **36**



entry	conditions	result ^a
1	InCl ₃ (20 mol %) MeOH, rt, 12h	Recovered S.M.
2	BF ₃ ·OEt ₂ , Toluene, rt, 12 h	Decomposition
3	Sc(OTf) ₃ (10 mol %), THF	Decomposition
4	TiCl _x (OiPr) _y (Various conditions)	Decomposition
5	TiF ₄ , rt, THF, 12 h	Imine Cleavage
6	TFAA, CH ₂ Cl ₂ , reflux, 12 h	>15%
7	TBAF, -20 °C, CH ₂ Cl ₂ , 12 h	8%
8	110 °C, Toluene, 3 days	Recovered S.M.

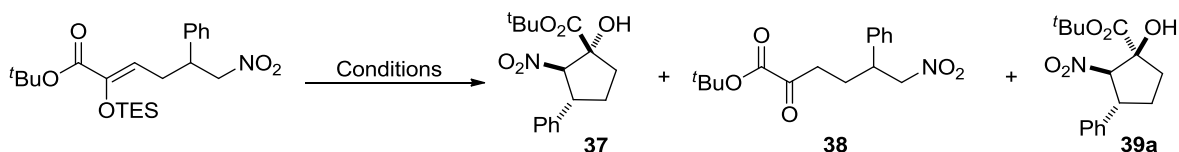
^aIsolated Yield.

1.4.2. Henry Cyclization

Since the enolsilanes **22a-i** are assembled in the correct oxidation state to enable a silyl enol ether deprotection/Henry cyclization cascade, we envisioned furnishing highly functionalized cyclopentanols with three contiguous stereocenters from these simple enolsilane starting materials. The intramolecular Henry reaction is infrequently deployed in organic chemistry due to the difficulty in synthesizing the requisite bifunctional nitrocarbonyl precursors.²⁵ These enolsilanes provide the desired bifunctionality by virtue of the silyl enol ether serving as a masked α -keto ester. An investigation was conducted to enable the desired cascade of enolsilane **22a** with the results summarized in Table 1-9. Initial studies employed fluoride-based deprotections since they are the most common

method for deprotecting silyl protecting groups. Subjecting enolsilane **22a** to TBAF deprotection conditions at room temperature (entry 1) provided the desired Henry cascade albeit in an unsatisfactory yield of 43% and a 4:1 diastereomeric ratio favoring diastereomer **37**. Employing hydrogen fluoride/pyridine conditions (entry 2) enabled the silyl deprotection, but not the Henry cyclization resulting in the α -keto ester **38** being obtained in a 92% yield. Substituting the fluoride deprotections for a basic methanol deprotection at -5 °C (entry 3) provided the desired cyclization in a 78% yield with a greater than 20:1 diastereoselection in favor of diastereomer **39a**.

Table 1-9. Optimization of the Henry Cyclization Cascade



entry	conditions	product	dr	yield (%) ^b
1	TBAF, THF, 4 hrs, rt	37	4:1	43
2	HF*pyridine, 3 hrs, rt	38	N/A	92
3	NaOH, MeOH/CH ₂ Cl ₂ , 3 hrs, 0 °C	39a	20:1	78

1.4.3. Optimization

Although the reaction parameters provided excellent diastereoselectivity for **39a**, the diastereoselectivity was not equally impressive for other examples. Even very similar compounds such as **39b** provided only 2:1 diastereoselection under the original reaction conditions. To correct this poor diastereoselectivity, a series of conditions were screened on enolsilane **22b** to find conditions that provide for excellent diastereoselectivity to be

imparted to a larger substrate scope. Strangely, employing an equal amount of dichloromethane to methanol as a cosolvent provided a dramatic jump in diastereoselectivity as illustrated in Table 1-10. While the role of dichloromethane in the reaction is unknown, the effect on the diastereoselection is clear and the yield remained unaffected.

Table 1-10 Effects of Dichloromethane as Cosolvent

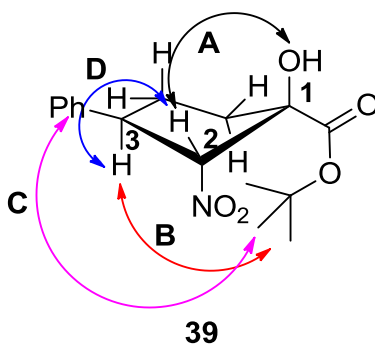
entry	R	d.r. without CH ₂ Cl ₂	d.r. with CH ₂ Cl ₂	yield (%) ^b
1	4-ClPh	2:1	20:1	69
2	<i>i</i> Pr	2:1	>20:1	56
3	<i>t</i> Bu	1:1	>20:1	59

1.4.4. Determination of Relative Stereochemistry

The relative stereochemistry of **39a** was deduced by NOESY analysis and represented in Figure 1-16. The identities of all other substrates were assigned using the same rationale. The relative stereochemistry at C1-C2 was assigned based on an observed nOe between the C2 α -nitro methine proton and the C1 alcohol proton (A) which establishes these two substituents as *syn*. A strong nOe correlation observed between the C3 benzylic proton and the C1 *tert*-butyl ester (B) suggests that these two groups must also be *syn*. The relatively weak correlation between the *tert*-butyl ester and the α -nitro methine proton imply these groups are in a *trans* orientation. By corollary, this means that the substituents at C2 and C3 are also *trans*. Although it is odd to see a *tert*-butyl

ester orienting itself towards the ring for steric reasons, we proposed that hydrogen bonding between the *tert*-butyl ester carbonyl and the alcohol likely orients the *tert*-butyl group over the ring thus explaining the observed nOe correlations. Moreover, the comparatively small nOe for the C3 phenyl substituent with the *tert*-butyl group (C) suggests that these substituents do not significantly interact with one another. Although there is a nOe between the benzylic proton at C3 and the α -nitro methylene proton at C2 (D), we have previously observed that a nOe between the vicinal protons on a 5-membered ring does not preclude the possibility of a *trans* orientation.²⁹ This rationale, in conjunction with the stronger nOe between the C3 phenyl group and the C2 α -nitro methine proton, further supports the *trans* assignment. This NOESY analysis was justified by obtaining an x-ray crystal structure of the carboxylic acid derivative (**S1**) which was obtained by a TFA deprotection of **39a**.³⁰

Figure 1-16 Representative nOe Correlations for **39**

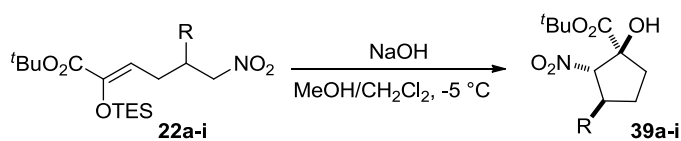


1.4.5. Reaction Scope and Trends

The enolsilanes **22a-i** were exposed to the optimized conditions for the diastereoselective Henry cyclization with the results chronicled in Table 1-11. The yields ranged from 58-94% with alkyl, alkenyl, aryl, and heteroaryl examples all being well

tolerated. The diastereocontrol was complete for all examples except substrates **39e**, **39f**, **39g** (entries 5-7). The common attribute of these three examples is that they possess linear R groups, or no substitution in the case of **39f** (entry 7) which provides the lowest diastereomeric ratio of 1.5:1. All the substrates that have branched R groups provide complete diastereocontrol. While the cause of the importance of branching at the R position is unknown, it is clear that the sterics of the side chain controls diastereoselection.

Table 1-11 Substrate Scope for the Diastereoselective Henry Cyclization Cascade



entry	product	R	yield (%) ^b	d.r.
1	39a	Ph	78	>20:1
2	39b	4-Cl-C ₆ H ₄	69	20:1
3	39c	2-theinyl	94	20:1
4	39d	2-furyl	54	20:1
5	39e	(<i>E</i>)-styryl	64	3:1
6	39f	H	70	1.5:1
7	39g	<i>n</i> -pentyl	58	5:1
8	39h	<i>i</i> Pr	56	>20:1
9	39i	<i>t</i> Bu	59	>20:1

^aReagents: Enolsilane **22a-i** (1 equiv.), NaOH (1.2 equiv), conducted [**22**]₀ = 0.01 M in (1:1) MeOH:CH₂Cl₂. ^bIsolated Yield. See section 1.6 for additional experimental details.

1.4.6. Attempts at Aza-Henry Cyclization Variant

Based on the success of the Henry cyclization cascade, an aza-Henry variant was envisioned which would give rise to aminocyclopentanes as illustrated in Figure 1-17.

The requisite α -keto ester **38** can be obtained via a mild silyl enol ether deprotection as demonstrated earlier in the Henry cyclization experiments. Once formed, imine formation would provide the α -imino ester **40** which would undergo an aza-Henry reaction with the nitronate to provide **41**. If successful, these aminocyclopentanes could find utility as building blocks to various oroidin alkaloids which are known for their highly challenging structures. Some illustrative examples of these natural products are depicted in Figure 1-18 with the core structure obtained via the aza-Henry cascade highlighted in blue. A more straight forward application of these aminocyclopentanes would be deprotection of the *tert*-butyl ester to provide α,α -disubstituted amino acid derivatives. Similar quaternary amino acid derivatives have received attention due to their medicinal importance and this three step route would provide a highly efficient synthesis of these compounds.³¹

Figure 1-17 Proposed Synthesis of α,α -Disubstituted Amino Acids

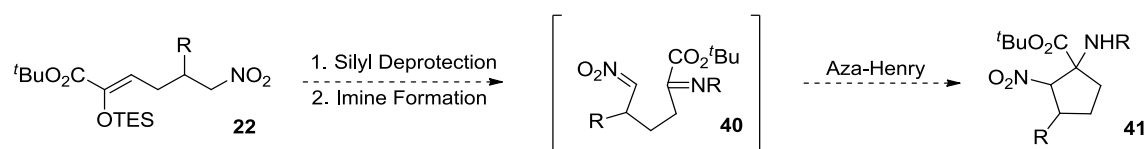
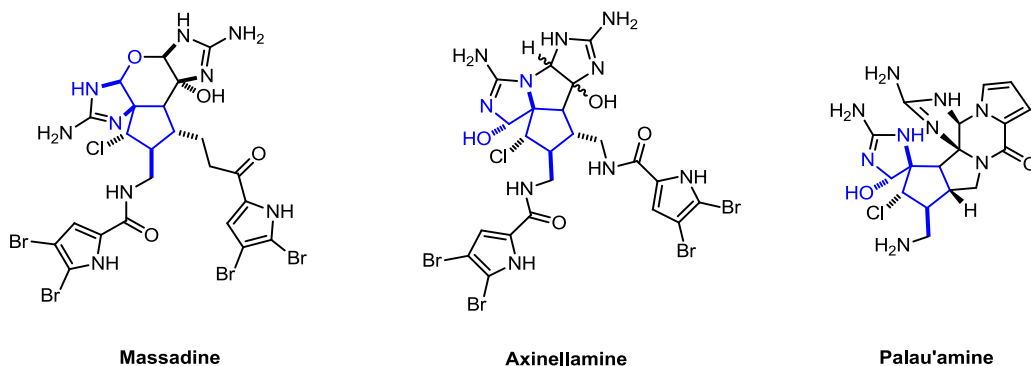


Figure 1-18. Oroidin Alkaloid Natural Products



Utilizing HF-pyridine as a mild silyl enol ether deprotection method, **38** was cleanly converted into the desired α -keto ester in a 92% yield. Various conditions were then investigated to access the desired imine formation/aza-Henry cyclization with instructive examples illustrated in Table 1-12. Treating the α -keto ester with benzylamine at ambient temperature (entry 1) provided the known Henry cyclization to **39a**. In this case, the basicity of benzylamine was sufficient to catalyze the Henry cyclization before the requisite imine was formed. Benzylamine was then substituted with aniline, a less basic amine. Employing aniline in an AcOH buffered solution to pH = 7, was successful in slowing the Henry reaction; however no imine formation was observed after 24 hrs (entry 2). To facilitate imine formation, the α -keto ester was treated with aniline in an AcOH buffered solution to pH = 7 in refluxing toluene. These conditions were too aggressive and only decomposition was observed after 2 hr.

Table 1-12. Attempted Aza-Henry Cyclization Conditions

entry	conditions	product
1	Benzylamine, THF, rt, 2 hrs	39a
2	Aniline, AcOH, THF, pH = 7, rt 24 hrs	Starting Material
3	Aniline, AcOH, refluxing toluene, 2 hrs	Decomposition

Based on these observations, the aza-Henry cyclization variant was deemed untenable due to the predominance of the base-catalyzed Henry cyclization. The standard Henry cyclization is too facile for the α -keto substrate to allow for imine formation in the

presence of an amine. Although buffering the solution did serve to halt the Henry cyclization, it was not sufficient to provide the desired imine formation.

1.5. Conclusion

A novel reactivity pattern for silyl glyoxylates, vinylmagnesium bromide, and nitroalkenes to provide for the regio- and stereoselective synthesis of (*Z*)-enolsilanes is disclosed. The reported three-component coupling provides good to very good yields for a variety of alkyl, alkenyl, aryl, and heteroaryl nitroalkenes while allowing for no variation on the nucleophilic partner. A likely mechanism for this methodology was deduced from the selectivity factors that governed reactivity. Furthermore, this methodology provides a rare example of a vinylogous Michael reaction arising from a simple metallodienolate precursor. The heretofore unreported nitroenolsilanes were utilized in a highly diastereoselective silyl deprotection/Henry cyclization cascade under basic methanol conditions. This cascade enabled the expeditious synthesis of nitrocyclopentanol with three contiguous stereocenters in two steps from readily available starting materials. All substrates possessing a branched R group provided complete diastereoselection.

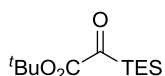
1.6 Experimental Details

Materials and Methods: General. Infrared (IR) spectra were obtained using a Nicolet 560-E.S.P. infrared spectrometer. Proton and carbon nuclear magnetic resonance spectra (^1H and ^{13}C NMR) were recorded on either a Bruker model Avance 500 (^1H at 500 MHz and ^{13}C NMR at 125 MHz), or a Bruker model Avance 400 (^1H NMR at 400 MHz and ^{13}C NMR at 100 MHz) spectrometer with solvent resonance as the internal standard (^1H NMR: CDCl_3 at 7.26 ppm; ^{13}C NMR: CDCl_3 at 77.0 ppm). ^1H NMR data are reported as

follows: chemical shift, multiplicity (s = singlet, br s = broad singlet, d = doublet, t = triplet, q = quartet, sept = septet, m = multiplet), coupling constants (Hz), and integration. Analytical thin layer chromatography (TLC) was performed on Whatman 0.25 mm silica gel 60 plates. Visualization was accomplished with UV light and aqueous ceric ammonium molybdate solution followed by heating. Purification of the reaction products was carried out by flash chromatography using Sorbent Technologies silica gel 60 (32-63 μm). All reactions were carried out under an atmosphere of nitrogen in oven-dried glassware with magnetic stirring. Yield refers to isolated yield of analytically pure material. Yields are reported for a specific experiment and as a result may differ slightly from those found in the tables, which are averages of at least two experiments. Dichloromethane, tetrahydrofuran, and toluene were dried by passage through a column of neutral alumina under nitrogen prior to use.^[32] Nitroalkenes **21a**, **21b**, **21d** are commercially available from Sigma-Aldrich. Nitroalkenes **21c**,^[33] **21g**,^[33] **21h**,^[33] **21e**,^[34] and **21f**^[35] were prepared according to literature procedures. Nitroalkene **21i** was prepared by substituting pivalaldehyde for isobutyraldehyde in the procedure for **21h**.

Synthesis of Triethylsilyl Glyoxylate

Triethylsilyl glyoxylate was obtained by modifying the published method for *tert*-butyldimethylsilyl glyoxylate by substituting TESOTf for TBSOTf in the silylation step.



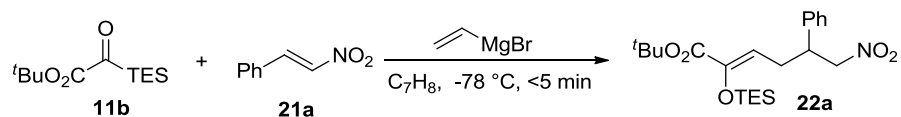
Triethylsilyl glyoxylate (11b): Analytical data for **11b**: **IR** (thin film, cm^{-1})

¹) 2958, 2913, 2878, 2359, 1713, 1661, 1460, 1370, 1289, 1159; ¹**H** NMR

(400 MHz, CDCl_3) δ 1.55 (s, 9H), 0.98 (t, J = 7.8 Hz, 9H), 0.85 – 0.79 (m, 6H); ¹³**C**

NMR (100 MHz, CDCl₃): δ 233.0, 162.5, 83.3, 27.9, 7.0, 2.3; **TLC** (5% Ether/petroleum ether) R_f = 0.50. **LRMS** (ESI) Calcd. for C₁₂H₂₄O₃SiNa 244.15, Found: 244.2.

Synthesis of Silyl Enol Ethers (22a-i)



Synthesis of Silyl Enol Ethers: General Procedure A: The triethylsilyl glyoxylate (1.5 equiv) and nitroalkene (1.0 equiv) were added to an oven-dried vial. The vial was then purged with N₂ and toluene (0.1 M) was added. The resulting solution was cooled to -78 °C using an acetone/dry ice bath and vinylmagnesium bromide (1.5 equiv) was added dropwise to the solution. Once the addition was complete the reaction was allowed to warm to room temperature, diluted with ethyl acetate (5 mL), and quenched with saturated ammonium chloride (5 mL). The resulting mixture was stirred for 10 min. The layers were separated, and the aqueous layer was extracted with ethyl acetate (3 X 5 mL). The organic extracts were combined, washed with brine (5 mL), dried with magnesium sulfate, and concentrated *in vacuo*. The crude mixture was purified by flash chromatography with 2.5% EtOAc/hexanes yielding the desired product.

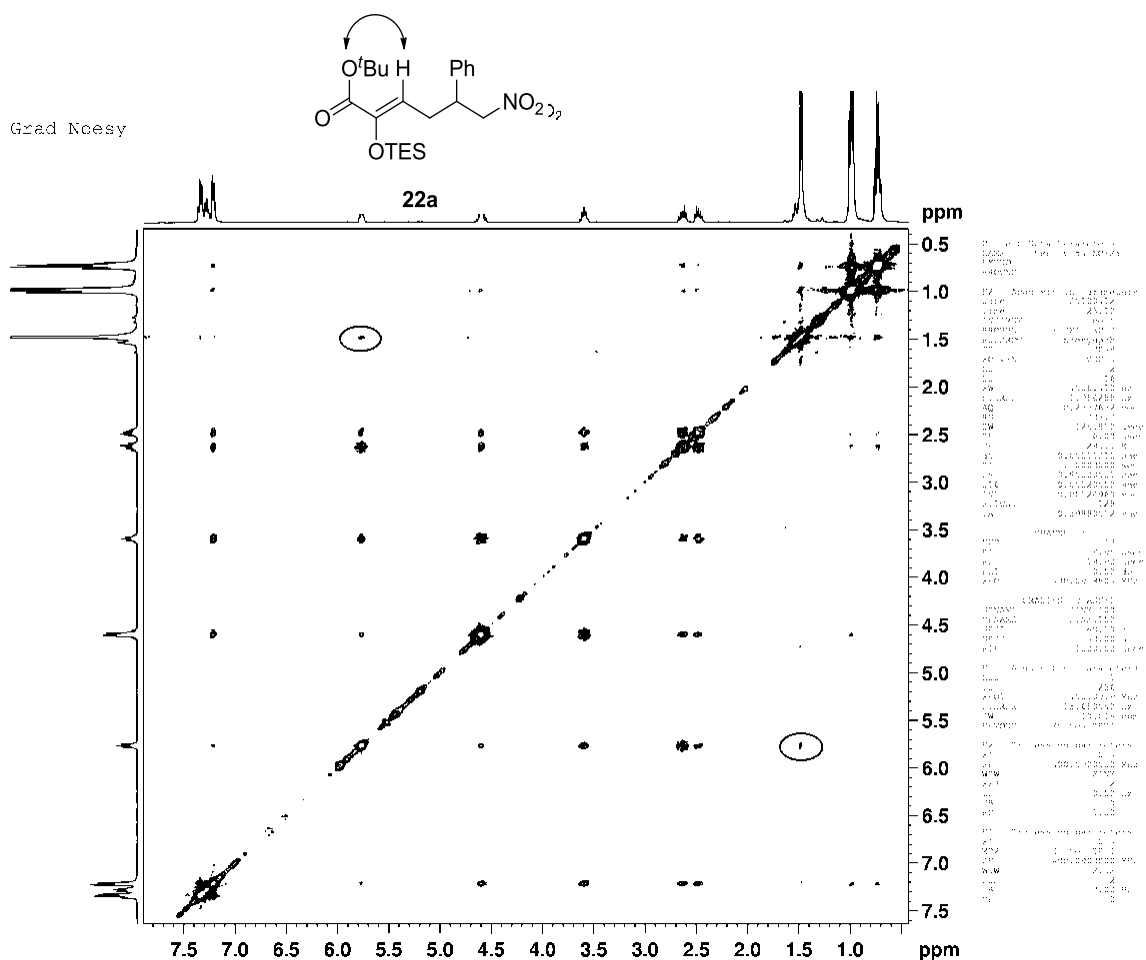
Synthesis of Silyl Enol Ethers: General Procedure B: For certain nitroalkenes that are insoluble in toluene at -78 °C, a mixture of the silyl glyoxylate (1.5 equiv) and the nitroalkene (1.0 equiv) were dissolved in toluene and added dropwise to a solution of vinylmagnesium bromide and toluene at -78°C. Once the addition was complete the reaction was allowed to warm to room temperature, diluted with ethyl acetate (5 mL), and

quenched with saturated ammonium chloride (5 mL). The resulting mixture was stirred for 10 minutes. The layers were separated, and the aqueous layer was extracted with ethyl acetate (3 X 5 mL). The organic extracts were combined, washed with brine (5 mL), dried with magnesium sulfate, and concentrated *in vacuo*. The crude mixture was purified by flash chromatography with 2.5% EtOAc/hexanes yielding the desired product.

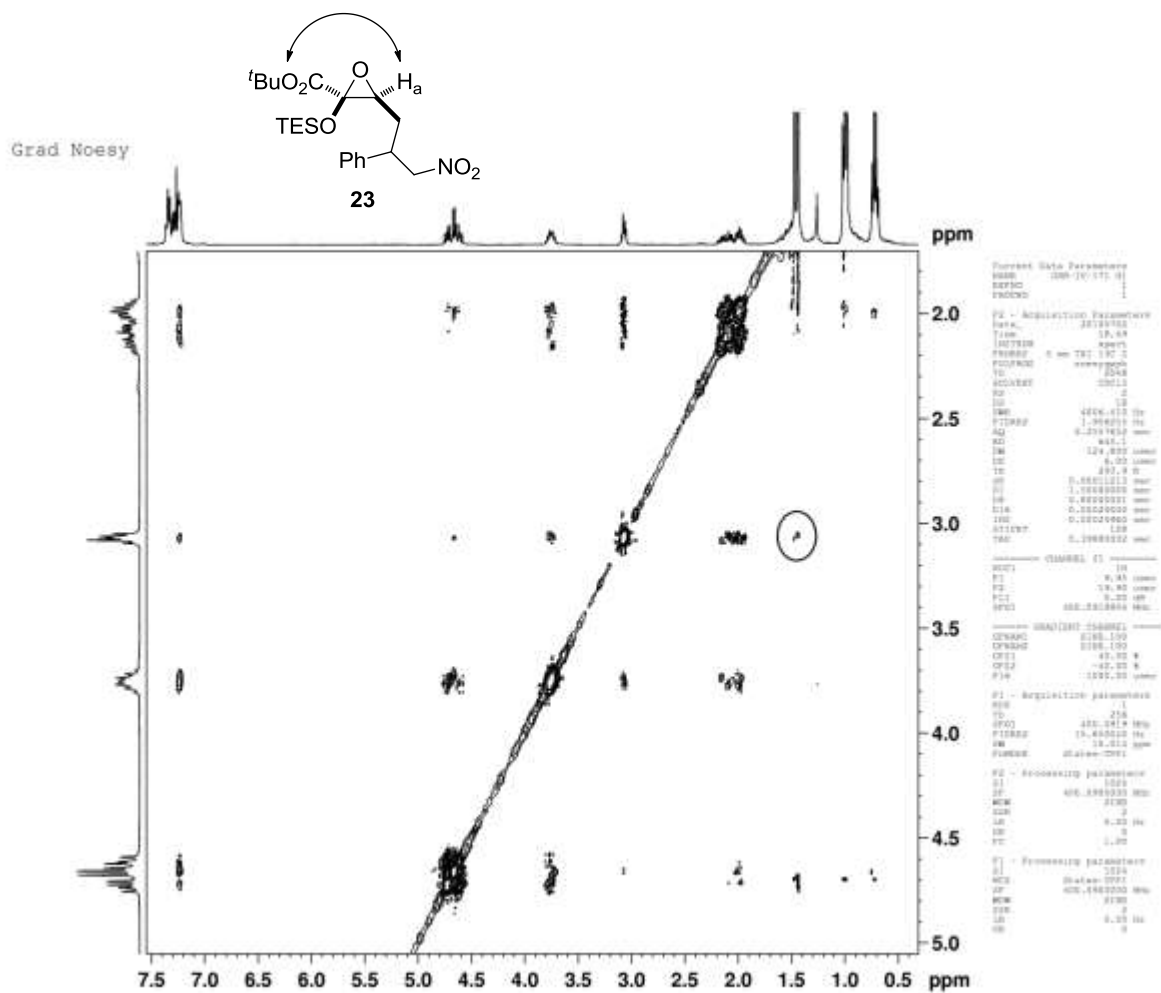
Synthesis of Silyl Enol Ethers: General Procedure C: For certain substrates that were difficult to separate from the silylglyoxylate oligomers byproduct, the reagent ratios were altered to limit the formation of offending byproduct. The triethylsilyl glyoxylate (1 equiv) and nitroalkene (1.5 equiv) were added to an oven-dried vial. The vial was then purged with N₂ and toluene (0.1 M) was added. The resulting solution was cooled to -78 °C using an acetone/dry ice bath and vinylmagnesium bromide (1.5 equiv) was added dropwise to the solution. Once the addition was complete the reaction was allowed to warm to room temperature, diluted with ethyl acetate (5 mL), and quenched with saturated ammonium chloride (5 mL). The resulting mixture was stirred for 10 minutes. The layers were separated, and the aqueous layer was extracted with ethyl acetate (3 X 5 mL). The organic extracts were combined, washed with brine (5 mL), dried with magnesium sulfate, and concentrated *in vacuo*. The crude mixture was purified by flash chromatography with 2.5% EtOAc/hexanes yielding the desired product.

Structural Assignment for the (Z)-Silyl Enol Ethers based on NOESY Analysis:

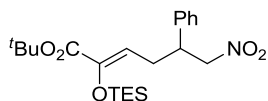
The stereochemistry of the silyl enol ethers was assigned based on the observed nOe between the vinyl proton at C3 and the C1 *tert*-butyl ester which establishes the two substituents as *cis* (see circled nOe below). The lack of any nOe between the C3 vinyl proton and the C2 triethylsilyl ether corroborates the (Z)-geometry assignment.



The stereochemical assignment was further corroborated by the observed nOe between H_a at C3 and the C1 *tert*-butyl ester of the silyloxyepoxide derivative (**23**). The lack of any nOe between the triethylsilyl group and H_a confirms the (*Z*)-geometry assignment.

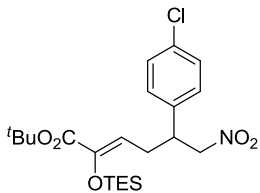


Analytical Data for the Silyl Enol Ethers (22a-i)



(Z)-tert-butyl 6-nitro-5-phenyl-2-((triethylsilyl)oxy)hex-2-enoate (22a): The title compound was prepared according to

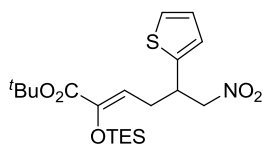
General Procedure A using **11b** (0.123 g, 0.503 mmol, 1.5 equiv), vinylmagnesium bromide (1 M, .500 mL, .500 mmol, 1.5 equiv) and β -nitrostyrene (0.050 g, 0.335 mmol, 1 equiv). After addition of the vinylmagnesium bromide, the reaction was warmed to room temperature and quenched. Purification by flash chromatography (2.5% EtOAc/hexanes) yielded 102 mg (72%) of the product as a yellow oil. Analytical data for **22a**: **IR** (thin film, cm^{-1}): 3054, 2986, 1715, 1555, 1421, 1370, 1265, 740; **^1H NMR** (400 MHz, CDCl_3): δ 7.36-7.21 (m, 5H), 5.77 (t, $J = 6.8$ Hz, 1H), 4.63-4.56 (m, 1H), 3.64-3.58 (m, 1H), 2.68-2.60 (m, 1H), 2.52-2.45 (m, 1H), 1.48 (s, 9H), 0.99 (t, $J = 7.6$ Hz, 9H), 0.73 (q, $J = 7.6$ Hz, 6H); **^{13}C NMR** (100 MHz, CDCl_3): δ 163.4, 144.0, 139.4, 128.94, 127.7, 127.3, 115.5, 81.4, 79.9, 43.7, 29.7, 28.0, 6.8, 5.6; **TLC** (20% EtOAc/hexanes) R_f 0.64. **LRMS** (ESI) Calcd. for $\text{C}_{22}\text{H}_{35}\text{NO}_5\text{SiNa}$: 444.22. Found: 444.2.



(Z)-tert-butyl 5-(4-chlorophenyl)-6-nitro-2-((triethylsilyl)oxy)hex-2-enoate (22b): The title compound was prepared according to General Procedure A using **11b** (0.140 g,

0.572 mmol, 1.5 equiv), vinylmagnesium bromide (1 M, 0.580, 0.580 mmol, 1.5 equiv)

and (*E*)-1-chloro-4-(2-nitrovinyl)benzene (0.070 g, 0.381 mmol, 1 equiv). After addition of the vinylmagnesium bromide, the reaction was warmed to room temperature and quenched. Purification by flash chromatography (2.5% EtOAc/hexanes) yielded 122 mg (70%) of the product as a colorless oil. Analytical data for **22b**: **IR** (thin film, cm^{-1}): 2957, 2914, 2877, 1716, 1645, 1556, 1494, 1458, 1370, 1288, 1255, 1141, 1094, 1014, 826; **^1H NMR** (400 MHz, CDCl_3) δ 7.30 (d, J = 8.4 Hz, 2H), 7.14 (d, J = 8.4 Hz, 2H), 5.78 (dd, J = 8.0, 7.2 Hz, 1H), 4.62-4.50 (m, 2H), 3.60 (m, 1H), 2.62-2.54 (m, 2H), 1.47 (s, 9H), 0.97 (t, J = 8.0 Hz, 9H), 0.71 (q, J = 8.0 Hz, 6H); **^{13}C NMR** (100 MHz, CDCl_3): δ 163.3, 144.2, 137.9, 133.6, 129.2, 129.1, 128.6, 114.8, 81.5, 79.7, 43.1, 29.6, 28.0, 6.7, 5.6; **TLC** (20% EtOAc/hexanes) R_f 0.62. **LRMS** (ESI) Calcd. for $\text{C}_{22}\text{H}_{34}\text{ClNO}_5\text{SiNa}$: 478.18. Found: 478.2.



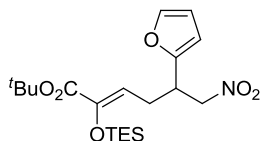
(*Z*)-*tert*-butyl

6-nitro-5-(thiophen-2-yl)-2-

((triethylsilyl)oxy)hex-2-enoate (**22c**): The title compound was

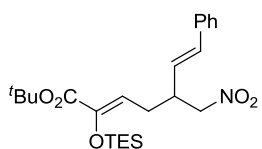
prepared according to General Procedure A using **11b** (0.177 g, 0.725 mmol, 1.5 equiv), vinylmagnesium bromide (1 M, .730, 0.730 mmol, 1.5 equiv) and (*E*)-2-(2-nitrovinyl)thiophene (0.075 g, -0.483 mmol, 1 equiv). After addition of the vinylmagnesium bromide, the reaction was warmed to room temperature and quenched. Purification by flash chromatography (2.5% EtOAc/hexanes) yielded 132 mg (65%) of the product as a yellow oil. Analytical data for **22c**: **IR** (thin film, cm^{-1}): 2956, 2912, 2877, 1715, 1645, 1556, 1456, 1369, 1286, 1249, 1143, 1007, 850; **^1H NMR** (400 MHz, CDCl_3) δ 7.22 (dd, J = 0.8, 4.8 Hz, 1H), 6.95 (dd, J = 5.2, 3.6 Hz, 1H), 6.89 (d, J = 3.6 Hz, 1H), 5.81 (dd, 8.4, 6.8 Hz, 1H), 4.61 (dd, J = 12.8, 6.4 Hz, 1H), 4.53 (dd, J = 12.4,

8.8 Hz, 1H), 3.95-3.91 (m, 1H), 2.67-2.51 (m, 2H), 1.48 (s, 9H), 0.98 (t, $J = 7.6$ Hz, 9H), 0.72 (q, $J = 7.6$ Hz, 6H); ^{13}C NMR (100 MHz, CDCl_3): δ 163.3, 144.3, 142.4, 126.9, 125.1, 124.5, 114.7, 81.4, 80.3, 39.0, 30.6, 28.0, 6.7, 5.6; **TLC** (20% EtOAc/hexanes) R_f 0.63. **LRMS** (ESI) Calcd. for $\text{C}_{20}\text{H}_{33}\text{NO}_5\text{SSiNa}$: 450.17. Found: 450.2.



(Z)-tert-butyl 5-(furan-2-yl)-6-nitro-2-((triethylsilyl)oxy)hex-2-enoate (22d): The title compound was prepared according to

General Procedure B using **11b** (0.198 g, 0.809 mmol, 1.5 equiv), vinylmagnesium bromide (1 M, 0.810 mL, 0.810 mmol, 1.5 equiv) and (*E*)-2-(2-nitrovinyl)furan (0.075 g, 0.539 mmol, 1 equiv). After addition of the vinylmagnesium bromide, the reaction was warmed to room temperature and quenched. Purification by flash chromatography (2.5% EtOAc/hexanes) yielded 142 mg (64%) of the product as a yellow oil. Analytical data for **22d**: **IR** (thin film, cm^{-1}): 2957, 2913, 2877, 2360, 1717, 1646, 1557, 1506, 1458, 1372, 1286, 1247, 1167, 1143, 1012, 915, 850, 806; ^1H NMR (400 MHz, CDCl_3) δ 7.35 (d, $J = 0.4$ Hz, 1H), 6.30 (s, 1H), 6.15 (d, $J = 3.2$ Hz, 1H), 5.78 (t, $J = 7.6$ Hz, 1H), 4.63 (dd, $J = 12.8, 8.4$ Hz, 1H), 4.53 (dd, $J = 12.8, 6.0$ Hz, 1H), 3.77-3.69 (m, 1H), 2.57 (t, $J = 7.2$ Hz, 1H), 1.48 (s, 9H), 0.97 (t, $J = 8.0$ Hz, 9H), 0.72 (q, $J = 8.0$ Hz, 6H); ^{13}C NMR (100 MHz, CDCl_3): δ 163.3, 152.4, 144.2, 142.2, 114.8, 110.3, 106.9, 81.4, 77.6, 37.3, 28.0, 27.3, 6.7, 5.6; **TLC** (20% EtOAc/hexanes) R_f 0.56. **LRMS** (ESI) Calcd. for $\text{C}_{20}\text{H}_{33}\text{NO}_5\text{SiNa}$: 434.20. Found: 434.3.



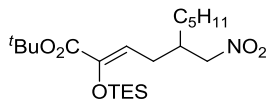
(Z)-tert-butyl 5-(4-chlorophenyl)-6-nitro-2-((triethylsilyl)oxy)hex-2-enoate (22e): The title compound was

prepared according to General Procedure A using **11b** (0.146 g, 0.599 mmol, 1.5 equiv), vinylmagnesium bromide (1 M, 0.600 mL, 0.600 mmol, 1.5 equiv) and ((1*E*, 3*E*)-4-nitrobuta-1,3-dien-1-yl)benzene (0.070 g, 0.400 mmol, 1 equiv). After addition of the vinylmagnesium bromide, the reaction was warmed to room temperature and quenched. Purification by flash chromatography (2.5% EtOAc/hexanes) yielded 118 mg (66%) of the product as a pale yellow oil. Analytical data for **22e**: **IR** (thin film, cm⁻¹): 2957, 2912, 2877, 1716, 1645, 1556, 1455, 1370, 1288, 1255, 1141, 1007, 966, 849; **¹H NMR** (400 MHz, CDCl₃) δ 7.33-7.20 (m, 5H), 6.50 (d, *J* = 16, 1H), 5.99 (dd, *J* = 15.6, 8.8 Hz, 1H), 5.84 (t, *J* = 7.6 Hz, 1H), 4.45 (dd, *J* = 12.0, 6.0 Hz, 1H), 4.45 (dd, *J* = 12.0, 9.2 Hz, 1H), 3.20-3.15 (m, 1H), 2.42-2.33 (m, 2H), 1.47 (s, 9H), 0.96 (t, *J* = 7.6 Hz, 9H), 0.71 (q, *J* = 7.6 Hz, 6H); **¹³C NMR** (100 MHz, CDCl₃): δ 163.4, 144.2, 136.5, 133.3, 128.5, 127.8, 127.8, 127.4, 115.1, 81.5, 79.3, 41.6, 28.0, 6.8, 5.6; **TLC** (20% EtOAc/hexanes) *R_f* 0.65. **LRMS** (ESI) Calcd. for C₂₄H₃₇NO₅SiNa: 470.23. Found: 470.3.



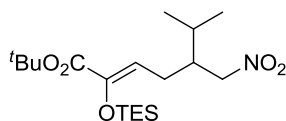
The title compound was prepared according to General Procedure C using **11b** (0.150 g, 0.614 mmol, 1 equiv), vinylmagnesium bromide (1 M, 0.680 mL, 0.680 mmol, 1.1 equiv) and nitroethylene (0.176 g, 1.23 mmol, 2 equiv). After addition of the vinylmagnesium bromide, the reaction was warmed to room temperature and quenched. The yield of the crude product (58%) was determined using ¹H NMR by comparing to an internal standard of mesitylene. **22f** was found to be unstable to flash chromatography due to deprotection of the silyl enol ether and subsequent transformations however the analytically pure product can isolated by flash chromatography (2.5% EtOAc/hexanes)

16mg (31%) of the product as a yellow oil. In general, a short silica plug provides material that is sufficiently pure to employ in subsequent reactions. Separation from byproducts after the Henry cyclization is trivial and is the preferred method. Analytical data for **8f**: **IR** (thin film, cm^{-1}): 2957, 2913, 2878, 1716, 1645, 1556, 1370, 1141; **^1H NMR** (400 MHz, CDCl_3) δ 5.81 (t, $J = 7.2$ Hz, 1H), 4.37 (t, $J = 7.2$ Hz, 2H), 2.25 (q, $J = 7.2$ Hz, 2H), 2.11 (p, $J = 7.2$, 2H), 1.49 (s, 9H), 0.96 (t, $J = 8.0$ Hz, 9H), 0.70 (q, $J = 8.0$ Hz, 6H); **^{13}C NMR** (100 MHz, CDCl_3): δ 163.6, 143.7, 117.2, 81.4, 75.0, 28.1, 26.5, 22.3, 6.7, 5.6; **TLC** (20% EtOAc/hexanes) R_f 0.75. **LRMS** (ESI) Calcd. for $\text{C}_{16}\text{H}_{31}\text{NO}_5\text{SiNa}$: 368.19. Found: 368.2.



(Z)-tert-butyl 5-(nitromethyl)-2-((triethylsilyl)oxy)dec-2-enoate (22g): The title compound was prepared according to

General Procedure C using **11b** (0.150 g, 0.614 mmol, 1 equiv), vinylmagnesium bromide (1 M, 0.680 mL, 0.680 mmol, 1.1 equiv) and (*E*)-1-nitrohept-1-ene (0.176 g, 1.23 mmol, 2 equiv). After addition of the vinylmagnesium bromide, the reaction was warmed to room temperature and quenched. Purification by flash chromatography (2.5% EtOAc/hexanes) yielded 148 mg (58%) of the product as a colorless oil. Analytical data for **22g**: **IR** (thin film, cm^{-1}): 2957, 2876, 1715, 1555, 1369, 1145, 1007, 739; **^1H NMR** (400 MHz, CDCl_3): δ 5.82 (t, $J = 7.6$ Hz, 1H), 4.34-4.24 (m, 2H), 2.36-2.15 (m, 3H), 1.49 (s, 9H), 1.35-1.28 (m, 8H), 0.96 (t, $J = 7.6$ Hz, 9H), 0.88 (t, $J = 7.2$ Hz, 3H), 0.71 (q, $J = 7.6$ Hz, 6H); **^{13}C NMR** (100 MHz, CDCl_3): δ 163.5, 144.0, 115.8, 81.3, 79.3, 37.4, 31.7, 31.5, 28.0, 27.4, 25.9, 22.4, 13.9, 6.7, 5.6; **TLC** (20% EtOAc/hexanes) R_f 0.57. **LRMS** (ESI) Calcd. for $\text{C}_{21}\text{H}_{41}\text{NO}_5\text{SiNa}$: 438.27. Found: 438.3.

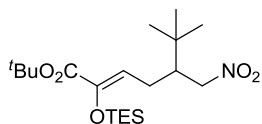


(*Z*)-*tert*-butyl

6-methyl-5-(nitromethyl)-2-

((triethylsilyl)oxy)hept-2-enoate(**22h**):

The title compound was prepared according to General Procedure C using **11b** (0.150 g, 0.614 mmol, 1 equiv), vinylmagnesium bromide (1 M, 0.680 mL, 0.680 mmol, 1.1 equiv) and (*E*)-3-methyl-1-nitrobut-1-ene (0.142 g, 1.23 mmol, 2 equiv). After addition of the vinylmagnesium bromide, the reaction was warmed to room temperature and quenched. The yield of the crude product (53%) was determined using ^1H NMR by comparing to an internal standard of mesitylene. Purification by flash chromatography (2.5% EtOAc/hexanes) yielded 93 mg (39%) of the product as a colorless oil. In general, a short silica plug provides material that is sufficiently pure to employ in subsequent reactions. Separation from byproducts after the Henry cyclization is trivial and is the preferred method. Analytical data for **22h**: **IR** (thin film, cm^{-1}): 2960, 2912, 2877, 1715, 1644, 1555, 1458, 1370, 1253, 1145, 1006, 739; ^1H NMR (400 MHz, CDCl_3): δ 5.81 (t, $J = 7.2$ Hz, 1H), 4.34 (dd, $J = 12.4, 7.2$ Hz, 1H), 4.25 (dd, $J = 12.4, 6.4$ Hz, 1H), 2.27-2.10 (m, 1H), 1.81-1.77 (m, 1H), 1.49 (s, 9H), 0.98-0.92 (m, 15H), 0.71 (q, $J = 7.6$ Hz, 6H); ^{13}C NMR (100 MHz, CDCl_3): δ 163.5, 144.0, 116.6, 81.4, 77.4, 43.1, 28.6, 28.1, 24.4, 19.1, 18.4, 6.7, 6.6, 5.6; **TLC** (20% EtOAc/hexanes) R_f 0.56. **LRMS** (ESI) Calcd. for $\text{C}_{19}\text{H}_{37}\text{NO}_5\text{SiNa}$: 410.23. Found: 410.2.



(*Z*)-*tert*-butyl

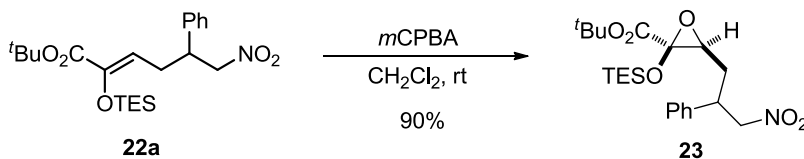
6,6-dimethyl-5-(nitromethyl)-2-

((triethylsilyl)oxy)hept-2-enoate(**22i**):

The title compound was prepared according to General Procedure C using **11b** (0.200 g, 0.818 mmol, 1 equiv

vinylmagnesium bromide (1 M, 0.900 mL, 0.900 mmol, 1.1 equiv) and (*E*)-3,3-dimethyl-1-nitrobut-1-ene (0.236 g, 1.64 mmol, 2 equiv). After addition of the vinylmagnesium bromide, the reaction was warmed to room temperature and quenched. The yield of the crude product (36%) was determined using ^1H NMR by comparing to an internal standard of mesitylene. Purification by flash chromatography (2.5% EtOAc/hexanes) yielded 19 mg (24%) of the product as a colorless oil. In general, a short silica plug provides material that is sufficiently pure to employ in subsequent reactions. Separation from byproducts after the Henry cyclization is trivial and is the preferred method. Analytical data for **22i**: **IR** (thin film, cm^{-1}): 2959, 2878, 1716, 1369, 1332, 1141; ^1H **NMR** (400 MHz, CDCl_3): δ 5.84 (dd, $J = 8.0, 5.6$ Hz, 1H), 4.42 (dd, $J = 13.6, 5.6$ Hz, 1H), 4.15 (dd, $J = 13.6, 5.6$ Hz, 1H), 2.34-2.12 (m, 3H), 1.49 (s, 9H), 0.99-0.93 (m, 18H), 0.72 (q, $J = 7.6$ Hz, 6H); ^{13}C **NMR** (100 MHz, CDCl_3): δ 163.5, 143.6, 117.6, 81.3, 46.9, 33.4, 28.1, 28.0, 27.3, 25.0, 6.75, 5.6; **TLC** (20% EtOAc/hexanes) R_f 0.73. **LRMS** (ESI) Calcd. for $\text{C}_{20}\text{H}_{39}\text{NO}_5\text{SiNa}$: 424.25. Found: 424.3.

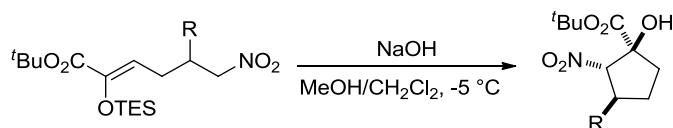
Preparation of *tert*-butyl 3-(3-nitro-2-phenylpropyl)-2-((triethylsilyl)oxy)oxiranes-2-carboxylate (23**):**



A 20-mL scintillation vial was charged with **22a** (163 mg, 0.387 mmol, 1.0 equiv), *m*CPBA (130 mg, 0.580 mmol, 1.5 equiv) and CH_2Cl_2 (4 mL, 0.1 M) and stirred for 3 h. Once the reaction was complete the solution was diluted with CH_2Cl_2 (5 mL) and quenched with sodium thiosulfate (10 mL) and stirred for 30 minutes. The layers were

separated and the aqueous layer was extracted with methylene chloride (3 x 5 mL). The combined organic extracts were washed with sodium bicarbonate (10 mL), brine (5 mL), dried with sodium sulfate, and concentrated *in vacuo* to provide 143 mg (85%) of the product as a colorless oil. Analytical data for **23**: IR (thin film, cm^{-1}): 2957, 2878, 2360, 2341, 1740, 1556, 1332, 1155; *mixture of diastereomers*: ^1H NMR (400 MHz, CDCl_3): δ 7.35-7.21 (m, 5H), 4.72-4.60 (m, 2H), 3.79-3.71 (m, 1H), 3.07-3.04 (m, 1H), 2.19-1.92 (m, 2H), 1.46 (s, 9H), 1.42 (s, 9H), 1.00-0.97 (m, 9H), 0.71 (q, $J = 6.4$ Hz, 6H); ^{13}C NMR (100 MHz, CDCl_3): δ 166.9, 166.9, 138.8, 138.4, 129.0, 129.0, 127.9, 127.8, 127.4, 127.3, 82.9, 82.8, 80.1, 79.6, 79.4, 60.8, 60.2, 41.9, 41.2, 31.1, 30.6, 27.7, 27.7, 6.5, 5.2; TLC (20% EtOAc/hexanes) R_f 0.46. LRMS (ESI) Calcd. for $\text{C}_{22}\text{H}_{35}\text{NO}_6\text{SiNa}$: 460.59. Found: 460.2.

Synthesis of Nitrocyclopentanols: General Procedure D (39a-i)



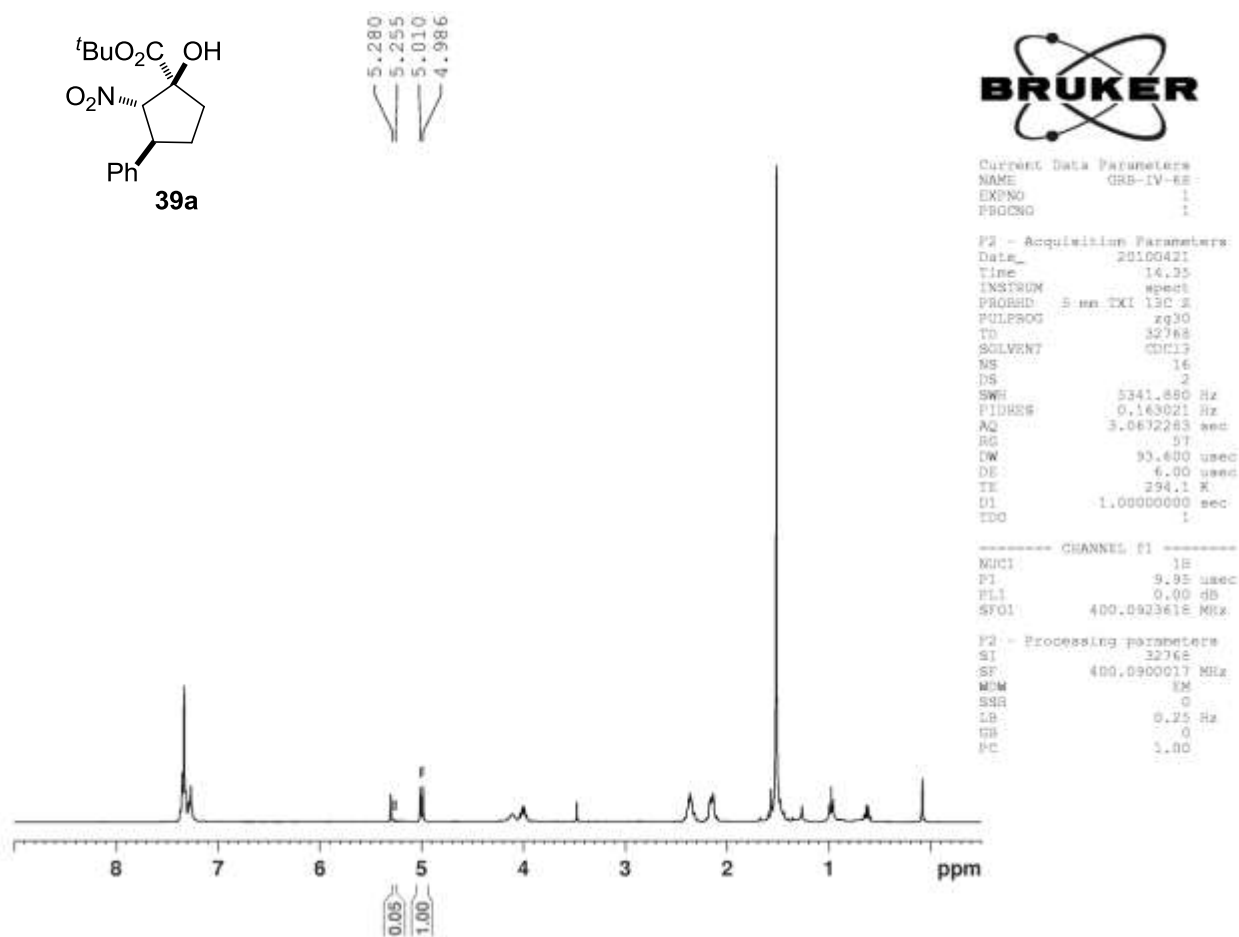
The silyl enol ether was dissolved in 1:1 mixture of methanol (0.1 M) and methylene chloride (0.1 M). The resulting solution was cooled in an ice/brine bath to -5°C . Sodium hydroxide (1.2 equiv) was added at once and the resulting solution was stirred at -5°C till the reaction was judged complete by TLC analysis. Once the reaction was complete the solution was diluted with methylene chloride (5 mL) and quenched with saturated ammonium chloride (5 mL). The resulting solution was stirred for 5 minutes. The layers were separated and the aqueous layer was extracted with methylene chloride (3 x 5 mL). The combined organic extracts were washed with brine (5 mL), dried with sodium

sulfate, and concentrated *in vacuo*. The resulting cyclopentanol (**39a-i**) were purified by flash chromatography using the indicated solvent system.

General Information for the Structural Assignments from NOESY Spectra

Calculation of Diastereomeric Ratios:

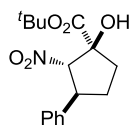
The diastereomeric ratios for the nitrocyclopentanol were calculated using the ratio of the α -nitro methine proton for each diastereomer. In the following example the diastereomeric ratio for the crude material obtained from the reaction with **22a** shows compound **39a** in a 20:1 d.r.:



General Method for the Structural Assignment of the Nitrocyclopentanol based on NOESY Analysis and X-ray Crystallography:

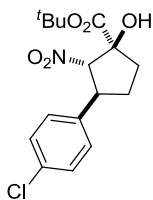
The identity of the major diastereomer **39a** was assigned as illustrated by the following NOESY spectrum. All other nitrocyclopentanol examples (**39b-i**) were assigned using the same rationale (see **XII** for analyzed spectra). The relative stereochemistry at C1-C2 was assigned based on an observed nOe between the C2 α -nitro methine proton and the C1 OH group (**A**) which establishes these two substituents as *cis*. A very weak nOe is observed between the α -nitro methine proton at C2 and the *tert*-butyl ester at C1 (**B**). The *trans* orientation assigned at C2-C3 is supported by the observed strong nOe between the C3 benzylic proton and the C1 *tert*-butyl ester (**C**). Hydrogen bonding between the ester carbonyl and the alcohol likely orients the *tert*-butyl group over the ring thus explaining the observed nOe. This nOe would not be observed if the C3 benzylic proton and the C1 OH group were *cis* as evidenced in the C1-C2 analysis. Moreover, the comparatively small nOe for the C3 phenyl substituent with the *tert*-butyl group (**D**) (similar in magnitude to interaction **B**) suggests that these substituents do not significantly interact with one another. Although there is a nOe between the benzylic proton at C3 and the α -nitro methylene proton at C2 (**E**), we have previously observed that a nOe between the vicinal protons on a 5-membered ring does not preclude the possibility of a *trans* orientation.^[6] This rationale in conjunction with the stronger nOe between the C3 phenyl group and the C2 α -nitro methine proton further supports the *trans* assignment.

Analytical Data for the Trisubstituted Nitrocyclopentanols (39a-i)



(±)-(1*S*, 2*S*, 3*S*)-*tert*-butyl 1-hydroxy-2-nitro-3-phenylcyclopentanecarboxylate (**39a**):

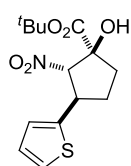
The title compound was prepared according to General Procedure D using **22a** (0.056 g, 0.133 mmol, 1 equiv) and NaOH (0.006 g, 0.159 mmol, 1.2 equiv). After stirring for 3 h, the reaction was complete as determined by TLC analysis. The reaction was worked up and purified by flash chromatography (10% EtOAc/hexanes) to afford 32 mg (78%) of the product as a white solid in >20:1 dr. Analytical data for **39a**: mp 60 °C; IR (thin film, cm⁻¹): 3479, 2979, 2933, 1731, 1552, 1371, 1154, 841; ¹H NMR (400 MHz, CDCl₃): δ 7.37-7.27 (m, 5H), 4.99 (d, *J* = 10.0 Hz, 1H), 4.07 (s, 1H), 4.03-3.96 (m, 1H), 2.39-2.31 (m, 2H), 2.17-2.10 (m, 2H), 1.51 (s, 9H); ¹³C NMR (100 MHz, CDCl₃): δ 171.1, 140.4, 128.9, 127.4, 127.3, 100.5, 84.9, 83.3, 48.2, 37.4, 31.1, 27.6; TLC (20% EtOAc/hexanes) R_f 0.38. LRMS (ESI) Calcd. for C₁₆H₂₁NO₅Na: 330.13. Found: 330.0.



(±)-(1*S*, 2*S*, 3*S*)-*tert*-butyl 3-(4-chlorophenyl)-1-hydroxy-2-nitrocyclopentanecarboxylate (**39b**):

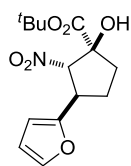
The title compound was prepared according to General Procedure D using **22b** (0.064 g, 0.140 mmol, 1 equiv) and NaOH (0.007 g, 0.168 mmol, 1.2 equiv). After stirring for 7 h, the reaction was complete as determined by TLC analysis. The reaction was worked up and purified by flash chromatography (10% EtOAc/hexanes) to afford 33 mg (69%) of the product as a white solid in 20:1 dr. Analytical data for **39b**: mp 92 °C; IR (thin film, cm⁻¹): 3480,

2954, 2925, 2360, 2341, 1731, 1552, 1154, 838; **¹H NMR** (400 MHz, CDCl₃): δ 7.31 (d, *J* = 8.4 Hz, 2H), 7.25 (d, *J* = 8.4 Hz, 2H), 4.99 (d, *J* = 10 Hz, 1H), 4.10 (s, 1H), 3.96 (dd, *J* = 17.6, 9.6 Hz, 1H), 2.39-2.28 (m, 2H), 2.16-2.06 (m, 2H), 1.49 (s, 9H); **¹³C NMR** (100 MHz, CDCl₃): δ 170.9, 138.8, 133.3, 129.0, 128.7, 100.3, 85.1, 83.2, 47.6, 37.4, 31.0, 27.6; **TLC** (20% EtOAc/hexanes) *R_f* 0.31. **LRMS** (ESI) Calcd. for C₁₆H₂₀NO₅Na: 364.09. Found: 364.10.



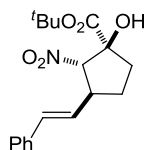
(±)-(1*S*, 2*S*, 3*R*)-*tert*-butyl 1-hydroxy-2-nitro-3-(thiophen-2-yl)cyclopentanecarboxylate (**39c**): The title compound was prepared according to General Procedure D using **22c** (0.045 g, 0.105 mmol, 1 equiv)

and NaOH (0.005 g, 0.126 mmol, 1.2 equiv). After stirring for 3 h, the reaction was complete as determined by TLC analysis. The reaction was worked up and purified by flash chromatography (10% EtOAc/hexanes) to afford 31 mg (94%) of the product as a colorless oil in 20:1 dr. Analytical data for **39c**: **IR** (thin film, cm⁻¹): 3480, 2977, 1730, 1554, 1371, 1154, 839; **¹H NMR** (400 MHz, CDCl₃): δ 7.20 (dd, *J* = 4.8, 1.2 Hz, 1H), 6.97-6.94 (m, 2H), 4.93 (d, *J* = 10.0 Hz, 1H), 4.29 (dd, *J* = 17.6, 9.6 Hz, 1H), 4.07 (s, 1H), 2.45-2.11 (m, 4H), 1.50 (s, 9H); **¹³C NMR** (100 MHz, CDCl₃): δ 170.9, 143.5, 127.0, 124.8, 124.2, 100.8, 85.1, 83.3, 43.2, 37.1, 31.3, 27.6, 0.98; **TLC** (20% EtOAc/hexanes) *R_f* 0.33. **LRMS** (ESI) Calcd. for C₁₄H₁₉NO₅SNa: 336.09. Found: 336.10.



(±)-(1*S*, 2*S*, 3*R*)-*tert*-butyl 3-(furan-2-yl)-1-hydroxy-2-nitrocyclopentanecarboxylate (**39d**): The title compound was prepared

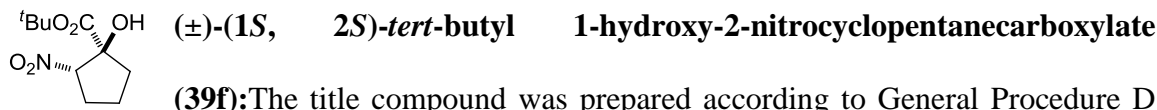
according to General Procedure D using **22d** (0.074 g, 0.180 mmol, 1 equiv) and NaOH (0.009 g, 0.216 mmol, 1.2 equiv). After stirring for 3 h, the reaction was complete as determined by TLC analysis. The reaction was worked up and purified by flash chromatography (10% EtOAc/hexanes) to afford 29 mg (54%) of the product as a white solid in 20:1 dr. Analytical data for **39d**: mp 80 °C; IR (thin film, cm⁻¹): 3481, 2978, 2928, 2360, 2341, 1730, 1552, 1371, 1154, 840; ¹H NMR (400 MHz, CDCl₃): δ 7.35-7.34 (m, 1H), 6.31 (dd, *J* = 5.0, 3.2 Hz, 1H), 6.18 (d, *J* = 3.2 Hz, 1H), 5.04 (d, *J* = 9.6 Hz, 1H), 4.15-4.07 (m, 1H), 4.00 (s, 1H), 2.34-2.10 (m, 4H), 1.50 (s, 9H); ¹³C NMR (125 MHz, CDCl₃): δ 171.1, 153.0, 141.9, 110.4, 106.3, 97.3, 85.0, 82.9, 41.2, 36.7, 27.59; TLC (20% EtOAc/hexanes) R_f 0.33. LRMS (ESI) Calcd. for C₁₄H₁₉NO₆Na: 320.11. Found: 320.1.



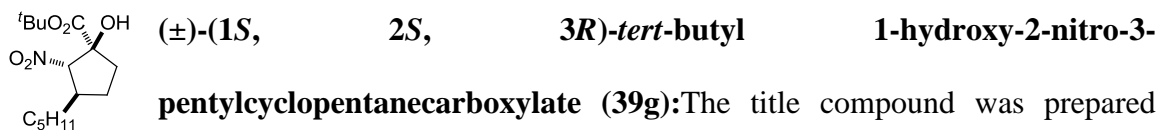
(±)-(1*S*, 2*S*, 3*S*)-*tert*-butyl 1-hydroxy-2-nitro-3-((*E*)-styryl)cyclopentanecarboxylate (**39e**): The title compound was prepared according to General Procedure D using **22e** (0.101 g, 0.226 mmol, 1 equiv)

and NaOH (0.011 g, 0.271 mmol, 1.2 equiv). After stirring for 12 h, the reaction was complete as determined by TLC analysis. The reaction was worked up and purified by flash chromatography (10% EtOAc/hexanes) to afford 48 mg (64%) of the product as a white solid in 20:1 dr. Analytical data for **39e**: mp 78 °C; IR (thin film, cm⁻¹): 3466, 2982, 2360, 1718, 1555, 1370, 1160, 1020; ¹H NMR (400 MHz, CDCl₃): δ 7.37-7.22 (m, 5H), 6.55 (d, *J* = 16 Hz, 1H), 6.17 (dd, *J* = 16, 8 Hz, 1H), 4.73 (d, *J* = 10.0 Hz, 1H), 4.03 (s, 1H), 3.62-3.58 (m, 1H), 2.32-2.19 (m, 2H), 2.08-1.92 (m, 2H), 1.50 (s, 9H); ¹³C NMR (125 MHz, CDCl₃): δ 171.3, 136.5, 132.3, 128.6, 128.4, 127.7, 126.3, 98.8, 84.9, 45.8,

36.8, 28.6, 27.6; **TLC** (20% EtOAc/hexanes) R_f 0.31. **LRMS** (ESI) Calcd. for $C_{18}H_{23}NO_5Na$: 356.15. Found: 356.2.

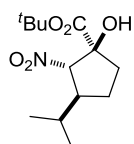


using **22f** (0.073 g, 0.211 mmol, 1 equiv) and NaOH (0.010 g, 0.285 mmol, 1.2 equiv). After stirring for 12 h, the reaction was complete as determined by TLC analysis. The reaction was worked up and purified by flash chromatography (15% EtOAc/hexanes) to afford 20 mg (41%) of the product as a white solid in 1.6:1 dr. Analytical data for **39f**: mp 67 °C; **IR** (thin film, cm^{-1}): 3482, 2979, 1730, 1551, 1154, 967, 841; *major diastereomer*: 1H NMR (400 MHz, $CDCl_3$): δ 4.83 (dd, $J = 16, 8$ Hz, 1H), 3.92 (s, 1H), 2.48-2.33 (m, 2H), 2.26-2.18 (m, 1H), 2.05-1.88 (m, 3H), 1.45 (s, 9H); ^{13}C NMR (125 MHz, $CDCl_3$): δ 171.6, 94.3, 84.5, 82.8, 37.4, 29.0, 27.6, 21.4; *minor diastereomer*: 1H NMR (400 MHz, $CDCl_3$): δ 5.08 (dd, $J = 9.2, 8.4$ Hz, 1H), 3.67 (s, 1H), 2.60-2.52 (m, 1H), 2.30-1.97 (m, 3H), 1.85-1.78 (m, 1H), 1.55 (s, 9H); ^{13}C NMR (125 MHz, $CDCl_3$): δ 172.4, 90.6, 84.1, 81.1, 37.2, 27.8, 26.3, 20.6; **TLC** (20% EtOAc/hexanes) R_f 0.33. **LRMS** (ESI) Calcd. for $C_{10}H_{17}NO_5Na$: 254.10. Found: 254.1.



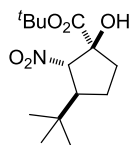
according to General Procedure D using **22g** (0.146 g, 0.351 mmol, 1 equiv) and NaOH (0.17 g, 0.422 mmol, 1.2 equiv). After stirring for 12 h, the reaction was complete as determined by TLC analysis. The reaction was worked up and purified by flash chromatography (10% EtOAc/hexanes) to afford 68 mg (64%) of the product as a

colorless oil in 5:1 dr. Analytical data for **39g**: **IR** (thin film, cm^{-1}): 3486, 2931, 1732, 1556, 1156, 843; **^1H NMR** (400 MHz, CDCl_3): δ 4.50 (d, $J = 9.2$ Hz, 1H), 3.91 (s, 1H), 2.79-2.73 (m, 1H), 2.21-2.10 (m, 2H), 1.97-1.91 (m, 1H), 1.73-1.65 (m, 1H), 1.46 (s, 9H), 1.38-1.29 (m, 8H), 0.88 (t, $J = 8$ Hz, 3H); **^{13}C NMR** (100 MHz, CDCl_3): δ 171.5, 99.5, 84.5, 83.3, 42.4, 36.5, 34.1, 31.7, 27.9, 27.6, 22.5, 13.9; **TLC** (20% EtOAc/hexanes) R_f 0.32. **LRMS** (ESI) Calcd. for $\text{C}_{15}\text{H}_{27}\text{NO}_5\text{Na}$: 324.18. Found: 324.2.



(±)-(1S, 2S, 3S)-*tert*-butyl 1-hydroxy-3-isopropyl-2-nitrocyclopentanecarboxylate (**39h**):

The title compound was prepared according to General Procedure D using **22h** (0.078 g, 0.201 mmol, 1 equiv) and NaOH (0.010 g, 0.242 mmol, 1.2 equiv). After stirring for 16 h, the reaction was complete as determined by TLC analysis. The reaction was worked up and purified by flash chromatography (10% EtOAc/hexanes) to afford 31 mg (56%) of the product as a white solid in >20:1 dr. Analytical data for **39h**: **IR** (thin film, cm^{-1}): 3481, 2964, 2875, 2360, 1726, 1553, 1371, 1157, 840; **^1H NMR** (400 MHz, CDCl_3): δ 4.64 (d, $J = 8.4$ Hz, 1H), 3.88 (s, 1H), 2.72-2.67 (m, 1H), 2.27-1.65 (m, 5H), 1.47 (s, 9H), 0.93 (d, $J = 6.8$ Hz, 6H); **^{13}C NMR** (100 MHz, CDCl_3): δ 171.2, 97.9, 84.6, 83.8, 48.6, 36.4, 30.8, 27.6, 25.2, 20.7, 18.8; **TLC** (20% EtOAc/hexanes) R_f 0.34. **LRMS** (ESI) Calcd. for $\text{C}_{13}\text{H}_{23}\text{NO}_5\text{Na}$: 296.15. Found: 296.0.

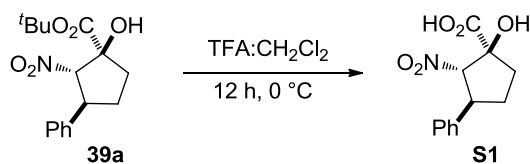


(±)-(1S, 2S, 3S)-*tert*-butyl 3-(*tert*-butyl)-1-hydroxy-2-nitrocyclopentanecarboxylate (**39i**):

The title compound was prepared according to General Procedure D using **22i** (0.028 g, 0.070 mmol, 1.0 equiv) and NaOH

(0.003 g, 0.084 mmol, 1.2 equiv). After stirring for 16 h, the reaction was complete as determined by TLC analysis. The reaction was worked up and purified by flash chromatography (10% EtOAc/hexanes) to afford 12 mg (59%) of the product as a white solid in >20:1 dr. Analytical data for **39i**: mp 68 °C; IR (thin film, cm⁻¹): 3473, 2965, 1719, 1555, 1370, 1155, 839; ¹H NMR (400 MHz, CDCl₃): δ 4.69 (d, *J* = 7.6 Hz, 1H), 3.83 (s, 1H), 2.88-2.82 (m, 1H), 2.22-1.72 (m, 4H), 1.47 (s, 9H), 0.91 (s, 9H); ¹³C NMR (100 MHz, CDCl₃): δ 170.8, 97.3, 84.6, 84.3, 52.6, 36.6, 32.4, 27.6, 27.2, 24.7; TLC (20% EtOAc/hexanes) R_f 0.37. LRMS (ESI) Calcd. for C₁₄H₂₅NO₅Na: 310.16. Found: 310.2.

Preparation of (±)-(1*S*, 2*S*, 3*S*)-1-hydroxy-2-nitro-3-phenylcyclopentanecarboxylic acid (S1**):**



A 20-mL scintillation vial was charged with **39a** (42.0 mg, 0.137 mmol, 1.0 equiv), trifluoroacetic acid (1 mL, 0.13 M) and CH₂Cl₂ (1 mL, 0.13 M) and stirred at 0 °C for 12 h. The crude mixture was then concentrated *in vacuo* and purified by flash chromatography (60% EtOAc/Hexanes) to afford 32 mg (93%) of the product as an off-white solid. The material was dissolved in pentane and allowed to slowly evaporate which provided a single crystal suitable for X-ray analysis. Analytical data for **S1**: IR (thin film, cm⁻¹): 3031, 1732, 1549, 1374, 1222, 699; ¹H NMR (400 MHz, CDCl₃): 7.36-7.26 (m, 5H), 5.09 (d, *J* = 10.0 Hz, 1H), 4.07 (q, *J* = 9.2 Hz, 1H), 2.55-2.43 (m, 2H), 2.28-2.14 (m, 2H); ¹³C NMR (125 MHz, CDCl₃): δ 176.8, 140.0 128.9, 127.5, 127.2,

100.2, 83.5, 47.9, 36.7, 30.7; **TLC** (100% EtOAc/hexanes) R_f 0.24 **LRMS** (ESI) Calcd. for $C_{12}H_{13}NO_5Na$: 274.07. Found: 274.05.

1.7 References

- [1] Seebach, D. *Angew. Chem. Int. Ed.* **1979**, *18*, 239-258.
- [2] Moser, W. H. *Tetrahedron*, **2001**, *57*, 2065-2084.
- [3] Brook, A. G. *Acc. Chem. Res.* **1981**, *14*, 77-84.
- [4] Linghu, X.; Nicewicz, D. A.; Johnson, J. S. *Org. Lett.* **2002**, *4*, 2957-2960.
- [5] Nicewicz, D. A.; Johnson, J. S. *J. Am. Chem. Soc.* **2005**, *127*, 6170-6171.
- [6] Nicewicz, D. A.; Brétéché, G.; Johnson, J. S. *Org. Synth.* **2008**, *85*, 278-286.
- [7] (a) Linghu, X.; Satterfield, A. D.; Johnson, J. S. *J. Am. Chem. Soc.* **2006**, *128*, 9302-9303. (b) Greszler, S. N.; Johnson, J. S. *Angew. Chem. Int. Ed.* **2009**, *48*, 3689-3691. (c) Schmitt, D. C.; Johnson, J. S. *Org. Lett.* **2010**, *12*, 944-947. (d) Yao, M.; Lu, C.-D. *Org. Lett.* **2011**, *13*, 2782-2785. (e) Greszler, S. N.; Malinowski, J. T.; Johnson, J. S. *J. Am. Chem. Soc.* **2010**, *132*, 17393-17395. (f) Nicewicz, D. A.; Satterfield, A. D.; Schmitt, D. C.; Johnson, J. S. *J. Am. Chem. Soc.* **2008**, *130*, 17281-17283.
- [8] Greszler, S. N.; Malinowski, J. T.; Johnson, J. S. *Org. Lett.* **2011**, *13*, 3206-3209.
- [9] Schmitt, D. C. Unpublished results.
- [10] Xue, D.; Chen, Y.-C.; Wang, Q.-W.; Cun, L.-F.; Zhu, J.; Deng, J.-D. *Org. Lett.* **2005**, *7*, 293-296.
- [11] Brown, S. P.; Goodwin, N. C.; MacMillan, D. W. C. *J. Am. Chem. Soc.* **2003**, *125*, 1192-1194.
- [12] Hitche, J.; Trost, B. M. *J. Am. Chem. Soc.* **2009**, *131*, 4572-4573.
- [13] Quintard, A.; Lefranc, A.; Alexakis, A. *Org. Lett.* **2011**, *13*, 1540-1543.
- [14] Terada, M.; Kenichi, A. *Org. Lett.* **2011**, *13*, 2026-2029.
- [15] (a) Rassu, G.; Appendino, G.; Casiraghi, G.; Zanardi, F. *Chem. Rev.* **2000**, *100*, 1929-1972. (b) Denmark, S. E.; Heemstra Jr., J. R.; Beutner, G. L. *Angew. Chem. Int. Ed.* **2005**, *44*, 4682-4698.

- [16] Sheperd, N. E.; Tanabe, H.; Xu, Y.; Matsunaga, S.; Shibasaki, M. *J. Am. Chem. Soc.* **2010**, *132*, 3666-3667.
- [17] (a) Huang, H.; Jin, Z.; Zhu, K.; Liang, X.; Ye, J. *Angew. Chem. Int. Ed.* **2011**, *50*, 3232- 3235. (b) Zhang, Y.; Shao, Y.-L.; Xu, H.-S.; Wang, W. *J. Org. Chem.* **2011**, *76*, 1472-1474.
- [18] Tanaka, K.; Takeda, K. *Tetrahedron Lett.* **2004**, *45*, 7859-7861.
- [19] Bencivenni, G.; Galzerano, P.; Mazzanti, A.; Bartoli, G.; Melchiorre, P. *PNAS* **2010**, *107*, 20642-20647.
- [20] Casiraghi, G.; Battistini, L.; Curti, C.; Rassu, G.; Zanardi, F. *Chem. Rev.* **2011**, *111*, 3076-3154.
- [21] Ono, N. *The Nitro Group in Organic Synthesis*, Wiley-VCH, Weinheim, **2001**.
- [22] Cuellar, R. D. Unpublished results
- [23] Ziegler, F. E.; Chakraborty, U. R.; Wester, R. T. *Tetrahedron Lett.* **1982**, *23*, 3237-3240.
- [24] (a) Kuwajima, I.; Kato, M. *J. Chem. Soc. Chem. Commun.* **1979**, 708-709. (b) Reich, H. J.; Olsen, R. E.; Clark, M. C. *J. Am. Chem. Soc.* **1980**, *102*, 1423-1424. (c) Kato, M.; Mori, A.; Oshino, H.; Enda, J., Kobayashi, K.; Kuwajima, I. *J. Am. Chem. Soc.* **1984**, *106*, 1773-1778. (d) Enda, J.; Kuwajima, I. *J. Am. Chem. Soc.* **1985**, *107*, 5495-5501. (e) Ahlbrecht, H.; Beyer, U. *Synthesis* **1999**, 365-390.
- [25] Luzzio, F. A. *Tetrahedron* **2001**, *57*, 915-945.
- [26] Buffat, M. G. P. *Tetrahedron* **2004**, *60*, 1701-1729.
- [27] Lloyd, D. H.; Nichols, D. E. *J. Org. Chem.* **1986**, *51*, 4294-4295.
- [28] Matsuda, Y.; Kitajima, M.; Takayama, H. *Org. Lett.* **2008**, *10*, 125-128.
- [29] Pohlhaus, P. D.; Bowman, R. K.; Johnson, J. S. *J. Am. Chem. Soc.* **2004**, *126*, 2294-2295.
- [30] CCDC 788056 contains the supplementary crystallographic data for this paper. These data can be obtained free of charge from The Cambridge Crystallographic Data Centre via www.ccdc.cam.ac.uk/data_request/cif.

- [31] For reviews see: (a) Jung, M. J. *Chemistry and Biochemistry of the Amino Acids*; Barrett, G. C., Ed.; Chapman and Hall: New York, 1985. (b) Williams, R. W. *Synthesis of Optically Active R-Amino Acids*; Pergamon: Oxford, 1989.
- [32] P. J. Alaimo, P. J.; Peters, D. W.; Arnold J.; Bergman R. G. *J. Chem. Ed.* **2001**, 78, 64.
- [33] Hitce, J.; Trost, B.M. *J. Am. Chem. Soc.* **2009**, 131, 4572-4573.
- [34] Dockendorff, C.; Sahli, S.; Olsen, M.; Milhau, L.; Lautens, M. *J. Am. Chem. Soc.* **2005**, 127, 15028-15029.
- [35] Y. Chi, Y.; Guo, L.; Kopf, N. A.; Gellman, S. H. *J. Am. Chem. Soc.* **2008**, 130, 5608-5609.

CHAPTER TWO

ACETYLIDE-INITIATED VINYLOGOUS MICHAEL CASCADE OF SILYL GLYOXYLATES AND ELABORATION TO CYCLOPENTANOL DERIVATIVES

2.1 Introduction

The efficient synthesis of densely functionalized cyclopentane derivatives remains a vital task in organic synthesis due to the ubiquity of this structure in Nature. Cyclopentitols, polyhydroxylated cyclopentanes, are of particular significance due to their presence in a variety of medicinally relevant natural products as well as current drug targets. Additionally, cyclopentenols are also highly relevant due to their incorporation in numerous biologically active targets and a variety of carbonucleosides. Although there are known processes for synthesizing various cyclopentanol derivatives, efficient methodologies that deliver functional group-rich cyclopentanols from simple starting materials would be welcome additions to the synthetic toolbox. In this chapter, a strategy for the diastereoselective synthesis of densely functionalized cyclopentane derivatives utilizing tetrasubstituted silyloxyallene starting materials is disclosed. These silyloxyallenes are prepared via a diastereoselective three-component coupling employing silyl glyoxylates, alkynyl nucleophiles and nitroalkenes via an acetylide-initiated Kuwajima-Reich rearrangement¹/vinylogous Michael cascade. The reported

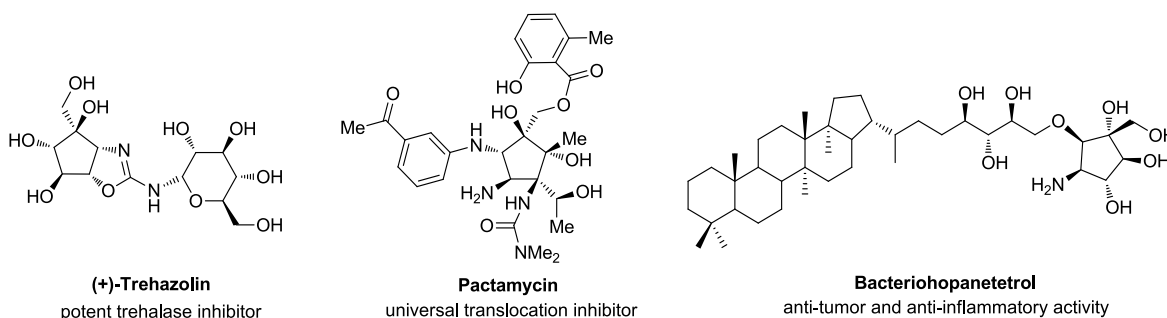
strategy provides a three-step synthesis of fully substituted cyclopentitols with moderate to excellent diastereoselectivity.

2.2 Background

2.2.1. Prevalence of Cyclopentitols in Nature

The cyclopentitol moiety is found in the core structure of numerous natural products of biological importance.² More specifically, aminocyclitols, a subset of this class of compounds, possess significant biological activity as antibiotics, anticancer therapeutics and glycoside inhibitors. Although cyclopentitol natural products are valuable from both a biological as well as synthetic organic standpoint, no widely applicable, succinct methodology exists for their construction. The dearth of general methodologies applicable to their synthesis is likely due to their densely functionalized structures. Figure 2-1 illustrates some representative examples from the aminocyclopentitol class of natural products along with their reported biological activity. Each example possesses a fully functionalized, stereodefined core structure which makes these natural products some of the most complex molecular scaffolds known for five membered rings.

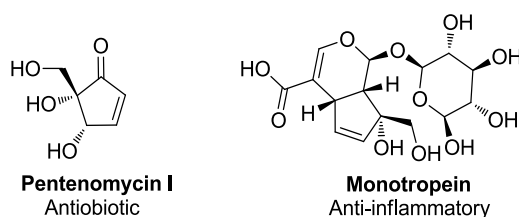
Figure 2-1. Representative Examples of Aminocyclopentitol Natural Products²



2.2.2. Prevalence of Cyclopentenols in Medicinally Relevant Molecules

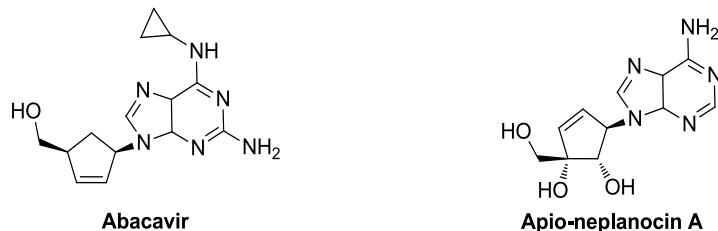
The cyclopentenol moiety is present in a vast array of biologically relevant natural products and synthetic drug targets. The biologically active natural products, pentenomycin I³ and monotropein⁴ illustrated in Figure 2.2 with their reported biological activity serve as representative examples of this structural moiety in natural products. Cyclopentenols also frequently serve as advanced intermediates in the synthesis of various cyclopentane based natural products due to the functional versatility imparted by the olefin.²

Figure 2-2. Representative Examples of Cyclopentenol Natural Products



Additionally, this structural unit is particularly prevalent in carbanucleosides, which are nucleoside analogs where the heteroatom of the core structure has been replaced by a methylene. Carbanucleosides have received significant attention due to their biological activities and potential as therapeutic agents. Additionally, carbocyclic nucleosides are usually chemically and enzymatically more stable than the corresponding natural nucleosides. Relevant examples of medicinally important carbanucleosides are illustrated in Figure 2.3 to highlight the structural motif. While interest in these compounds remains high, production of these nucleoside analogs frequently require step-intensive syntheses.²

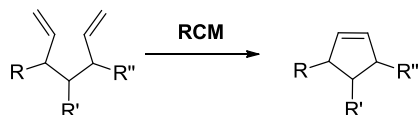
Figure 2-3. Representative Examples of Medicinally Relevant Carbanucleosides



2.2.3 Synthetic Approaches to Cyclopentanol Derivatives

Due to the medicinal relevance highlighted in Section 2.2.2, a variety of synthetic strategies have been utilized in the synthesis of densely functionalized cyclopentanol derivatives. In the synthesis of cyclopentenols, the olefin functionality has frequently been incorporated by implementing a ring-closing metathesis strategy employing the Schrock catalyst or various types of the Grubbs catalysts as illustrated in Figure 2-4. This strategy provides for a late stage, highly functional group tolerant cyclization of an acyclic precursor. Although ring-closing metathesis is recognized as one of the cornerstones of organic synthesis, several drawbacks to this method exist. Among these drawbacks are the multistep syntheses required to prepare the requisite acyclic diene and the high cost of the ruthenium catalyst.

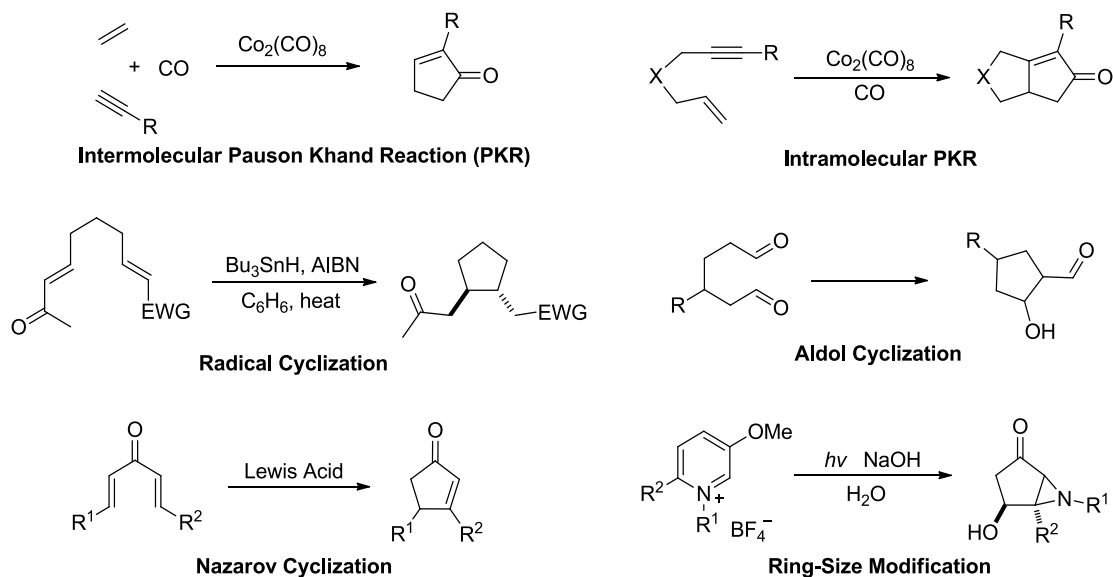
Figure 2-4. Ring-Closing Metathesis as a General Method for the Synthesis of Cyclopentenols



When ring-closing metathesis is determined to be untenable, a variety of alternative methodologies have been utilized in the synthesis of cyclopentanol

derivatives. These other methodologies include the Pauson-Khand reaction, various radical cyclizations, intramolecular aldol condensations, Nazarov cyclizations, photochemical reactions, and ring-size modification reactions.² Selected examples from these common strategies are presented in Figure 2-5.

Figure 2-5. Examples of Other Common Synthetic Routes to Cyclopentane Derivatives

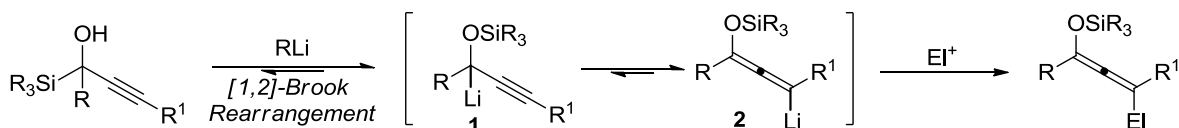


2.2.4. Kuwajima-Reich Rearrangement

Discovered independently by both researchers in 1980, the Kuwajima-Reich rearrangement has become the most common method for the synthesis of silyloxyallenes. The rearrangement occurs when α -hydroxypropargyl silanes undergo a [1,2]-Brook rearrangement in the presence of strong base and engage a secondary electrophile in a vinylogous fashion as illustrated in Figure 2-6. The isomerization to the allenyl anion **1** is favored due to the anion stabilizing effect of the higher s-character of the sp^2 orbital over the sp^3 -centered silyloxy propargyl anion **2**. This rearrangement has been shown to provide excellent γ -selectivity for a variety of electrophiles such as alkyl halides,

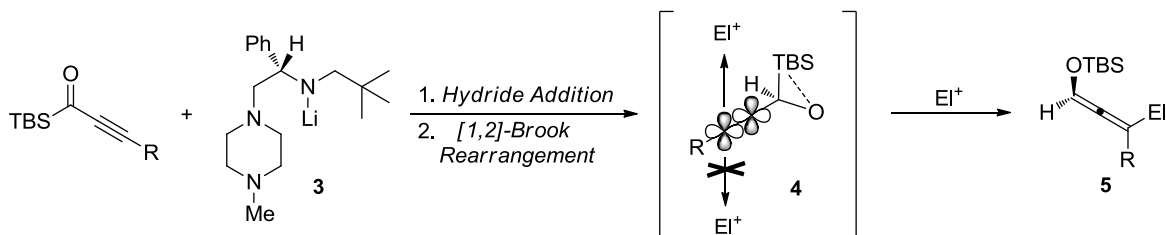
disulfides, H^+ , and DMF.¹ Most relevant to the present investigation is the precedent that 1-silyloxyallen-3-ylcopper reagents generated by lithiation and transmetalation of silyloxyallenes undergo conjugate additions with enones.⁵

Figure 2-6. The Kuwajima-Reich Rearrangement



Recently, the Takeda group disclosed the only example of an enantioselective Kuwajima-Reich rearrangement for the enantioselective synthesis of silyloxyallenes.⁶ This methodology was accomplished by employing an enantioselective Meerwein-Ponndorf-Verley-type reduction of acylsilanes by a chiral lithium amide **3** to provide the requisite α -silyl alkoxide **4** *in situ*. The α -silyl alkoxide can then undergo [1,2]-Brook rearrangement resulting in the transient secondary nucleophile, the allenyl anion, that can undergo a subsequent $\text{S}_{\text{E}}2'$ electrophilic substitution to provide optically active 1-unsubstituted silyloxyallenes **5** as illustrated in Scheme 2-1.

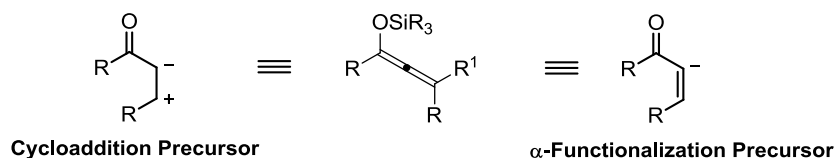
Scheme 2-1. Enantioselective Kuwajima-Reich Rearrangement



2.2.5. Utility of Silyloxyallenes

Although categorized as a subset class of allenes, silyloxyallenes have been recognized for possessing their own unique reactivity profile. Silyloxyallenes have found utility in various α -functionalizations including as α -acylvinyl anion equivalents with various electrophiles including carbonyls, α,β -unsaturated carbonyls and alkylidene malonates, and imines.⁷ Silyloxyallenes have been utilized in numerous cycloadditions including [3+2],^{7a,7b} [4+2],^{7c} [5+3]^{7d} which fully exploit the reactivity of the silyloxyallene moiety. Figure 2-7 summarizes the synthons represented by silyloxyallenes.

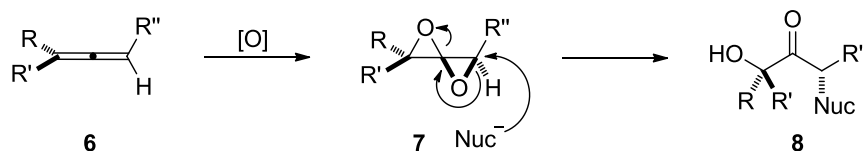
Figure 2-7. Utility of Silyloxallenes as Various Synthons



2.2.6. Spirodiepoxidation of Allenes

Dioxidation of allenes is a unique reactivity common to all types of allenes leading to spirodiepoxides. Although not frequently employed in organic chemistry, the reactivity of spirodiepoxides has been studied by Crandall⁸ and expounded upon by Lawrence in various total syntheses and new methodologies.⁹ The transformation of the allene **6** to the spirodiepoxide frequently employs dry DMDO in chloroform, as illustrated in Scheme 2-2. The less-substituted position of the spirodiepoxide **7** is susceptible to nucleophilic attack which provides α -hydroxyketone **8** after the nucleophile-induced ring opening. The potent electrophilicity of spirodiepoxides derives from the release of the highly strained structure.

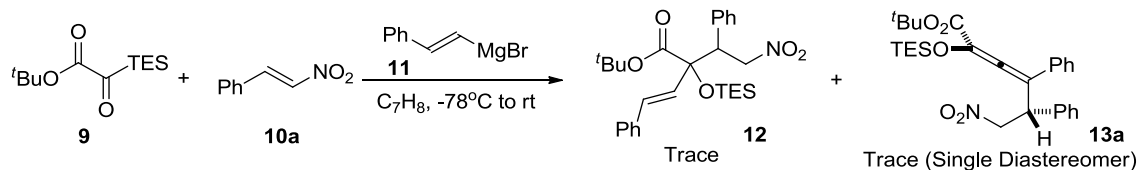
Scheme 2-2. Synthesis and Reactivity of Spirodiepoxides



2.2.7. Origin of the Title Reaction

The disclosed work arose from a byproduct obtained during studies on the attempted incorporation of β -substituted vinylmagnesium bromide reagents in the three-component coupling of silyl glyoxylate **9**, nitroalkene **10a** and vinylmagnesium bromide summarized in Chapter 1. When β -styrylmagnesium bromide **11** was exposed to the reaction parameters none of the desired vinylogous coupling product was observed. Instead, a trace amount of the α -addition product **12** was observed via NMR as well as an unexpected byproduct **13a** obtained as a single diastereomer as illustrated in Scheme 2-3.

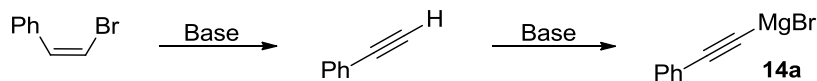
Scheme 2-3. Three-Component Coupling Leading to Silyloxyallene **13a**



The most likely explanation for the isolation of **13a** is a vinylogous Michael reaction arising from the addition of a phenyl acetylide nucleophile. Although unanticipated, the conditions to form the styryl nucleophile likely also produced the acetylide. β -Styrylmagnesium bromide was synthesized from β -bromostyrene and magnesium filings in THF reflux.¹⁰ The conditions for the Grignard formation provided the necessary requirements for the formation of the undesired byproduct, 1-

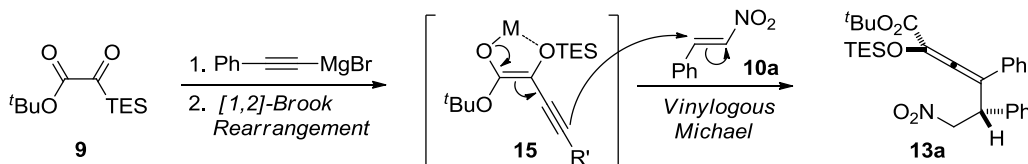
phenylethynylmagnesium bromide **14a**, by basic elimination of the bromine to form phenylacetylene followed by a subsequent deprotonation as illustrated in Figure 2-8.

Figure 2-8. Hypothesized Formation of the Unexpected Alkynyl Nucleophile



The phenylethynylmagnesium bromide could undergo nucleophilic attack on the silyl glyoxylate **9** providing glycolate enolate **15**, after Kuwajima-Reich rearrangement. The presumed transient secondary nucleophile **15** could then engage the β -nitrostyrene **10a** secondary electrophile through the π -system in a vinylogous fashion providing the silyloxyallene **13a** as the product of the three-component coupling as illustrated in Figure 2-9.

Figure 2-9. Proposed Mechanism for the Formation of the Silyloxyallene **13a**

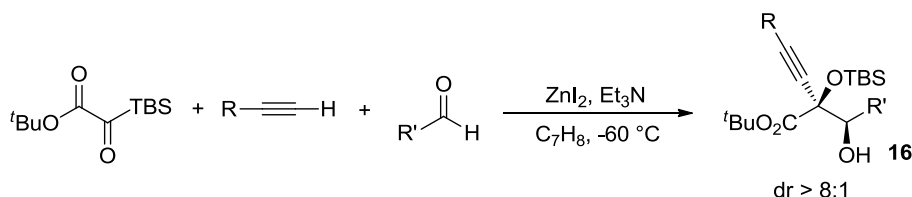


Intentionally employing phenylethynylmagnesium bromide (2 equiv) in the reaction conditions with silyl glyoxylate (1 equiv) and β -nitrostyrene (1.5 equiv) provided the same silyloxyallene product in a 60% yield as one diastereomer. This result supports the hypothesis that the silyloxyallene **13a** that was unintentionally formed in the β -styrylmagnesium bromide trial was the result of the phenylethynylmagnesium bromide byproduct engaging the silyl glyoxylate in a novel three-component coupling.

2.2.8. Comparison to Precedented Silyl Glyoxylate Coupling with Acetylide Nucleophiles

The coupling of silyl glyoxylates and acetylide nucleophiles is known when the secondary electrophile is an aldehyde as depicted in Scheme 2-4.¹¹ In the reported aldehyde coupling, however, the glycolate enolate intermediate similar to **15** provided α -addition aldol products **16** instead of undergoing a vinylogous pathway via the Kuwajima-Reich rearrangement. The heretofore unknown coupling of silyl glyoxylates, acetylides, and nitroalkenes diverges from this previously observed reactivity to provide solely the γ -addition product. This observation further corroborates the hypothesis that the dominant selectivity (α vs. γ) in silyl glyoxylate chemistry is strongly related to the type of electrophile employed.^{11,12}

Scheme 2-4. Precedented Silyl Glyoxylate Three-Component Coupling with Acetylide Nucleophiles



2.3. Results and Discussion

2.3.1. Optimization of Reaction Parameters

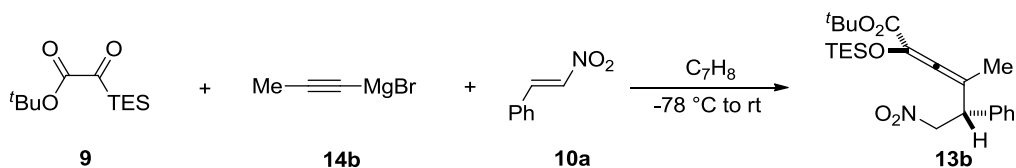
Due to the procedural similarity between the (*Z*)-enol silane three-component coupling and the developing silyloxyallene three-component coupling as well as the overall success of the first example discussed in Section 2.2.7., the optimized conditions strongly resembled that of the preceding methodology. Attempting the three-component

coupling at a higher temperature resulted in significant decomposition, and cooling the reaction to -100 °C had no beneficial effect in comparison to the -78°C trial. Solvent variation also had little effect on the efficiency of the reaction; except for some adverse effects in the solubility of the nitroalkene substrates. Similar to aldehyde-terminated three-component coupling,¹¹ the acetylide acted as a highly discriminant nucleophile chemoselectively attacking the silyl glyoxylate over the secondary electrophile. This high level of selectivity enabled the incorporation of both electrophilic reagents (silyl glyoxylate and nitroalkene) in the reaction flask concurrently. This was a fortuitous result since addition of the acetylide to the silyl glyoxylate without the nitroalkene being present, leads to extensive silyl glyoxylate oligomerization.

Since the major byproduct for this coupling methodology was silyl glyoxylate oligomerization, the equivalence of the reagents was adjusted to compensate for this competing pathway as seen in Table 2-1. Adjusting the equivalence of the acetylide **14b** had little effect on the yield, however adding a 50% excess of silyl glyoxylate significantly improved the yield of **13b** from 50% to 83%.

The axial chirality of the allene of the silyloxyallene **13b** could not be determined using NMR analysis and although **13b** was isolated as a solid, the product was not of sufficient quality for x-ray diffraction. In the hopes that the larger silyl group would allow for a more crystalline product, the coupling was attempted with the TIPS silyl glyoxylate **S1**. Using the same reaction conditions, the TIPS silyl glyoxylate **S1** provided the desired three-component coupling product as the TIPS silyloxyallene **S2** (see Section 2.7 for more details) in a 30% yield as a crystalline solid. Gratifyingly, a sample suitable for x-ray diffraction was obtained by slow evaporation of the **S2** in EtOAc.

Table 2-1. Stoichiometry Screen for the Acetylide-Initiated Cascade

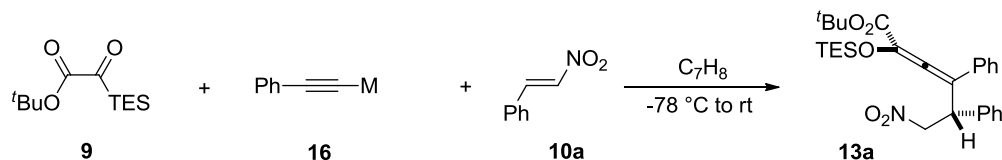


entry	9 (equiv)	14b (equiv)	10a (equiv)	yield ^b
1	1	1.3	1.5	50%
2	1	2	1.5	52%
3	1.3	2	1	61%
4	1.5	1	1	83%

^aAll reactions were conducted [**10a**]₀ = 0.1 M with the reaction warmed to room temperature immediately after the addition was complete. ^bIsolated Yield.

Since varying the cation can impact the rate of the [1,2]-Brook rearrangement,¹³ the metal counterion of the nucleophile was screened as shown in Table 2-2. Phenylethynyllithium **16a** and phenylethynylzinc **16b** reagents were subjected to the reaction conditions; however neither nucleophile was competent in this coupling. The lithium reagent provided trace γ -adduct with silyl glyoxylate oligomerization being the major product and the organozinc reagent interestingly provided trace α -adduct as the sole coupling product with the rest of the crude mixture being silyl glyoxylate oligomerization.

Table 2-2. Nucleophile Variation



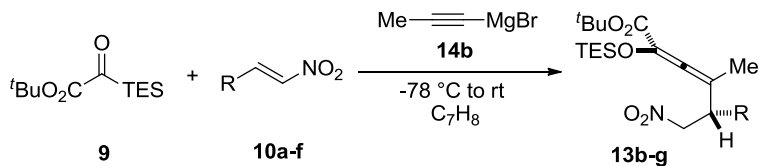
entry	M	product
1	16a Li	Trace γ -adduct
2	16b ZnX ₂	Trace α -adduct

^aAll reactions were conducted [**10a**]₀ = 0.1 M with the reaction warmed to room temperature immediately after the addition was complete. ^bYields determined by ¹H NMR spectroscopy.

2.3.2. Reaction Scope

With the optimized conditions in hand for the acetylide-initiated Kuwajima-Reich cascade, the scope of the amenable nucleophilic and electrophilic partners was investigated. Using commercially available 1-propynylmagnesium bromide as the nucleophilic partner, the versatility of the nitroalkene was examined. The results presented in Table 2-3 demonstrate that various alkyl aryl and heteroaryl nitroalkenes were all well tolerated by the reaction conditions. The aryl (entry 1) and heteroaryl (entries 2 and 3) nitroalkenes performed best with yields ranging from 67-83% while the alkyl (entries 4 and 5) nitroalkenes provided satisfactory yields ranging from 42-56%. Unlike the vinylation-initiated silyl glyoxylate cascade reported in Chapter 1, 3,3-dimethyl-1-nitrobut-1-ene (entry 6) provided only trace product. This is likely due to the diminished nucleophilic character of glycolate enolate **15** deriving from the greater s-character of the species when compared to the vinylmagnesium bromide derived glycolate enolate. The less active nucleophile is likely more sensitive to the steric bulk of the *t*-butyl moiety.

Table 2-3. Nitroalkene Substrate Scope for the Three-Component Coupling

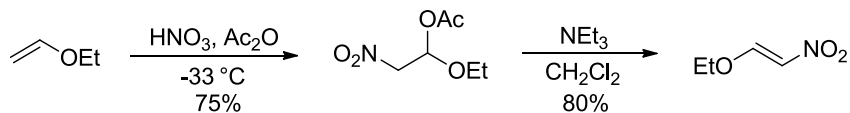


entry	product	R	yield (%)	d.r.
1	13b	Ph	83	>20:1
2	13c	2-thienyl	77	>20:1
3	13d	2-furyl	67	>20:1
4	13e	C ₅ H ₁₁	42	>20:1
5	13f	<i>i</i> -Pr	56	>20:1
6	13g	<i>t</i> -Bu	Trace	N.D.

^aAll reactions were conducted $[\text{X}]_0 = 0.01 \text{ M}$ with the reaction warmed to room temperature immediately after the addition was complete. ^bIsolated Yield. See section 2.7 for additional experimental details.

Incorporation of heteroatom substitution on the nitroalkene was of particular interest due to the value such compounds would have in secondary transformations (see section 2.5) by potentially providing fully oxidized cyclopentane rings in three steps from silyl glyoxylates. The requisite 2-nitrovinyl ether electrophile was synthesized in a 60% overall yield as illustrated in Scheme 2-5.¹⁴ This heteroatom containing nitroalkene was then used as the secondary electrophile partner in the three-component coupling under a variety of conditions summarized in Table 2-4. Ethynylmagnesium bromide **14j** was used as the nucleophile since the silyloxyallene arising from this three-component coupling would provide the core structure of trehazolin (illustrated in Figure 2.2.1) if successfully employed in a Henry cyclization cascade (see Section 2.5).

Scheme 2-5. Synthesis of 2-Nitrovinyl Ether

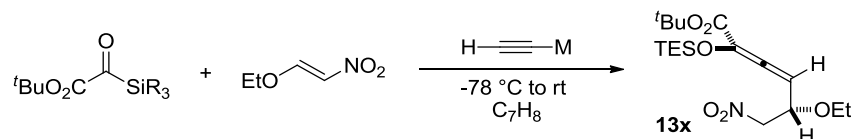


The attempts to incorporate the correct substitution parameters to access the core structure of trehazolin were regrettably unsuccessful with the most instructive entries provided in Table 2-4. At $-78\text{ }^\circ\text{C}$, the oligomerization of silyl glyoxylate was the predominant pathway for the concurrent addition of the silyl glyoxylate **9** and 2-nitrovinyl ether to the acetylide nucleophile (entry 1) resulting in no desired product. The sequential addition of silyl glyoxylate followed by 2-nitrovinyl ether to the acetylide nucleophile (entry 2) provided the desired product, but in an unusable yield of less than 10%. The isoelectronic alkynylzinc reagent was employed (entry 3), in the hopes of slowing the [1,2]-Brook rearrangement by varying the nucleophile's cation to halt the oligomerization pathway. This approach was also unsuccessful; providing no benefit over the magnesium cation.

Another potential solution to the silyl glyoxylate oligomerization pathway would be to slow the [1,2]-Brook rearrangement by altering the temperature. Running the reaction at $-100\text{ }^\circ\text{C}$ (entry 4) also provided no desired product and a mixture of unidentified byproducts. Previous studies¹⁵ have noted that the kinetics of the [1,2]-Brook rearrangement are related to the size of the migrating silyl group (with larger silyl groups migrating more slowly). To exploit this trend, the TIPS substituted silyl glyoxylate (entry 5, 6, 7) was utilized under for the same reaction conditions employed for the TES silyl glyoxylate. Although this variation did provide the highest yield to date at 14% (entry 7) of the desired product as one diastereomer by ^1H NMR analysis, it remains too inefficient

to be synthetically useful. With no clear alternatives available to attain the desired heteroatom functionalization for this specific coupling, the coupling with 2-nitrovinyl ether was abandoned and the versatility of the acetylide nucleophile was investigated.

Table 2-4. Screen of Conditions to Accommodate 2-Nitrovinyl Ether as the Secondary Electrophile.



entry	SiR ₃	M	temp	Type of Addition	yield (%) ^b
1	TES	MgBr	-78 °C	Concurrent	NDP
2	TES	MgBr	-78 °C	Sequential	<10%
3	TES	ZnBr	-78 °C	Concurrent	<10%
4	TES	MgBr	-100 °C	Concurrent	NDP
5	TIPS	MgBr	-78 °C	Sequential	NDP
6	TIPS	MgBr	-78 °C	Concurrent	Trace Pdt
7	TIPS	MgBr	-100 °C	Sequential	14%

^aAll reactions were conducted [9]₀ = 0.01 M with the reaction warmed to room temperature immediately after the addition was complete. ^bYields determined by ¹H NMR spectroscopy versus an internal standard of mesitylene. See section 2.7 for additional experimental details.

Utilizing β-nitrostyrene as the generic secondary electrophile, the versatility of the acetylide nucleophile was investigated with the results summarized in Table 2-5. Aryl (entry 1), alkenyl (entry 2), and alkyl (entry 3) substituted acetylides provided yields ranging from 71-77%. The isopropenyl derivative (entry 2) opens this methodology to being effective [4+2] cycloaddition precursor as illustrated by Takeda and coworkers by the application of similar vinylsilyloxyallenes in such reactions.⁶ The unsubstituted acetylide (entry 4) provided a low yield (18%) by NMR analysis. The main product for this entry was silyl glyoxylate oligomerization, which implies that the lack of steric bulk

facilitates oligomerization. To augment the utility of this coupling, a variety of heteroatom containing acetylide nucleophiles were screened to achieve a more expansive functional group tolerance.

Table 2-5. Acetylide Substrate Scope for the Three-Component Coupling

entry	product	R'	yield (%)	d.r.
1	13a	Ph	77 ^b	>20:1
2	13h	<i>i</i> -propenyl	76 ^b	>20:1
3	13i	C ₅ H ₁₁	71 ^b	>20:1
4	13j	H	18% ^c	>20:1
5	13k	TMS	39 ^b	>20:1
6	13l	-CH ₂ NMe ₂	0% ^c	N/A
7	13m	CO ₂ Et	0% ^c	N/A

^aAll reactions were conducted [**9**]₀ = 0.01 M with the reaction warmed to room temperature immediately after the addition was complete. ^bIsolated Yield. ^cYields determined by ¹H NMR spectroscopy versus and internal standard of mesitylene. See section 2.7 for additional experimental details.

The incorporation of a silyl group on the acetylide would provide considerable functional group diversity to the coupling through protodesilylation¹⁶ and well as the Tamao Fleming oxidation.¹⁷ Trimethylsilylethynylmagnesium bromide (entry 5) was exposed to the three-component coupling conditions and provided a 39% yield as a single diastereomer. This mediocre yield is likely a function of the added steric bulk of the trimethylsilyl group blocking the reactive site of the *in situ* generated (*Z*)-glycolate enolate. The direct incorporation of oxygen and nitrogen containing acetylides was then attempted. Employing 3-dimethylamino-1-propynylmagnesium bromide (entry 6) as the

nucleophile resulted in no desired product. In this case, the *in situ* (Z)-glycolate enolate eliminated the amine substituent as a leaving group providing the 1,1-unsubstituted silyloxycumulene instead of engaging the nitroalkene secondary electrophile. The Grignard reagent of ethyl propiolate (entry 7) was also subjected to the reaction conditions, however no desired product was observed. In this entry, the anionic character of the diester intermediate is likely too delocalized to function as a competent secondary nucleophile.

With the scope of this three-component coupling being extensively studied, our focus shifted to understanding the high levels of selectivity observed in the reaction. Specifically, since no explanation for the complete diastereoselectivity (20:1) observed for all substrates was apparent, we initiated a collaboration with Dr. Shubin Liu, a computational chemist, to investigate the transition state of the three-component coupling.

2.4. Computational Studies

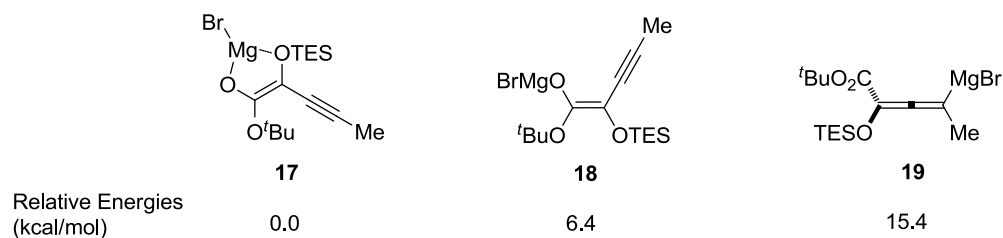
To gain a better understanding of the exquisite level of diastereo- and regioselectivity observed in this three-component coupling, the hypothesized mechanism was investigated through a quantum mechanical evaluation of the intermediates and transition states using the density functional theory (DFT) approach at the level of B3LYP/6-311G(d).¹⁸ Although the causative agent of the observed selectivity was not readily apparent, we hypothesized that the coordination of the nitroalkene to the magnesium cation of the (Z)-glycolate enolate during the transition state likely played a role in selectivity. We also felt such an investigation would be a fruitful endeavor because the vinylogous Michael reaction has rarely been studied computationally.¹⁹

2.4.1. Thermodynamics of the Secondary Nucleophile

The computational studies commenced with an analysis of the thermodynamic stability of the three possible isomers of the transient secondary nucleophile that arises from the addition of the acetylide nucleophile to the silyl glyoxylate. Upon completion of the [1,2]-Brook rearrangement, the three possible anionic species are the (*Z*)-glycolate enolate **17**, the (*E*)-glycolate enolate **18**, and the allenyl anionic species **19**. Although previous studies have demonstrated that the (*Z*)-glycolate enolate is the kinetic product of the [1,2]-Brook rearrangement of silyl glyoxylates due to FMO constraints,²⁰ geometric isomerization is possible in certain cases.²¹ With this in mind, a study of the thermodynamic stabilities of the intermediates appeared warranted.

Calculations performed by collaborator Dr. Shubin Liu provided the relative energies for the potential identities of the secondary nucleophiles summarized in Figure 2-10. The calculations found that the (*Z*)-glycolate enolate **17** is more stable than the (*E*)-glycolate enolate **18** by 6.4 kcal/mol and more stable than the allenyl anion species **19** by a staggering 15.4 kcal/mol. These data demonstrate that even if a mechanism for equilibration between the isomers existed, the (*Z*)-glycolate enolate would still be the predominant isomer. Assured that the (*Z*)-glycolate enolate was the functioning secondary nucleophile, the transition state of the reaction for the (*Z*)-glycolate enolate **17** and the nitroalkene secondary electrophile **10a** was calculated using the density functional theory approach.

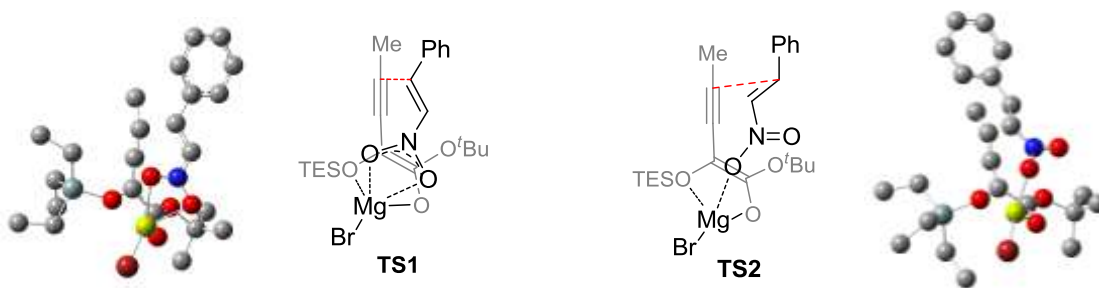
Figure 2-10. Relative Energies of the Potential Identities of the Secondary Nucleophilic Species



2.4.2. DFT-Optimized Transition States

The transition states for the formation of both possible diastereomers were optimized at the level of B3LYP/6-311G(d) using density functional theory. The calculations returned the two optimized transition states depicted in Figure 2-11. The barrier height between the two optimized transition states corresponds to a 3.0 kcal/mol difference in favor of **TS1** over **TS2**. This barrier height variance roughly corresponds to a 100-fold increase in reactivity favoring **TS1** over **TS2**. This analysis corresponds well with the empirical data since the favored transition state **TS1** leads to the experimentally-observed diastereomer. The crucial distinction between these two transition states is a function of the type of coordination the nitro group performs with respect to the coordinated magnesium cation of the (*Z*)-glycolate enolate **17**.

Figure 2-11. DFT-Optimized Transition States for **TS1** Leading to the Observed Diastereomer and **TS2** Which Would Lead to the Unobserved Diastereomer.



TS1 stabilizes the incipient negative charge by delocalizing the charge between the two oxygens of the nitro group equally via chelation to the magnesium cation; leading to a pentacoordinate magnesium species. In contrast, **TS2** stabilizes the developing anionic charge through a monodentate coordination which serves to differentiate the oxygen atoms and leads to a tetracoordinate magnesium species. Although monodentate coordination appears to be the predominant interaction invoked in synthetic organic literature, previous studies²² as well as crystal structures²³ have shown that both modes of nitro group coordination are possible.

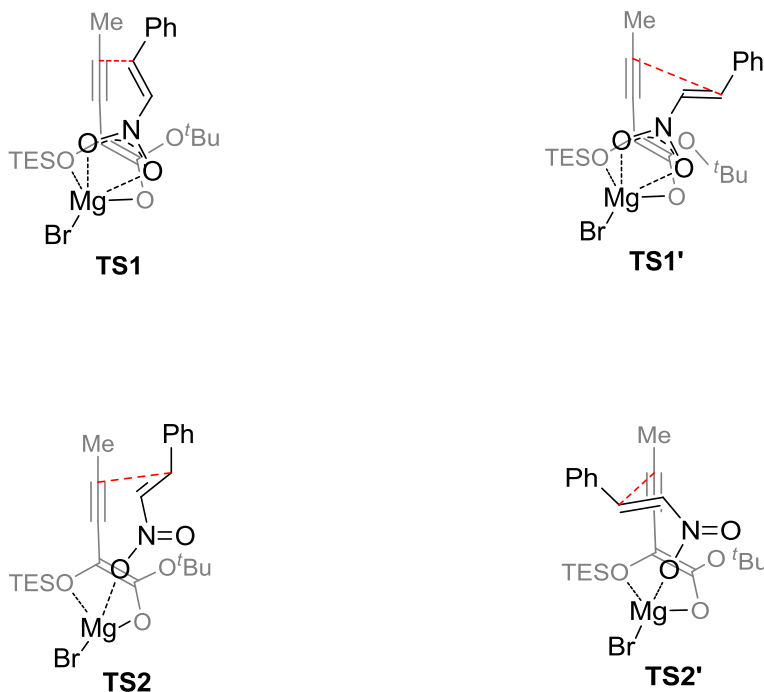
2.4.3 Implications on the Regio- and Diastereoselectivity

The DFT-optimized transition states **TS1** and **TS2** provide a plausible explanation for the regioselectivity observed in the three-component coupling. The vinylogous reactivity is rationalized by the dual coordination of the nitro group in **TS1** that requires the electrophilic site of the nitroalkene to possess favorable overlap with the γ -position of the (*Z*)-glycolate enolate while providing no possible overlap with the α -position. This variance in the orbital overlap distinguishes between the two nucleophilic sites of the (*Z*)-glycolate enolate **17** and provides a possible rationale for the complete regioselectivity observed in this coupling.

The DFT-optimized transition states also serve to justify the excellent level of diastereoselectivity observed in the reaction. Both diastereomers are still possible regardless of whether **TS1** or **TS2** is analyzed due to the possibility for a C–N bond rotation on the approaching nitroalkene. This expands the analysis to four distinct rotamers (two for **TS1** and two for **TS2**) as illustrated in Figure 2-12. **TS1'** and **TS2'** do not lead to productive reactivity though, due to the inability for rotamers **TS1'** and **TS2'**

to overlap favorably with either the α - or γ -reactive site on the (Z)-glycolate enolate nucleophile.

Figure 2-12. Comparison of **TS1** and **TS2** with the Non-Reactive Rotamers **TS1'** and **TS2'**

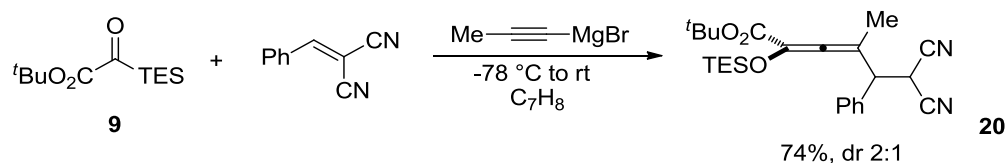


2.4.4. Additional Mechanistic Support for the Theoretical Studies from the Benzylidenemalononitrile-Terminated Three-Component Coupling

Although the calculated transition states provided a reasonable explanation for the observed selectivity, a test to experimentally corroborate this theoretical study of the importance of the type of nitro group coordination would add significant validity to the role of **TS1**. To probe the validity of **TS1**, a suitable electrophilic species that could enter the same three-component reaction manifold, but be incapable of chelation, would be required. Benzylidenemalononitrile emerged as a reasonable candidate since α,α -

dicyanoolefins react only in a Michael fashion (unlike α,β -unsaturated carbonyls) and the cyano groups should provide negligible coordination to the magnesium cation relative to the coordination of the nitro group. Exposing benzylidenemalononitrile to the three-component reaction conditions as the secondary electrophile substitute for the nitroalkene provided the desired vinylogous adduct **20** in a 74% yield and 2:1 diastereoselectivity as illustrated in Scheme 2-6. The poor diastereoselectivity observed in the benzylidenemalononitrile-terminated coupling provides strong corroboration for our hypothesized mechanism as well as the qualitative applicability of the theoretical studies.

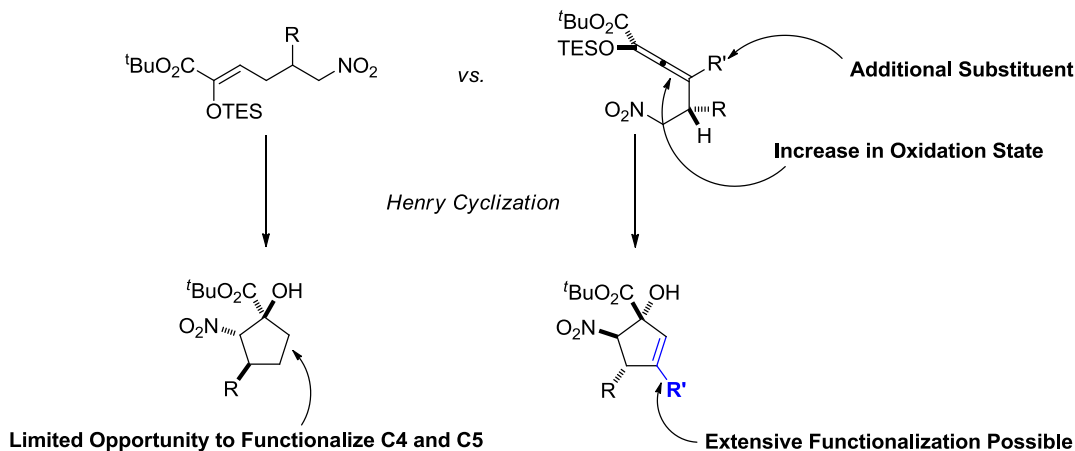
Scheme 2-6. α,α -Dicyanoolefin Three-Component Coupling Employing Benzylidenemalononitrile



2.5. Secondary Transformations to Cyclopentanol Derivatives

In addition to the many known transformations of allenes and the distinct reactivity imparted to silyloxyallenes, we hypothesized that these heretofore unknown 5-nitrosilyloxyallenes compounds would be poised to undergo interesting and unique subsequent transformations. Specifically, these 5-nitrosilyloxyallenes could be utilized as latent 5-nitroketoesters which would be useful in various Henry type cyclizations to form nitrocyclopentanol derivatives. This methodology is conceptually similar to the nitrocyclopentanol methodology covered in Chapter 1; however, the altered oxidation state of the C3 carbon adds new challenges and opportunities as seen by the comparison presented in Scheme 2-7.

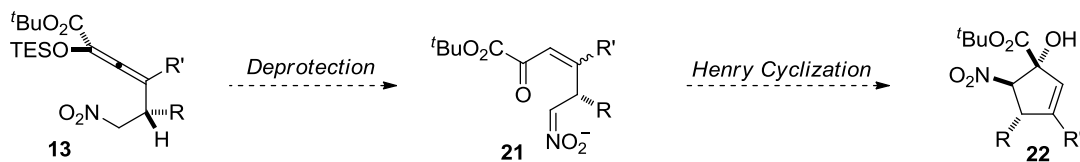
Scheme 2-7. Comparison of Silyloxyallene Cyclization Potential vs. Enolsilanes



2.5.1. Henry Cyclization of Silyloxyallenes

To affect successful Henry cyclization, the 5-nitrosilyloxyallene **13** must first undergo deprotection to the enone **21**, followed by deprotonation of one of the acidic α -nitro methylene protons and subsequent cyclization onto the α -ketoester to provide cyclopentenol **22** as depicted in Figure 2-13. The presence of the olefin after deprotection could lead to several challenges. First, the olefin is in conjugation with the α -ketoester which makes intermolecular Michael addition instead of intramolecular Henry reaction a potential obstacle. Also, the geometry of the olefin is not known and the added strain of the unsaturation may prevent the desired cyclization.

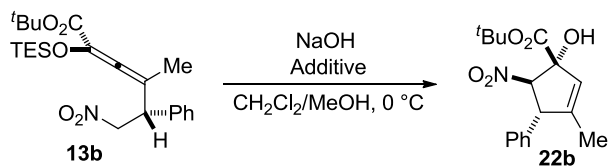
Figure 2-13. Proposed Henry Cyclization Sequence



2.5.2. Optimization

An examination of various cyclization conditions was conducted with the results summarized in Table 2-6. Exposing the 5-nitrosilyloxyallene **13b** to the known cyclization conditions disclosed in Chapter 1 (entry 1) provided a complex product mixture. Assuming the issue resides with the presence of the olefin, an investigation into whether a Lewis acid could interact with the olefin in a suitable manner to enable the desired cyclization was undertaken with AuCl₃ and Ti(OiPr)₄ screened as additives in the cyclization conditions. The AuCl₃ trial (entry 2) provided some product based on ¹H NMR analysis, however the yield was low due to a variety of byproducts being present in the crude mixture. Gratifyingly, Ti(OiPr)₄ (entry 3) provided the desired cyclization in a 75% yield and a >20:1 diastereomeric ratio. Although the incorporation of the Lewis acid additive is vital for successful Henry cyclization cascade, the exact role of the Ti(OiPr)₄ remains unknown.

Table 2-6. Screen of Conditions to Induce Henry Cyclization



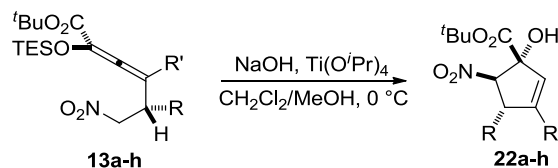
entry	Additive	yield (%) ^b	d.r.
1	None	NDP	N.D.
2	AuCl ₃	Trace	N.D.
3	Ti(OiPr) ₄	75 ^b	>20:1

^aAll reactions were conducted [**13b**]₀ = 0.01 M. ^bIsolated Yield.

2.5.3. Reaction Scope

With optimized conditions in hand for the efficient diastereoselective synthesis of nitrocyclopentenols, the scope of silyloxyallenes amenable to the reaction was investigated with the results disclosed in Table 2-7. The reaction proved to be reliable for a variety of substrates with R = aryl, heteroaryl, and alkyl moieties (entries 1-5) all being well tolerated. The products were obtained in yields ranging from 39-86% with complete diastereocontrol. The R' substituent was also amenable to a variety of functional groups including alkyl, alkenyl, and aryl groups (entries 6-8) providing yields ranging from 61-69% with complete diastereocontrol. When R' = TMS the diastereomeric ratio and the yield suffered significantly leading to this functional group being viewed as an untenable substrate for the cyclization (not shown). In contrast to the methodology presented in Chapter 1, the diastereoselectivity of this Henry cyclization appears to be largely independent of the identity and branching of the R group. The transition state which enables the excellent levels of diastereoselection remains unidentified.

Table 2-7. Substrate Scope for the Henry Cyclization



entry	product	R	R'	yield (%) ^b	d.r.
1	22a	Ph	Ph	61	>20:1
2	22b	Ph	Me	75	>20:1
3	22c	2-thienyl	Me	86	>20:1
4	22d	2-furyl	Me	60	>20:1
5	22e	C ₅ H ₁₁	Me	57	>20:1
6	22f	<i>i</i> -Pr	Me	39	>20:1
7	22g	Ph	C ₅ H ₁₁	69 ^b	>20:1
8	22h	Ph	<i>i</i> -propenyl	66	>20:1

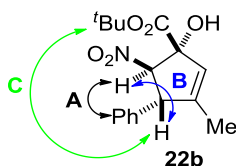
^aAll reactions were conducted [**13a-h**]₀ = 0.01 M with the reaction warmed to room temperature immediately after the addition was complete. ^bIsolated Yield. See section 2.7 for additional experimental details.

2.5.4. Determination of Relative Stereochemistry

The identity of the major diastereomer of **22a** and the identities of all other cyclopentenol examples (**22b-22e**) were assigned using the same rationale employing the nOe interactions represented in Figure 2-14 (see section 2.6 for complete details). The strong nOe between the C3 phenyl group and the C2 α -nitro methine proton of **22a** imply a *trans*-relationship (A) for the phenyl and nitro substituents. A very weak nOe is observed between the α -nitro methine proton at C2 and the benzylic methine at C3 (B) suggesting a *trans*-relationship for these protons. This assignment is further corroborated by a nOe correlation between the *t*-butyl ester and the benzylic methine proton, whereas no nOe correlation is observed between the *t*-butyl ester and the α -nitro methine (C). The

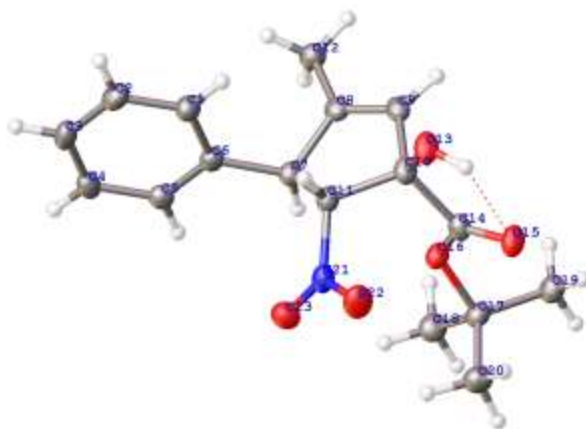
stereochemistry at C1 is challenging to assign based on the NOESY spectra since the alcohol and *t*-butyl ester possess no distinguishing nOe correlation for this position. A crystal structure was obtained to elucidate this stereochemical relationship.²⁴ The X-ray crystal structure verified the relative stereochemistry at C2-C3 as *trans* and provided the C1-C2 stereochemistry in terms of the alcohol and the nitro group as *trans*. The crystal structure also explained the absence of a nOe correlation between the nitro methine proton and the alcohol.

Figure 2-14. Representative nOe Correlations for **22b**



The crystal structure illustrates a coordination event between the alcohol proton and the ester carbonyl which directs the proton away from the ring, while also orienting the *t*-butyl group under the ring as seen in Figure 2-15. This provides a rational for the observed nOe's of the *t*-butyl ester with the benzylic methine proton as well as why the alcohol proton does not interact with the α -nitro methine proton. This interaction was hypothesized in the stereochemical justification provided for the nitrocyclopentanols synthesized in Chapter 1.

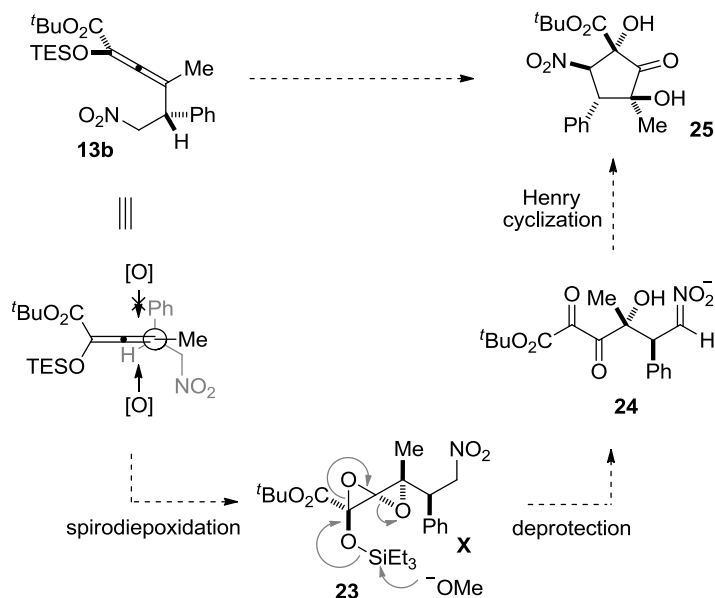
Figure 2-15. Illustration of the Crystal Structure of **22b** Solved by Dr. Peter White



2.5.5. Cyclopentitol Synthesis from Spirodiepoxides

To further exploit the allene functionality, a double oxidation to the spirodiepoxide was envisioned. This oxidation even could then be followed by a deprotection-initiated Henrycyclization cascade to provide fully substituted cyclopentitols. If the spirodiepoxidation of silyloxyallene **13b** is successful, the spirodiepoxide **23** could undergo the desired cascade as envisioned in Scheme 2-8. Deprotection of the silyloxy-spirodiepoxide would provide the vicinal tricarbonyl species **24**,²⁵ which could then cyclize under the basic conditions to provide fully substituted cyclopentitol **25**.

Scheme 2-8. Proposed Cascade for the Synthesis of Fully Substituted Cyclopentitols



2.5.6. Optimization of Reaction Parameters

The transformation of allenes to the derived spirodiepoxides typically employs dry DMDO in chloroform, however, our studies employed the more activate oxidant trifluoroperacetic acid since it was the only oxidant screened that provided complete consumption of the silyloxyallene **13b**. A screen of conditions to induce the desired cascade to provide the desired cyclopentitols was performed as illustrated in Table 2-8. The results demonstrate that the equivalents of trifluoroperacetic acid can be reduced to four (entry 1-2) without adversely affecting the consumption of the starting material. In regards to the cyclization, a trend emerged where the amount of NaOH had to be greater than the oxidant to induce cyclization. Regrettably, the optimization studies did not lead to a reliable method for the synthesis of **25**.

Table 2-8. Equivalence Screen for One-Pot Spirodiepoxidation/Henry Cyclization

$\text{13b} \xrightarrow[\text{NaOH (10 equiv), MeOH, 0 } ^\circ\text{C, 3 h}]{\text{TFPA (4 equiv), CH}_2\text{Cl}_2, \text{rt, 3 h}} \text{25}$

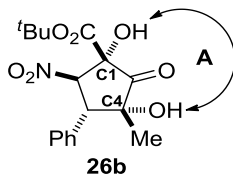
entry	TFPA	NaOH	yield ^b
1	10	2.0	NDP
2	6	2.5	NDP
3	4	8.0	NDP
4	4	10.0	Trace

^aAll reactions were conducted $[\text{13b}]_0 = 0.01 \text{ M}$. ^bIsolated Yield. See section 2.7 for additional experimental details.

2.5.7. Alternative Synthesis of Cyclopentitols

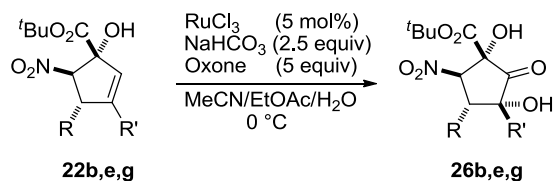
With the spirodiepoxidation route being viewed as untenable, an investigation into an alternative route to synthesize these cyclopentitols was then undertaken. Ketohydroxylation, the formation of an α -hydroxy ketone from an olefin pioneered by Plietker, provides a potential solution. Exposing cyclopentenol **22b** to modified ketohydroxylation conditions²⁶ provided cyclopentanone **26b** in 67% yield and a 3:1 mixture of diastereomers. The stereochemistry of the cyclopentitol **26b** was established by NOESY analysis. The relative stereochemistry at C1, C2 and C3 was set in the initial cyclization to the cyclopentenol which was discussed in Section 2.5.4. Assuming there is not a highly selective isomerization pathway (which seems unlikely since the reaction conditions are similar to the highly diastereoselective cyclization conditions) only the relative stereochemistry at C4 remains unsolved. Based on the large nOe observed between the C1-OH and the C4-OH these protons, these stereocenters were assigned as *syn* as illustrated in Figure 2-18.

Figure 2-18. Representative nOe Correlation for **26b**



Although cyclopentenones are reported to be problematic substrates for ketohydroxylation, increasing the catalyst loading to 5 mol % and extending the reaction time at 0 °C remedies the sluggish reactivity of these substrates with the results summarized in Table 2-9. Substrates **22e** and **22g** provide excellent levels of diastereoselectivity along with good yields. The cause of the diastereoselectivity has not been studied; however a possible explanation is polar group participation²⁷ from the C1 alcohol directing the ruthenium catalyst to the same face of the substrate. A global reduction of these substrates would provide highly complex aminocyclopentitol products. This simple three step protocol for the synthesis of densely functionalized cyclopentitols from silyl glyoxylate could provide opportunity for substantial derivatization for potential application in biological assays and in providing access to medicinal targets.

Table 2-9. Substrate Scope for the Ketohydroxylation



entry	product	R	R'	yield (%) ^b	d.r.
1	26a	Ph	Me	67	3:1
2	26b	C ₅ H ₁₁	Me	59	>20:1
3	26c	Ph	C ₅ H ₁₁	58	>10:1

^aAll reactions were conducted $[\text{22b,e,g}]_0 = 0.01 \text{ M}$. ^bIsolated Yield. See section 2.7 for additional experimental details.

2.6. Conclusion

A novel reactivity pattern for silyl glyoxylates, acetylides, and nitroalkenes to provide tetrasubstituted silyloxyallenes has been disclosed. The reported three-component coupling provides good to very good yields for a variety of alkyl, aryl and alkenyl and allows for limited heteroatom substitution. Each substrate screened provided the desired silyloxyallene product with complete diastereoselection. An explanation of the impressive chemo-, regio-, and diastereoselectivity was proposed based on quantum mechanical studies of the transition state employing density functional theory. Moreover, the unique reactivity of these heretofore unknown 5-nitrosilyloxyallenes has been exploited in the synthesis of cyclopentenols compounds by a Lewis acid-assisted Henry-type cyclization. Although a highly efficient methodology to access cyclopentitols directly from the silyloxyallenes was envisioned by implementing a novel oxidative Henry cyclization, all conditions screened failed to produce the desired cascade. Due to

the issues with the oxidative Henry cyclization, a ketohydroxylation was employed to convert the cyclopentenols to cyclopentitols in good yields and moderate to excellent diastereoselectivity.

2.7. Experimental Details

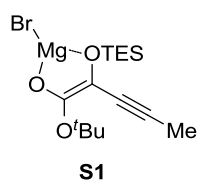
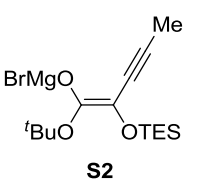
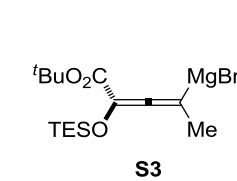
Materials and Methods: General. Infrared (IR) spectra were obtained using a Nicolet 560-E.S.P. infrared spectrometer. Proton and carbon nuclear magnetic resonance spectra (^1H and ^{13}C NMR) were recorded on a Varian 600 (^1H at 600 MHz and ^{13}C NMR at 150 MHz) spectrometer with solvent resonance as the internal standard (^1H NMR: CDCl_3 at 7.26 ppm; ^{13}C NMR: CDCl_3 at 77.0 ppm). ^1H NMR data are reported as follows: chemical shift, multiplicity (s = singlet, d = doublet, dd = doublet of doublets, t = triplet, q = quartet, m = multiplet), coupling constants (Hz), and integration. Analytical thin layer chromatography (TLC) was performed on Whatman 0.25 mm silica gel 60 plates. Visualization was accomplished with UV light and aqueous ceric ammonium molybdate solution followed by heating. Purification of the reaction products was carried out by flash chromatography using Sorbent Technologies silica gel 60 (32-63 μm). All reactions were carried out under an atmosphere of nitrogen in oven-dried glassware with magnetic stirring. Yield refers to isolated yield of analytically pure material. Yields are reported for a specific experiment and as a result may differ slightly from those found in the tables, which are averages of at least two experiments. Dichloromethane, tetrahydrofuran, and toluene were dried by passage through a column of neutral alumina under nitrogen prior to use.²⁸ Nitroalkenes **4a**, **4b**, **4d** are commercially available from Sigma-Aldrich. Nitroalkenes **4c**,²⁹ **4g**,²⁹ **4h**,²⁹ **4e**,³⁰ and **4f**³¹ were prepared according to

literature procedures. 1-Propynylmagnesium bromide was purchased from Sigma-Aldrich. All other alkynyl nucleophiles were synthesized by treating the appropriate terminal alkyne with one equivalent of 0.5M ethyl magnesiumbromide in THF and stirring for three hours at room temperature.

Computation Analysis of the Secondary Nucleophile Species Using B3LYP/6-

311G(d): A comparison of the relative energies of the three possible isomers of the transient secondary nucleophile; the (*Z*)-glycolate enolate **S1**, the (*E*)-glycolate enolate **S2**, and the allenyl anionic species **S3** is presented in Table S1. These results suggest that the (*Z*)-glycolate enolate is the thermodynamic transient secondary nucleophile compared to the (*E*)-glycolate enolate and the allenyl anionic species.

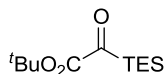
Table S1. Relative Energies of the Potential Identities of the Secondary Nucleophilic Species

		
S1	S2	S3

Entry	Relative Energies (kcal/mol)
S1	0.0
S2	6.4
S3	15.4

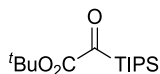
Synthesis of Silyl Glyoxylates

Triethylsilyl glyoxylate was obtained by modifying the published method for *tert*-butyldimethylsilyl glyoxylate by substituting TESOTf for TBSOTf in the silylation step.



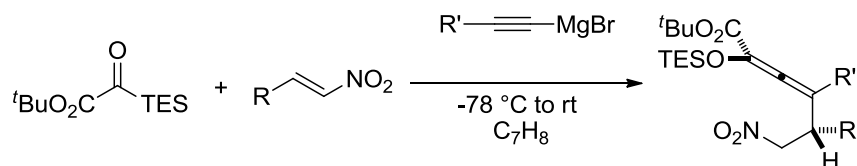
Triethylsilyl glyoxylate (9): The title compound was isolated as a yellow oil. Analytical data for **9**: **IR** (thin film, cm^{-1}) 2958, 2913, 2878, 2359, 1713, 1661, 1460, 1370, 1289, 1159; **^1H NMR** (600 MHz, CDCl_3) δ 1.55 (s, 9H), 0.98 (t, $J = 7.8$ Hz, 9H), 0.85 – 0.79 (m, 6H); **^{13}C NMR** (150 MHz, CDCl_3): δ 233.0, 162.5, 83.3, 27.9, 7.0, 2.3; **TLC** (5% Ether/petroleum ether) $R_f = 0.50$. **LRMS** (ESI) Calcd. for $\text{C}_{12}\text{H}_{24}\text{O}_3\text{SiNa}$ 267.14. Found: 267.2.

Triisopropylsilyl glyoxylate was obtained by modifying the published method for *tert*-butyldimethylsilyl glyoxylate by substituting TIPSOTf for TBSOTf in the silylation step.



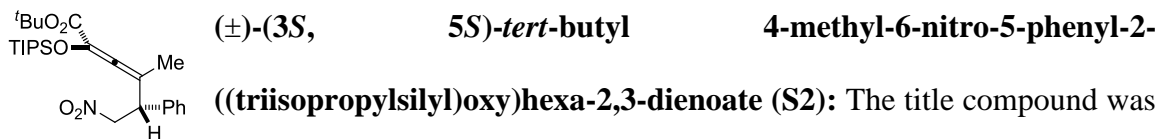
Triisopropylsilyl glyoxylate (S1): The title compound was isolated as a yellow oil. Analytical data for **S1**: **IR** (thin film, cm^{-1}) 2946, 2891, 2869, 2729, 1991, 1942, 1909, 1889, 1867; **^1H NMR** (600 MHz, CDCl_3) δ 1.54 (s, 9H), 1.43–1.38 (m, 3H), 1.11 (d, $J = 7.8$ Hz, 18H); **^{13}C NMR** (150 MHz, CDCl_3): δ 233.4, 163.5, 83.5, 27.9, 18.5, 11.1; **TLC** (5% EtOAc/petroleum ether) $R_f = 0.45$. **LRMS** (ESI) Calcd. for $\text{C}_{15}\text{H}_{30}\text{O}_3\text{SiNa}$ 309.19. Found: 309.2.

General Procedure for the Synthesis of Silyloxyallenes (S2, 13a-k)



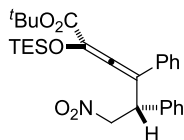
General Procedure for the Synthesis of Silyloxyallenes: A 0.23 M solution of triethylsilyl glyoxylate (1.5 equiv) and nitroalkene or α,α -dicyanoolefin (1.0 equiv) in dry toluene was added dropwise to a 0.027 M solution of alkynyl Grignard (1:2.7 THF/toluene) at $-78\text{ }^{\circ}\text{C}$. Once the addition was complete the reaction was allowed to warm to room temperature, then was diluted with diethyl ether (5 mL), and quenched with saturated ammonium chloride (5 mL). The resulting mixture was stirred for 10 min. The layers were separated, and the aqueous layer was extracted with diethyl ether (3 X 5 mL). The organic extracts were combined, washed with brine (5 mL), dried with magnesium sulfate, and concentrated *in vacuo*. The crude mixture was purified by flash chromatography with 5% EtOAc/hexanes yielding the desired product.

V. Analytical Data for the Silyloxyallenes (S2, 13a-k)



The title compound was prepared according to the general procedure using **S1** (0.165 g, 0.50 mmol, 1.5 equiv), 1-propynylmagnesium bromide (0.5 M, 1.00 mL, 0.50 mmol, 1.5 equiv) and β -nitrostyrene (0.050 g, 0.34 mmol, 1 equiv). After addition was complete, the reaction was warmed to

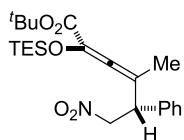
room temperature and quenched. Purification by flash chromatography (5% EtOAc/hexanes) yielded 52.0 mg (30%) of the product as a white solid. A sample suitable for x-ray diffraction was obtained by slow evaporation of the **S2** in EtOAc. Analytical data for **S2**: **IR** (thin film, cm^{-1}): 3031, 2945, 2893, 1949, 1726, 1603, 1495, 1392, 1140; **mp**: 43-46 °C **^1H NMR** (600 MHz, CDCl_3): δ 7.37-7.30 (m, 5H), 4.72 (dd, J = 7.2, 6.0 Hz, 1H), 4.56-4.51 (m, 1H), 4.12 (dd, J = 7.2, 6.0 Hz, 1H), 1.71 (s, 3H), 1.55 (s, 9H), 1.25-1.17 (m, 3H), 1.11-1.09 (m, 18H); **^{13}C NMR** (150 MHz, CDCl_3): δ 196.4, 164.3, 137.1, 129.0, 128.4, 128.3, 121.7, 111.8, 81.9, 79.4, 48.8, 28.2, 19.2, 17.8, 17.8, 12.3; **TLC** (20% EtOAc/hexanes) R_f 0.67. **LRMS** (ESI) Calcd. for $\text{C}_{26}\text{H}_{41}\text{NO}_5\text{SiNa}$: 498.27. Found: 498.3.



(±)-(3R,5S)-tert-butyl 6-nitro-4,5-diphenyl-2-((triethylsilyl)oxy)hexa-2,3-dienoate (13a): The title compound was prepared according to the

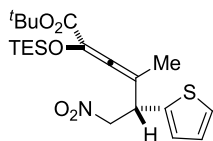
general procedure using **9** (0.123 g, 0.503 mmol, 1.5 equiv), 1-phenylethynylmagnesium bromide (0.5 M, 1.00 mL, .503 mmol, 1.5 equiv) and β -nitrostyrene (0.050 g, 0.335 mmol, 1 equiv). After addition was complete, the reaction was warmed to room temperature and quenched. Purification by flash chromatography (5% EtOAc/hexanes) yielded 127 mg (76%) of the product as a yellow solid. Analytical data for **13a**: **IR** (thin film, cm^{-1}): 2956, 2877, 2360, 2342, 1933, 1726, 1556, 1370, 1141; **mp**: 75-79 °C; **^1H NMR** (600 MHz, CDCl_3): δ 7.36-7.19 (m, 10H), 4.95-4.87 (m, 1H), 4.86-4.84 (m, 1H), 4.63-4.59 (m, 1H), 1.59 (s, 9H), 0.91 (t, J = 7.8 Hz, 9H), 0.61-0.57 (m, 6H); **^{13}C NMR** (125 MHz, CDCl_3): δ 163.5, 143.6, 117.6, 81.3, 46.9, 33.4, 28.1, 28.0, 27.3, 25.0, 6.75,

5.6; **TLC** (20% EtOAc/hexanes) R_f 0.48. **LRMS** (ESI) Calcd. for $C_{28}H_{37}NO_5SiNa$: 518.23. Found: 518.2.



(±)-(3*S*, 5*S*)-*tert*-butyl 4-methyl-6-nitro-5-phenyl-2-((triethylsilyl)oxy)hexa-2,3-dienoate (**13b**): The title compound was

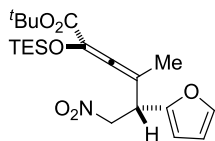
prepared according to the general procedure using **9** (0.245 g, 1.01 mmol, 1.5 equiv), 1-propynylmagnesium bromide (0.5 M, 2.01 mL, 1.01 mmol, 1.5 equiv) and β -nitrostyrene (0.100 g, 0.670 mmol, 1 equiv). After addition was complete, the reaction was warmed to room temperature and quenched. Purification by flash chromatography (5% EtOAc/hexanes) yielded 205 mg (70%) of the product as a white solid. Analytical data for **13b**: **IR** (thin film, cm^{-1}): 3438, 2956, 2877, 1950, 1731, 1557, 1156, 741; **mp**: 52-55 °C **1H NMR** (600 MHz, $CDCl_3$): δ 7.37-7.30 (m, 5H), 4.10 (dd, J = 13.2, 6.6 Hz, 1H), 4.49 (dd, J = 13.2, 9.0 Hz, 1H), 4.13 (dd, J = 8.4, 6.6 Hz, 1H), 1.74 (s, 3H), 1.55 (s, 9H), 1.00 (t, J = 7.8 Hz, 9H), 0.70 (q, J = 8.4, 7.8 Hz 6H); **^{13}C NMR** (150 MHz, $CDCl_3$): δ 196.3, 164.2, 137.0, 129.0, 128.4, 128.3, 121.2, 111.8, 81.9, 79.2, 48.8, 28.2, 19.4, 6.6, 4.7; **TLC** (20% EtOAc/hexanes) R_f 0.52. **LRMS** (ESI) Calcd. for $C_{25}H_{35}NO_5SiNa$: 456.22. Found: 456.2.



(±)-(3*S*, 5*S*)-*tert*-butyl 4-methyl-6-nitro-5-(thiophen-2-yl)-2-((triethylsilyl)oxy)hexa-2,3-dienoate (**13c**): The title compound was

prepared according to the general procedure using **9** (0.095 g, 0.389 mmol, 1.5 equiv), 1-propynylmagnesium bromide (0.5 M, 0.78 mL, 0.389 mmol, 1.5 equiv) and (*E*)-2-(2-nitrovinyl)thiophene (0.040 g, 0.259 mmol, 1 equiv). After addition was complete, the

reaction was warmed to room temperature and quenched. Purification by flash chromatography (5% EtOAc/hexanes) yielded 92 mg (81%) of the product as a yellow oil. Analytical data for **13c**: **IR** (thin film, cm^{-1}): 3428, 3120, 2957, 2878, 2253, 1951, 1724, 1557, 1370, 1144, 1012; **^1H NMR** (600 MHz, CDCl_3) δ 7.35 (d, $J = 0.6$ Hz, 1H), 6.33-6.31 (m, 2H), 4.68 (d, $J = 7.8$ Hz, 2H), 4.36-4.34 (m, 1H), 1.81 (s, 3H), 1.48 (s, 3H), 0.98-0.96 (m, 9H), 0.69-0.65 (m, 6H); **^{13}C NMR** (150 MHz, CDCl_3): δ 197.2, 164.0, 149.8, 142.8, 120.8, 110.5, 109.6, 108.7, 81.7, 76.2, 42.3, 28.0, 18.6, 6.5, 4.5; **TLC** (20% EtOAc/hexanes) R_f 0.40. **LRMS** (ESI) Calcd. for $\text{C}_{21}\text{H}_{33}\text{NO}_5\text{SSiNa}$: 462.17. Found: 462.2.



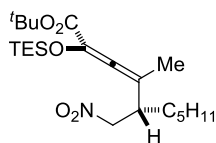
(±)-(3*S*,5*S*)-*tert*-butyl

5-(furan-2-yl)-4-methyl-6-nitro-2-

((triethylsilyl)oxy)hexa-2,3-dienoate (**13d**): The title compound was

prepared according to the general procedure using **9** (0.105 g, 0.431 mmol, 1.5 equiv), 1-propynylmagnesium bromide (0.5 M, 0.86 mL, .431 mmol, 1.5 equiv) and (*E*)-2-(2-nitrovinyl)furan (0.040 g, 0.288 mmol, 1 equiv). After addition was complete, the reaction was warmed to room temperature and quenched. Purification by flash chromatography (5% EtOAc/hexanes) yielded 82 mg (70%) of the product as a yellow oil. Analytical data for **13d**: **IR** (thin film, cm^{-1}): 2957, 2913, 2877, 2360, 1717, 1646, 1557, 1506, 1458, 1372, 1286, 1247, 1167, 1143, 1012, 915, 850, 806; **^1H NMR** (600 MHz, CDCl_3) δ 7.36-7.36 (m, 1H), 6.33-6.31 (m, 2H), 4.85 (d, $J = 7.8$ Hz, 2H), 4.37-4.34 (m, 1H), 1.82 (s, 3H), 1.48 (s, 9H), 0.99-0.96 (m, 9H), 0.70-0.66 (m, 6H); **^{13}C NMR** (150 MHz, CDCl_3): δ 197.3, 164.0, 149.9, 142.8, 120.9, 110.6, 109.6, 108.7, 81.7, 76.2, 42.3,

28.1, 27.9, 18.7, 6.5, 4.6; **TLC** (20% EtOAc/hexanes) R_f 0.42. **LRMS** (ESI) Calcd. for $C_{21}H_{33}NO_6SiNa$: 446.20. Found: 446.2.

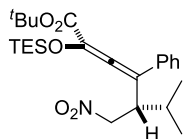


(±)-(3*S*,5*S*)-*tert*-butyl

4-methyl-5-(nitromethyl)-2-

((triethylsilyl)oxy)deca-2,3-dienoate (**13e**): The title compound was

prepared according to the general procedure using **9** (0.159 g, 0.651 mmol, 1.5 equiv), 1-propynylmagnesium bromide (0.5 M, 1.30 mL, .651 mmol, 1.5 equiv) and (*E*)-1-nitrohept-1-ene (0.050 g, 0.349 mmol, 1 equiv). After addition was complete, the reaction was warmed to room temperature and quenched. Purification by flash chromatography (5% EtOAc/hexanes) yielded 60 mg (42%) of the product as a yellow semisolid. Analytical data for **13e**: **IR** (thin film, cm^{-1}): 2957, 2877, 1948, 1724, 1556, 1369, 1290, 1146; **1H NMR** (600 MHz, $CDCl_3$): δ 4.44-4.43 (m, 1H), 4.34-4.31 (m, 1H), 2.97-2.92 (m, 1H), 1.87 (s, 3H), 1.46 (s, 9H), 1.46-1.28 (m, 8H), 1.00-0.95 (m, 9H), 0.89-0.87 (m, 3H), 0.68-0.667 (m, 6H); **^{13}C NMR** (150 MHz, $CDCl_3$): δ 197.7, 164.3, 120.0, 111.8, 81.4, 78.2, 43.0, 31.7, 30.6, 28.0, 26.1, 22.4, 18.5, 14.0, 6.5, 4.6; **TLC** (20% EtOAc/hexanes) R_f 0.56. **LRMS** (ESI) Calcd. for $C_{22}H_{41}NO_5SiNa$: 450.27. Found: 450.2.



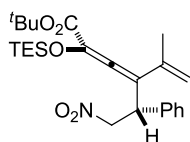
(±)-(3*S*,5*S*)-*tert*-butyl

4,6-dimethyl-5-(nitromethyl)-2-

((triethylsilyl)oxy)hept-2,3-dienoate(**13f**): The title compound was

prepared according to the general procedure using **9** (0.191 g, 0.781 mmol, 1.5 equiv), 1-propynylmagnesium bromide (0.5 M, 1.60 mL, 0.781 mmol, 1.5 equiv) and (*E*)-3-methyl-1-nitrobut-1-ene (0.060 g, 0.521 mmol, 1 equiv). After addition was complete, the

reaction was warmed to room temperature and quenched. Purification by flash chromatography (5% EtOAc/hexanes) yielded 108 mg (52%) of the product as a yellow oil. Analytical data for **13f**: **IR** (thin film, cm^{-1}): 2960, 2878, 2359, 1945, 1723, 1556, 1369, 1289; **^1H NMR** (600 MHz, CDCl_3): δ 4.41-4.39 (m, 2H), 2.80-2.77 (m, 1H), 1.91 (s, 3H), 1.45 (s, 9H), 1.03-1.02 (d, $J = 6.6$ Hz, 3H), 0.97-0.94 (m, 12H), 0.65 (q, $J = 7.8$ Hz, 6H); **^{13}C NMR** (150 MHz, CDCl_3): δ 197.9, 164.4, 120.4, 112.0, 81.5, 76.6, 48.9, 29.8, 28.0, 20.6, 20.3, 19.3, 6.5, 4.6; **TLC** (20% EtOAc/hexanes) R_f 0.54. **LRMS** (ESI) Calcd. for $\text{C}_{20}\text{H}_{37}\text{NO}_5\text{SiNa}$: 422.23. Found: 422.2.

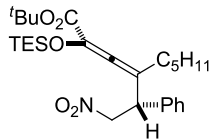


(\pm)-(*R*)-*tert*-butyl

5-methyl-4-((*S*)-2-nitro-1-phenylethyl)-2-

((triethylsilyl)oxy)hexa-2,3,5-trienoate (**13h**): The title compound was

prepared according to the general procedure using **9** (0.123 g, 0.503 mmol, 1.5 equiv), 1-propynylmagnesium bromide (0.5 M, 1.00 mL, .503 mmol, 1.5 equiv) and β -nitrostyrene (0.050 g, 0.335 mmol, 1 equiv). After addition was complete, the reaction was warmed to room temperature and quenched. Purification by flash chromatography (5% EtOAc/hexanes) yielded 122 mg (74%) of the product as a yellow oil. Analytical data for **13h**: **IR** (thin film, cm^{-1}): 2430, 2956, 2877, 2359, 2254, 1924, 1724, 1371, 1142; **^1H NMR** (600 MHz, CDCl_3): δ 7.39 (d, $J = 7.2$ Hz, 2H), 7.34-7.28 (m, 3H), 5.17 (s, 1H), 5.10 (s, 1H), 4.76-4.69 (m, 2H), 4.54-4.51 (m, 1H), 1.84 (s, 9H), 1.57 (s, 9H), 1.03-1.01 (m, 9H), 0.73 (q, $J = 7.8$ Hz, 6H); **^{13}C NMR** (150 MHz, CDCl_3): δ 201.4, 163.7, 137.8, 137.5, 128.9, 128.1, 127.9, 123.5, 117.9, 116.0, 82.2, 79.8, 44.9, 28.2, 22.1, 6.6, 4.9; **TLC** (20% EtOAc/hexanes) R_f 0.55. **LRMS** (ESI) Calcd. for $\text{C}_{25}\text{H}_{37}\text{NO}_5\text{SiNa}$: 482.23. Found: 482.2.

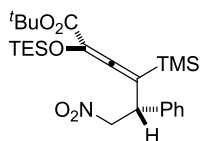


(*S*)-*tert*-butyl

4-((*S*)-2-nitro-1-phenylethyl)-2-

((triethylsilyl)oxy)nona-2,3-dienoate (**13i**): The title compound was

prepared according to the general procedure using **9** (0.123 g, 0.503 mmol, 1.5 equiv), 1-heptynylmagnesium bromide (0.5 M, 1.00 mL, .503 mmol, 1.5 equiv) and β -nitrostyrene (0.050 g, 0.335 mmol, 1 equiv). After addition was complete, the reaction was warmed to room temperature and quenched. Purification by flash chromatography (5% EtOAc/hexanes) yielded 106 mg (67%) of the product as a colorless oil. Analytical data for **13i**: **IR** (thin film, cm^{-1}): 3566, 2957, 2876, 2359, 2241, 1944, 1723, 1635, 1557, 1457, 1370, 1143; **^1H NMR** (600 MHz, CDCl_3): δ 7.36-7.30 (m, 5H), 4.72-4.69 (m, 1H), 4.51-4.47 (m, 1H), 4.16 (t, $J = 7.8$ Hz, 1H), 2.25-2.10 (m, 1H), 1.92-1.89 (m, 1H), 1.54 (s, 9H), 1.49-1.163 (m, 7H), 1.00-0.98 (m, 9H), 0.82-0.79 (m, 3H), 0.73-0.69 (m, 6H); **^{13}C NMR** (150 MHz, CDCl_3): δ 200.9, 163.9, 136.9, 134.2, 128.9, 128.5, 128.3, 128.3, 128.0, 127.1, 123.2, 117.0, 82.3, 79.7, 45.8, 28.3, 6.4, 4.6; **TLC** (20% EtOAc/hexanes) R_f 0.45. **LRMS** (ESI) Calcd. for $\text{C}_{27}\text{H}_{43}\text{NO}_5\text{SiNa}$: 512.25. Found: 512.3.



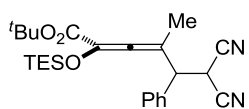
(\pm)-(*3R,5R*)-*tert*-butyl

6-nitro-5-phenyl-2-((triethylsilyl)oxy)-4-

(trimethylsilyl)hexa-2,3-dienoate (**13k**): The title compound was

prepared according to the general procedure using **9** (0.123 g, 0.503 mmol, 1.5 equiv), 2-methyl-1-buten-3-ynylmagnesium bromide (0.5 M, 1.00 mL, .503 mmol, 1.5 equiv) and β -nitrostyrene (0.050 g, 0.335 mmol, 1 equiv). After addition was complete, the reaction was warmed to room temperature and quenched. Purification by flash chromatography (5% EtOAc/hexanes) yielded 61 mg (37%) of the product as a white solid. Analytical

data for **13k**: mp: 73-76 °C IR (thin film, cm⁻¹): 3415, 2957, 2359, 2255, 2172, 1922, 1715, 1556, 1141; ¹H NMR (600 MHz, CDCl₃): 7.35-7.28 (m, 5H), 4.76-4.72 (m, 1H), 4.56-4.53 (m, 1H), 4.34-4.32 (m, 1H), 1.51 (s, 9H), 1.01-0.98 (m, 9H), 0.71 (q, *J* = 7.8 Hz, 6H), -0.01 (s, 9H); ¹³C NMR (150 MHz, CDCl₃): δ 204.2, 165.5, 137.5, 128.8, 128.7, 128.2, 121.0, 112.9, 81.5, 80.6, 46.0, 28.3, 6.7, 5.1, -1.29; TLC (20% EtOAc/hexanes) R_f 0.50. LRMS (ESI) Calcd. for C₂₅H₄₁NO₅Si₂Na: 514.24. Found: 514.2.



(±)-(3*S*)-*tert*-butyl

6,6-dicyano-4-methyl-5-phenyl-2-

((triethylsilyl)oxy)hexa-2,3-dienoate (**20**): The title compound was

prepared according to the general procedure using **9** (0.059 g, 0.243 mmol, 1.5 equiv), 1-propynylmagnesium bromide (0.5 M, 0.500 mL, .243 mmol, 1.5 equiv) and benzylidenemalononitrile (0.025 g, 0.162 mmol, 1 equiv). After addition was complete, the reaction was warmed to room temperature and quenched. Purification by flash chromatography (5% EtOAc/hexanes) yielded 52 mg (73%) of the product as a 2:1 diastereomeric ratio as a yellow oil. Analytical data for **20**: IR (thin film, cm⁻¹): 3065, 2957, 2254, 1952, 1724, 1455, 1293, 1140; ¹H NMR (600 MHz, CDCl₃): mixture of diastereomers: major diastereomer δ 7.48-7.35 (m, 5H), 4.01 (d, *J* = 7.2 Hz, 1H), 3.87-3.84 (m, 1H), 1.77 (s, 3H), 1.57 (s, 9H), 1.03-0.99 (m, 9H), 0.77-0.74 (m, 6H); minor diastereomer δ 7.48-7.35 (m, 5H), 4.13 (d, *J* = 7.8 Hz, 1H), 3.87-3.84 (m, 1H), 1.80 (s, 3H), 1.52 (s, 9H), 1.03-0.99 (m, 9H), 0.77-0.74 (m, 6H); ¹³C NMR (150 MHz, CDCl₃): mixture of diastereomers: δ 197.4, 163.7, 134.4, 129.4, 129.4, 129.3, 128.9, 128.5, 123.1, 112.1, 112.0, 111.4, 111.3, 110.8, 110.4, 82.5, 51.6, 20.0, 28.6, 28.1, 28.0, 27.2, 7.2, 6.6,

6.6, 5.8, 4.8; **TLC** (20% EtOAc/hexanes) R_f 0.37. **LRMS** (ESI) Calcd. for $C_{25}H_{34}N_2O_3SiNa$: 461.22. Found: 461.2.

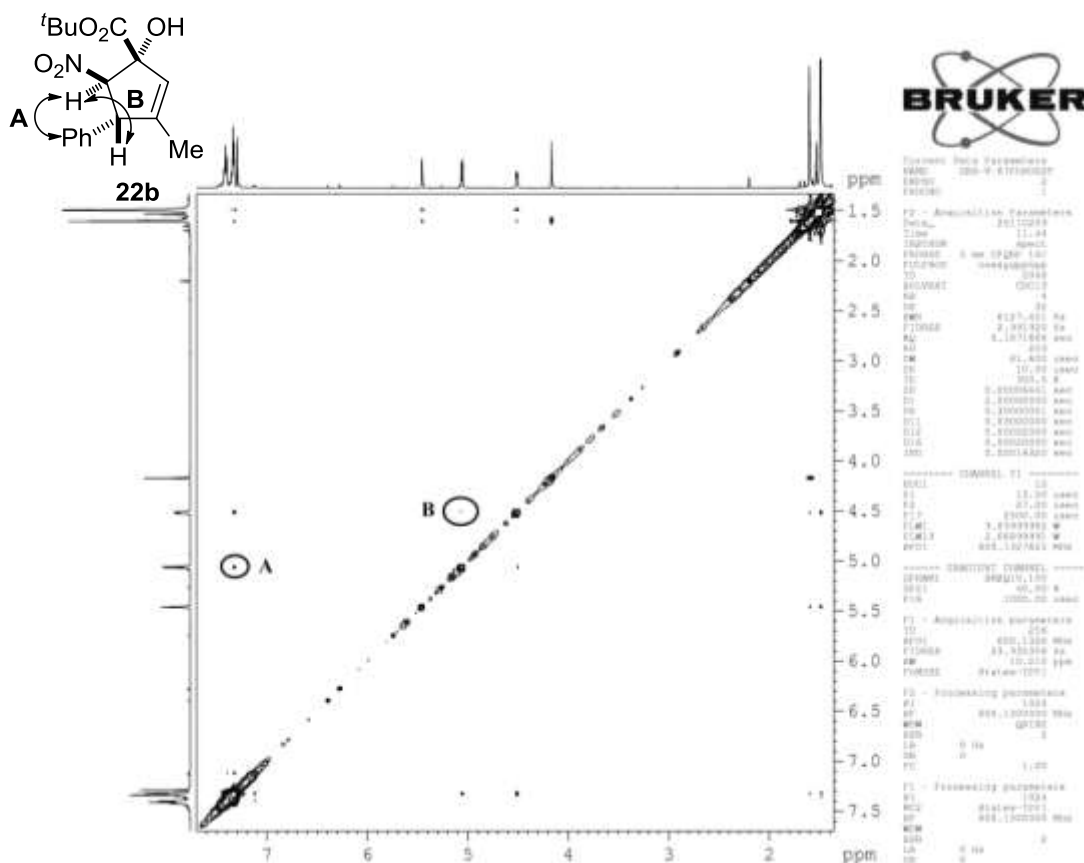
General Procedure for the Synthesis of Cyclopentenols (22a-h)

The silyloxyallene was dissolved in 1:1 mixture of methanol (0.1 M) and methylene chloride (0.1 M). The resulting solution was cooled in an ice/brine bath to -5 °C followed by the addition of $Ti(OiPr)_4$ (0.5 equiv). Sodium hydroxide (1.0 equiv) was added at once and the resulting solution was stirred at -5 °C until the reaction was judged complete by TLC analysis. Once the reaction was complete, the reaction mixture was diluted with methylene chloride (5 mL) and quenched with 1 M HCl (5 mL). The resulting mixture was stirred for 15 minutes. The layers were separated and the aqueous layer was extracted with methylene chloride (3 x 5 mL). The combined organic extracts were washed with brine (5 mL), dried with sodium sulfate, and concentrated *in vacuo*. The resulting cyclopentanols (**22a-h**) were purified by flash chromatography using 10% EtOAc/hexanes.

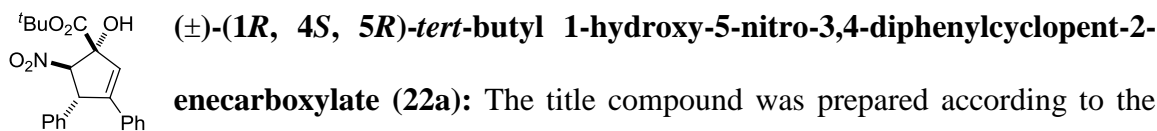
General Information for the Structural Assignments for Cyclopentenols

General Method for the Structural Assignment of the Cyclopentenols based on NOESY Analysis:

The identity of the major diastereomer **22b** was assigned as illustrated by the following NOESY spectrum. All other cyclopentenol examples (**22a,c-h**) were assigned using the same rationale (see **XII** for spectra). The strong nOe between the C3 phenyl group and the C2 α -nitro methine proton implies a *trans*-relationship (**A**). A very weak nOe correlation is observed between the α -nitro methine proton at C2 and the benzylic methine at C3 (**B**) suggesting a *trans*-relationship for these protons. The stereochemistry at C1 is challenging to assign based on the NOESY spectra since the alcohol and *tert*-butyl ester show no decisive nOe correlations. An x-ray crystal structure of **22b** was obtained to elucidate this stereochemical relationship. The solved structure verified the relative stereochemistry at C2-C3 as *trans* and provided the C1-C2 stereochemistry of the alcohol and the nitro group as *trans*. The crystal structure also explained why there was no nOe correlation observed between the α -nitro methine proton and the alcohol. The crystal structure illustrates a hydrogen bond between the alcohol proton and the ester carbonyl that pulls the proton away from the ring which orients the *t*-butyl group under the ring explaining why the *t*-butyl ester has nOe correlations with most protons on the ring (see attached cif). This interaction was hypothesized for a similar nitrocyclopentanol in the supporting information of *Angew. Chem. Int. Ed.* **2010**, 49, 8930-8933.

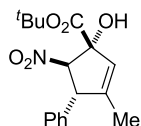


Analytical Data for the Cyclopentenols (22a-h)



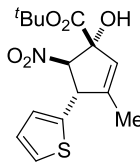
general procedure using **13a** (0.105 g, 0.212 mmol, 1 equiv), Ti(OiPr)₄ (0.030 mL, 0.106 mmol, 0.5 equiv) and NaOH (0.009 g, 0.212 mmol, 1.0 equiv). After stirring for 3 h, the reaction was complete as determined by TLC analysis. The reaction was worked up and purified by flash chromatography (10% EtOAc/hexanes) to afford 49 mg (61%) of the product as an orange semisolid in >20:1 dr. Analytical data for **22a**: IR (thin film, cm⁻¹): 3482, 3061, 2979, 1736, 1549, 1371, 1153; ¹H NMR (600 MHz, CDCl₃): δ 7.35-7.21 (m, 10H), 6.06 (s, 1H), 5.22-5.20 (m, 1H), 5.15 (d, *J* = 7.2 Hz, 1H), 4.36 (s, 1H), 1.48 (s, 9H);

¹³C NMR (150 MHz, CDCl₃): δ 170.1, 147.1, 139.9, 133.5, 128.9, 128.6, 128.6, 128.4, 127.6, 127.0, 126.7, 101.6, 85.6, 85.3, 52.8, 27.6; **TLC** (20% EtOAc/hexanes) R_f 0.30. **LRMS** (ESI) Calcd. for C₂₂H₂₃NO₅Na: 404.15. Found: 404.1.



(±)-(1*R*, 4*R*, 5*R*)-*tert*-butyl 1-hydroxy-3-methyl-5-nitro-4-phenylcyclopent-2-enecarboxylate (**22b**): The title compound was

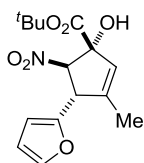
prepared according to the general procedure using **13b** (0.130 g, 0.300 mmol, 1 equiv), Ti(O*i*Pr)₄ (0.044 mL, 0.150 mmol, 0.5 equiv) and NaOH (0.012 g, 0.300 mmol, 1.0 equiv). After stirring for 2 h, the reaction was complete as determined by TLC analysis. The reaction was worked up and purified by flash chromatography (10% EtOAc/hexanes) to afford 67 mg (69%) of the product as an orange solid in >20:1 dr. Analytical data for **22b**: mp 85-89 °C; **IR** (thin film, cm⁻¹): 3501, 2978, 2916, 1733, 1371, 1155; **¹H NMR** (600 MHz, CDCl₃): δ 7.40-7.29 (m, 5H), 5.43 (s, 1H), 5.03 (d, *J* = 7.2 Hz, 1H), 4.49 (d, *J* = 7.2 Hz, 1H), 4.14 (s, 1H), 1.57 (s, 3H), 1.46 (s, 9H); **¹³C NMR** (150 MHz, CDCl₃): δ 170.6, 146.0, 139.1, 129.0, 128.5, 127.8, 126.5, 101.1, 85.7, 84.9, 55.7, 27.6, 15.5; **TLC** (20% EtOAc/hexanes) R_f 0.36. **LRMS** (ESI) Calcd. for C₁₇H₂₁NO₅Na: 342.12. Found: 342.2.



(±)-(1*R*, 4*S*, 5*R*)-*tert*-butyl 1-hydroxy-3-methyl-5-nitro-4-(thiophen-2-yl)cyclopent-2-enecarboxylate (**22c**): The title compound was prepared

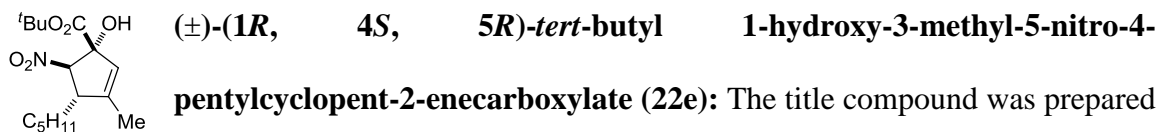
according to the general procedure using **13c** (0.065 g, 0.148 mmol, 1 equiv), Ti(O*i*Pr)₄ (0.020 mL, 0.074 mmol, 0.5 equiv) and NaOH (0.006 g, 0.148 mmol, 1.0 equiv). After stirring for 3 h, the reaction was complete as determined by TLC

analysis. The reaction was worked up and purified by flash chromatography (10% EtOAc/hexanes) to afford 40 mg (83%) of the product as a red oil in >20:1 dr. Analytical data for **13c**: **IR** (thin film, cm^{-1}): 3500, 2122, 2979, 2736, 2256, 1731, 1556, 1241; **^1H NMR** (600 MHz, CDCl_3): δ 7.39 (s, 1H), 6.36-6.34 (m, 2H), 5.37 (s, 1H), 5.26 (d, $J = 7.8$ Hz, 1H), 4.60 (d, $J = 6.6$ Hz, 1H), 4.11 (s, 1H), 1.61 (s, 3H), 1.44 (s, 9H); **^{13}C NMR** (150 MHz, CDCl_3): δ 170.4, 151.2, 144.3, 142.7, 125.9, 110.6, 108.6, 85.1, 84.9, 49.2, 27.6, 15.3; **TLC** (20% EtOAc/hexanes) R_f 0.36. **LRMS** (ESI) Calcd. for $\text{C}_{15}\text{H}_{19}\text{NO}_5\text{SNa}$: 348.09. Found: 348.1.

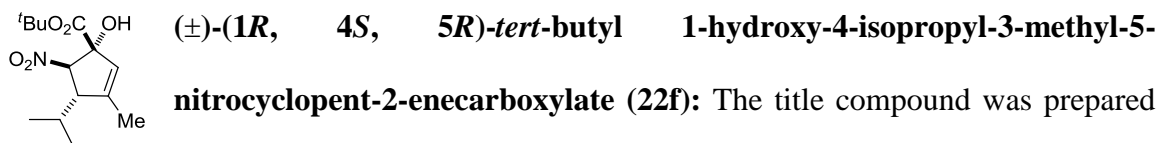


(±)-(1R, 4S, 5R)-*tert*-butyl 4-(furan-2-yl)-1-hydroxy-3-methyl-5-nitrocyclopent-2-enecarboxylate (**22d**): The title compound was prepared

according to the general procedure using **13d** (0.048 g, 0.114 mmol, 1 equiv), $\text{Ti}(\text{OiPr})_4$ (0.017 mL, 0.057 mmol, 0.5 equiv) and NaOH (0.005 g, 0.114 mmol, 1.0 equiv). After stirring for 8 h, the reaction was complete as determined by TLC analysis. The reaction was worked up and purified by flash chromatography (10% EtOAc/hexanes) to afford 21 mg (60%) of the product as a red oil in >20:1 dr. Analytical data for **22d**: **IR** (thin film, cm^{-1}): 3493, 2980, 2933, 2360, 1732, 1552, 1372, 1153; **^1H NMR** (600 MHz, CDCl_3): δ 7.39 (s, 1H), 6.36-6.35 (m, 2H), 5.37 (s, 1H), 5.26 (d, $J = 7.8$ Hz, 1H), 4.60 (d, $J = 6.6$ Hz, 1H), 4.11 (s, 1H), 1.61 (s, 3H), 1.44 (s, 9H); **^{13}C NMR** (150 MHz, CDCl_3): δ 170.4, 151.2, 144.3, 142.7, 125.9, 110.6, 108.6, 96.8, 85.1, 84.9, 49.2, 27.6, 15.3; **TLC** (20% EtOAc/hexanes) R_f 0.26. **LRMS** (ESI) Calcd. for $\text{C}_{15}\text{H}_{19}\text{NO}_6\text{Na}$: 332.11. Found: 332.1.

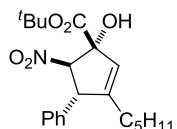


The title compound was prepared according to the general procedure using **13e** (0.055 g, 0.129 mmol, 1 equiv), Ti(OiPr)₄ (0.020 mL, 0.064 mmol, 0.5 equiv) and NaOH (0.005 g, 0.128 mmol, 1.0 equiv). After stirring for 3 h, the reaction was complete as determined by TLC analysis. The reaction was worked up and purified by flash chromatography (10% EtOAc/hexanes) to afford 23 mg (57%) of the product as a orange oil in >20:1 dr. Analytical data for **22e**: **IR** (thin film, cm⁻¹): 3498, 2932, 2860, 1731, 1550, 1371, 1158, 1081; **¹H NMR** (600 MHz, CDCl₃): δ 5.24 (s, 1H), 4.81 (d, *J* = 7.2 Hz, 1H), 4.01 (s, 1H), 3.46 (d, *J* = 5.4 Hz, 1H), 1.79 (s, 1H), 4.11 (s, 1H), 1.61 (s, 3H), 1.43 (s, 9H) 1.59-0.95 (m, 11H); **¹³C NMR** (150 MHz, CDCl₃): δ 170.7, 146.7, 125.2, 97.2, 85.8, 84.5, 48.7, 32.1, 30.3, 27.6, 25.1, 22.5, 15.3, 14.0, 6.6, 5.8; **TLC** (20% EtOAc/hexanes) *R_f* 0.38. **LRMS** (ESI) Calcd. for C₁₆H₂₇NO₅Na: 336.18. Found: 336.2.



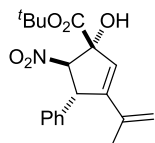
The title compound was prepared according to the general procedure using **13f** (0.058 g, 0.145 mmol, 1 equiv), Ti(OiPr)₄ (0.021 mL, 0.0073 mmol, 0.5 equiv) and NaOH (0.006 g, 0.145 mmol, 1.0 equiv). After stirring for 4 h, the reaction was complete as determined by TLC analysis. The reaction was worked up and purified by flash chromatography (10% EtOAc/hexanes) to afford 16 mg (39%) of the product as a opaque semisolid in >20:1 dr. Analytical data for **13f**: **IR** (thin film, cm⁻¹): 3495, 2970, 2349, 1731, 1555, 1370, 1237, 1157; **¹H NMR** (600 MHz, CDCl₃): δ 5.21 (s, 1H), 4.82 (d, *J* = 6.6 Hz, 1H), 4.14 (s, *J* = 16, 8 Hz, 1H), 3.51 (d, *J* =

2.4 Hz, 1H), 2.21-2.16 (m, 1H), 1.78 (s, 3H), 1.40 (s, 9H), 0.96 (d, $J = 7.2$ Hz, 3H), 0.86 (d, $J = 6.6$ Hz, 3H); ^{13}C NMR (150 MHz, CDCl_3): δ 170.6, 146.5, 125.6, 94.8, 86.6, 84.6, 53.7, 27.5, 27.0, 19.9, 16.8, 15.7; TLC (20% EtOAc/hexanes) R_f 0.42. LRMS (ESI) Calcd. for $\text{C}_{14}\text{H}_{23}\text{NO}_5\text{Na}$: 308.15. Found: 308.1.



(±)-(1R, 4R, 5S)-*tert*-butyl 1-hydroxy-5-nitro-3-pentyl-4-phenylcyclopent-2-enecarboxylate (**22g**): The title compound was

prepared according to the general procedure using **13g** (0.074 g, 0.151 mmol, 1 equiv), $\text{Ti}(\text{OiPr})_4$ (0.020 mL, 0.075 mmol, 0.5 equiv) and NaOH (0.006 g, 0.151 mmol, 1.0 equiv). After stirring for 12 h, the reaction was complete as determined by TLC analysis. The reaction was worked up and purified by flash chromatography (10% EtOAc/hexanes) to afford 39 mg (69%) of the product as a yellow oil in >20:1 dr. Analytical data for **22g**: IR (thin film, cm^{-1}): 3500, 2957, 2931, 2359, 1738, 1550, 1371, 1155; ^1H NMR (600 MHz, CDCl_3): δ 7.39-7.29 (m, 5H), 5.43 (s, 1H), 5.02 (d, $J = 7.2$ Hz, 1H), 4.54 (d, $J = 7.2$ Hz, 1H), 4.15 (s, 1H), 1.98-1.92 (m, 1H), 1.81-1.77 (m, 1H), 1.46 (s, 9H), 1.38-1.46 (m, 6H), 0.88-0.83 (m, 3H); ^{13}C NMR (150 MHz, CDCl_3): δ 170.7, 150.2, 139.2, 129.0, 128.6, 127.7, 125.8, 101.1, 85.6, 84.8, 54.3, 30.9, 29.1, 27.6, 26.2, 22.3, 13.9; TLC (20% EtOAc/hexanes) R_f 0.28. LRMS (ESI) Calcd. for $\text{C}_{21}\text{H}_{29}\text{NO}_5\text{Na}$: 398.19. Found: 398.2.



(±)-(1R, 4S, 5R)-*tert*-butyl 1-hydroxy-5-nitro-4-phenyl-3-(prop-1-en-2-yl)cyclopent-2-enecarboxylate (**22h**): The title compound was prepared

according to the general procedure using **13h** (0.053 g, 0.106 mmol, 1 equiv), $\text{Ti}(\text{OiPr})_4$ (0.016 mL, 0.053 mmol, 0.5 equiv) and NaOH (0.004 g, 0.106 mmol, 1.0 equiv). After

stirring for 4 h, the reaction was complete as determined by TLC analysis. The reaction was worked up and purified by flash chromatography (10% EtOAc/hexanes) to afford 25 mg (68%) of the product as an orange semisolid in >20:1 dr. Analytical data for **22h**: **IR** (thin film, cm^{-1}): 3482, 2978, 2932, 2359, 2254, 1732, 1555, 1371, 1229; **^1H NMR** (600 MHz, CDCl_3): δ 7.37-7.29 (m, 5H), 5.74 (s, 1H) 5.02 (d, J = 6.0 Hz, 1H), 4.98 (s, 1H), 4.91 (d, J = 7.2 Hz, 1H), 4.76 (s, 1H), 1.90 (s, 3H), 1.48 (s, 9H); **^{13}C NMR** (150 MHz, CDCl_3): δ 170.1, 147.8, 141.1, 136.6, 128.9, 128.2, 127.5, 127.2, 118.8, 101.6, 85.7, 85.2, 52.6, 27.6, 20.8; **TLC** (20% EtOAc/hexanes) R_f 0.17. **LRMS** (ESI) Calcd. for $\text{C}_{19}\text{H}_{23}\text{NO}_5\text{Na}$: 368.15. Found: 368.1.

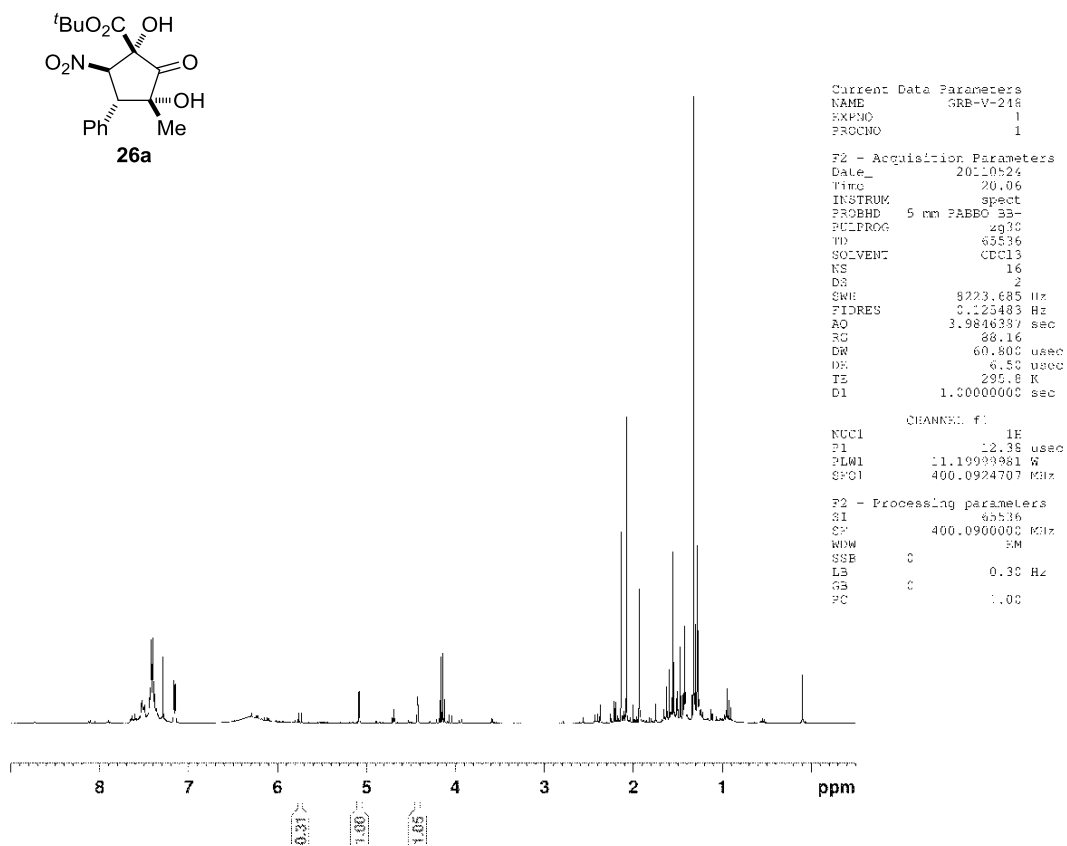
General Procedure for the Synthesis of Cyclopentitols (**26a,d,g**)

Oxone (5 equiv) was added to a mixture of NaHCO_3 (2.5 equiv) and RuCl_3 (0.05 equiv) 0.03 M solution in water, MeCN (0.16 M), EtOAc (0.16 M) at room temperature. The resultant mixture was stirred vigorously till the solution turned bright yellow and then was cooled to 0 °C with an ice bath. Once cooled, the cyclopentenol (1 equiv) was added and allowed to stir vigorously until the reaction was judged complete by TLC analysis. Once the reaction was complete the solution was diluted with EtOAc (5 mL) and filtered. The filtrate was neutralized with an excess of NaHCO_3 . The resulting mixture was stirred for 15 minutes. The solids were then filtered, washed with EtOAc, dried with MgSO_4 and concentrated *in vacuo*. The resulting cyclopentanol (**26a,d,g**) were purified by flash chromatography using 20% EtOAc/hexanes.

General Information for the Structural Assignment for Cyclopentitols 26a,d,g

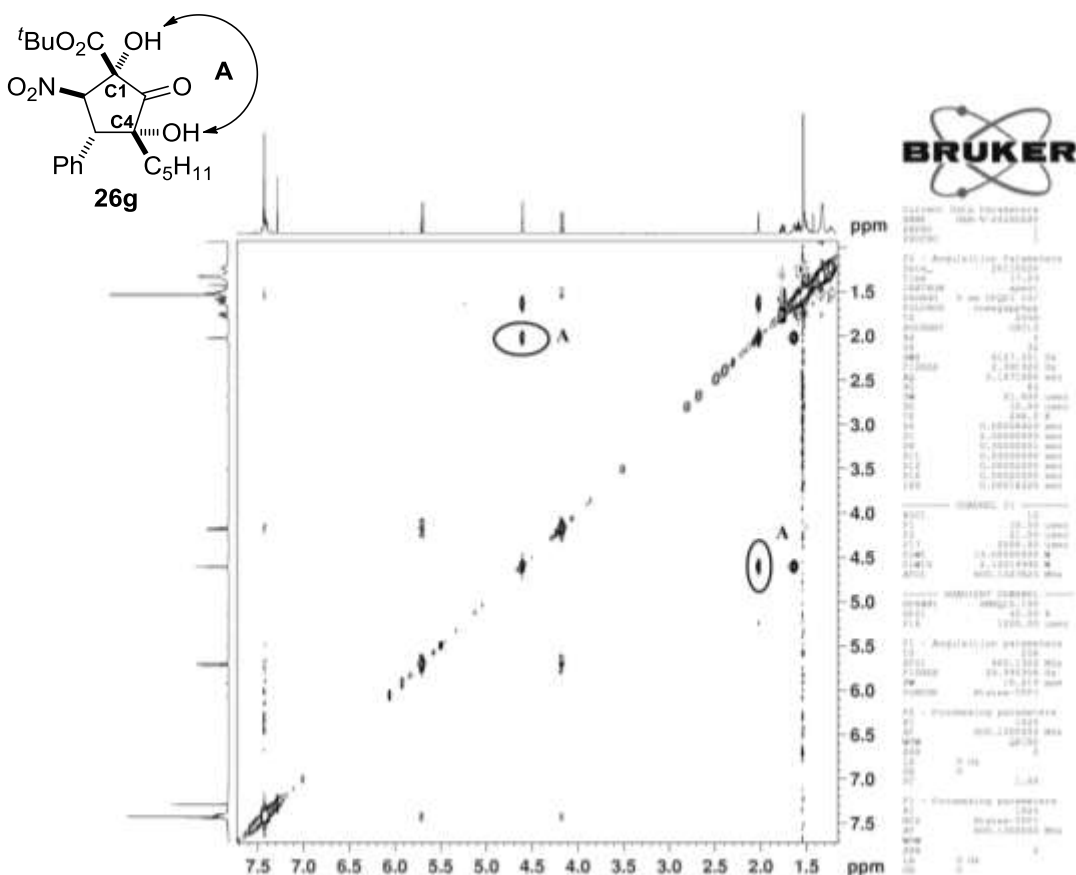
Calculation of Diastereomeric Ratios:

The diastereomeric ratios for the cyclopentitols were calculated using the ratio of the α -nitro methine proton for each diastereomer. In the following example the diastereomeric ratio for the crude material obtained from the reaction with **8a** shows compound **26a** in a 3:1 d.r.:

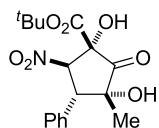


General Method for the Structural Assignment of the Nitrocyclopentanols based on NOESY Analysis:

The identity of the major diastereomer of **9g** was assigned as illustrated by the following NOESY spectrum. Other cyclopentitol examples (**9a,d**) were assigned using the same rationale. The relative stereochemistry at C1, C2 and C3 was set in the initial cyclization to the cyclopentenol. Assuming there is not a highly selective isomerization pathway, which seems unlikely since the reaction conditions are similar to the cyclization conditions (temperature, basic, solvent); only the relative stereochemistry at C4 remains unsolved. Based on the large nOe observed between the C1-OH and the C4-OH these protons, these stereocenters were assigned as *syn*.

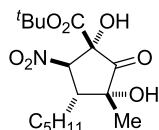


Analytical Data for the Cyclopentitols (26a,d,g)



(±)-(1*S*, 3*R*, 4*R*, 5*R*)-*tert*-butyl 1,3-dihydroxy-3-methyl-5-nitro-2-oxo-4-phenylcyclopentanecarboxylate (**26a**):

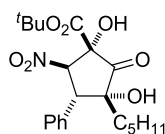
The title compound was prepared according to the general procedure using **22a** (0.034 g, 0.106 mmol, 1 equiv), 0.03 M RuCl₃ (0.18 mL, 0.053 mmol, 0.05 equiv), oxone (0.327 g, 0.532 mmol, 5 equiv), NaHCO₃ (0.022 g, 0.266 mmol, 2.5 equiv). After stirring for 2 h, the reaction was complete as determined by TLC analysis. The reaction was worked up and purified by flash chromatography (20% EtOAc/hexanes) to afford 29 mg (68%) of the product as a colorless oil in 3:1 dr. Analytical data for **26a**: **IR** (thin film, cm⁻¹): 3713, 3460, 2980, 2933, 1772, 1746, 1557, 1373, 1234, 807, 659; major diastereomer: **¹H NMR** (600 MHz, CDCl₃): δ 7.42-7.37 (m, 5H), 5.70 (d, *J* = 6.6 Hz, 1H), 4.52 (s, 1H), 4.03 (d, *J* = 12.6 Hz, 1H), 2.13 (s, 1H), 1.53 (s, 9H), 1.39 (s, 3H); **¹³C NMR** (150 MHz, CDCl₃): δ 205.0, 165.8, 131.5, 129.6, 128.7, 127.9, 91.7, 87.6, 82.0, 52.8, 27.7, 20.9; **TLC** (30% EtOAc/hexanes) R_f 0.36. **LRMS** (ESI) Calcd. for C₁₇H₂₁NO₇Na: 374.12. Found: 374.2.



(±)-(1*S*, 3*R*, 4*R*, 5*R*)-*tert*-butyl 1,3-dihydroxy-3-methyl-5-nitro-2-oxo-4-pentylcyclopentanecarboxylate (**26d**):

The title compound was prepared according to the general procedure using **22d** (0.020 g, 0.064 mmol, 1 equiv), 0.03 M RuCl₃ (0.11 mL, 0.003 mmol, 0.05 equiv), oxone (0.195 g, 0.315 mmol, 5 equiv), NaHCO₃ (0.013 g, 0.16 mmol, 2.5 equiv). After stirring for 2 h, the reaction was complete as determined by TLC analysis. The reaction was worked up and purified by flash chromatography (20% EtOAc/hexanes) to afford 15 mg (68%) of the product as a

colorless oil in >20:1 dr. Analytical data for **26d**: **IR** (thin film, cm^{-1}): 3766, 3480, 2956, 2923, 1772, 1741, 1556, 1148, 1071, 836, 663; **^1H NMR** (600 MHz, CDCl_3): δ 4.99 (d, J = 12.0 Hz, 1H), 4.28 (s, 1H), 2.89-2.85 (m, 1H), 1.91 (s, 1H), 1.85-1.80 (m, 1H), 1.66-1.38 (m, 8H), 1.58 (s, 3H), 1.50 (s, 9H), 1.33-1.32 (m, 3H); **^{13}C NMR** (150 MHz, CDCl_3): δ 207.2, 165.9, 94.3, 87.4, 82.5, 46.1, 32.0, 27.7, 26.4, 22.8, 22.4, 14.0; **TLC** (30% EtOAc/hexanes) R_f 0.31. **LRMS** (ESI) Calcd. for $\text{C}_{16}\text{H}_{27}\text{NO}_7\text{Na}$: 368.17. Found: 368.2.



(±)-(1S, 3R, 4R, 5R)-tert-butyl 1,3-dihydroxy-5-nitro-2-oxo-3-pentyl-4-phenylcyclopentanecarboxylate (26g): The title compound was prepared

according the general procedure using **22g** (0.080 g, 0.213 mmol, 1 equiv), 0.03 M RuCl_3 (0.35 mL, 0.011 mmol, 0.05 equiv), oxone (0.655 g, 1.07 mmol, 5 equiv), NaHCO_3 (0.045 g, 0.532 mmol, 2.5 equiv). After stirring for 2 h, the reaction was complete as determined by TLC analysis. The reaction was worked up and purified by flash chromatography (20% EtOAc/hexanes) to afford 47 mg (55%) of the product as a colorless oil in 20:1 dr. Analytical data for **26g**: **IR** (thin film, cm^{-1}): 3435, 2956, 2927, 2860, 1651, 1556, 1496, 1362, 1288, 1119; **^1H NMR** (600 MHz, CDCl_3): δ 7.42-7.36 (m, 5H) 5.68 (d, J = 12.0 Hz, 1H), 4.58 (s, 1H), 4.15 (d, J = 12.0 Hz, 1H), 1.99 (s, 1H), 1.76-1.29 (m, 8H), 1.55 (s, 9H), 0.93-0.89 (m, 3H); **^{13}C NMR** (150 MHz, CDCl_3): δ 170.9, 143.5, 127.0, 124.8, 124.2, 100.8, 85.1, 83.3, 43.2, 37.1, 31.3, 27.6, 0.98; **TLC** (30% EtOAc/hexanes) R_f 0.33. **LRMS** (ESI) Calcd. for $\text{C}_{21}\text{H}_{29}\text{NO}_7\text{Na}$: 430.18. Found: 430.2.

2.8. References

- [1] Kuwajima, I.; Kato, M. *Tetrahedron Lett.* **1980**, *21*, 623-626. (b) Reich, H. J.; Olson, R. E.; Clark, M. C. *J. Am. Chem. Soc.* **1980**, *102*, 1423-1424.
- [2] Kurteva, V. B.; Afonso, C. A. M. *Chem. Rev.* **2009**, *109*, 6809-6857.
- [3] (a) Umino, K.; Furama, T.; Matzuzawa, N.; Awataguchi, Y.; Ito, Y.; Okuda, T. *J. Antibiot.* **1973**, *26*, 506-512. (b) Umino, K.; Takeda, N.; Ito, Y.; Okuda, T. *Chem. Pharm. Bull.* **1974**, *22*, 1233-1238.
- [4] Choi, J.; Lee, K.-T.; Choi, M.-Y.; Nam, J.-H.; Jung, H.-J.; Park, S.-K.; Park, H.-J. *Biol. Pharm. Bull.* **2005**, *28*, 1915-1918.
- [5] Matsuoka, R.; Horiguchi, Y.; Kuwajima, I. *Tetrahedron Lett.* **1987**, *28*, 1299-1302.
- [6] Sasaki, M.; Kondo, Y.; Kawahata, M.; Yamaguchi, K.; Takeda, K. *Angew. Chemie. Int. Ed.* DOI: 10.1002/ange.201102430
- [7] (a) Reich, H. J.; Eisenhart, E. K.; Olson, R. E.; Kelly, M. J. *J. Am. Chem. Soc.* **1986**, *108*, 7791-7800. (b) Brekan, J. A.; Reynolds, T. E.; Scheidt, K. A. *J. Am. Chem. Soc.* **2010**, *132*, 1472-1473. (c) Sasaki, M.; Kondo, Y.; Kawahata, M.; Yamaguchi, K.; Takeda, K. *Angew. Chemie. Int. Ed.* DOI: 10.1002/ange.201102430. (d) Mitachi, K.; Yamamoto, T.; Kondo, F.; Shimizu, T.; Miyashita, M.; Tanino, K. *Chem. Lett.* **2010**, *39*, 630-632.
- [8] Crandall, J. K.; Batal, D. J. *J. Org. Chem.* **1988**, *53*, 1338-1340.
- [9] Zhang, Y.; Cusick, J. R.; Ghosh, P.; Shangguan, N.; Katukojvala, S.; Inghrim, J.; Emge, T. J.; Williams, L. J. *J. Org. Chem.* **2009**, *74*, 7707-7714.
- [10] Sato, F.; Oguro, K.; Watanabe, H.; Sato, M. *Tetrahedron Lett.* **1980**, *21*, 2869-2872.
- [11] Nicewicz, D. A.; Johnson, J. S. *J. Am. Chem. Soc.* **2005**, *127*, 6170-6171.
- [12] Boyce, G. R.; Johnson, J. S. *Angew. Chem. Int. Ed.* **2010**, *49*, 8930-8933.
- [13] Luzzio, F. A. *Tetrahedron* **2001**, *57*, 915-945.
- [14] Kogan, T. P.; Gaeta, F. C. A. *Synthesis* **1988**, 706-707.
- [15] Brook, A. G. *Acc. Chem. Res.* **1974**, *7*, 77-84.

- [16] Sommer, L. H.; Tyler, L. J.; Whitmore, F. C. *J. Am. Chem. Soc.* **1948**, *70*, 2872-2874.
- [17] (a) Tamao, K.; Ishida, N.; Tanaka, T.; Kumada, M. *Organometallics* **1983**, *2*, 1694-1696. (b) Fleming, I.; Henning, R.; Parker, D. C.; Plaut, H. E.; Sanderson, P. E. J. *J. Chem. Soc. Perkin Trans. 1* **1995**, 317-336.
- [18] (a) Becke, A. D. *J. Chem. Phys.* **1993**, *98*, 5648-5652. (b) Lee, C. T.; Yang, W. T.; Parr, R. G. *Phys. Rev. B* **1988**, *37*, 785-789. (c) Hariharan, P. C.; Pople, J. A. *Theor. Chim. Acta.* **1973**, *28*, 213-222. (d) Francl, M. M.; Pietro, W. J.; Henre, W. J.; Binkley, J. S.; Gordon, M. S.; DeFrees, D. J.; Pople, J. A. *J. Chem. Phys.* **1982**, *77*, 3654-3665.
- [19] Casiraghi, G.; Battistini, L.; Curti, C.; Rassu, G.; Zanardi, F. *Chem. Rev.* **2011**, *111*, 3076-3154.
- [20] Schmitt, D. C.; Johnson, J. S. *Org. Lett.* **2010**, *12*, 944-947.
- [21] Greszler, S. N.; Johnson, J. S. *Angew. Chem., Int. Ed.* **2009**, *48*, 3689-3691.
- [22] (a) Lecea, B.; Arrieta, A.; Morao, I.; Cossío, F. P. *Chem. Eur. J.* **1997**, *3*, 20-28. (b) Hara, K.; Tosaki, S.-Y.; Gnanadesikan, V.; Morimoto, H.; Harada, S.; Sugita, M.; Yamagiwa, N.; Matsunaga, S.; Shibasaki, M. *Tetrahedron* **2009**, *65*, 5030-5036.
- [23] (a) Ito, H.; Ito, T. *Chem. Lett.* **1985**, 1251. (b) Diel, B. N.; Hope, H. *Inorg. Chem.* **1986**, *25*, 4448. (c) Kovacs, T.; Speier, G.; Reglier, M.; Giorgi, M.; Vertes, A.; Vanko, G. *Chem Commun.* **2000**, 469. (d) Simonsen, O. *Acta Crystallogr., Sect B: Struct. Crystallogr. Cryst. Chem.* **1973**, *29*, 2600.
- [24] CCDC 827440 (5a-TIPS) and CCDC 830724 (8a) contain the supplementary crystallographic data for this paper. These data can be obtained free of charge from The Cambridge Crystallographic Data Centre via www.ccdc.cam.ac.uk/data_request/cif.
- [25] Wasserman, H. H.; Petersen, A. K.; Xia, M. *Acc. Chem. Res.* **2004**, *37*, 687-701.
- [26] Plietker, B. *J. Org. Chem.* **2004**, *69*, 8287-8296.
- [27] Donohoe, T. J.; Blades, K.; Moore, P. R.; Waring, M. J.; Winter, J. J. G.; Helliwell, M.; Newcombe, N. J.; Stemp, G. *J. Org. Chem.* **2002**, *67*, 7946-7956.
- [28] Alaimo, P. J.; Peters, D. W.; Arnold, J.; Bergman, R. G. *J. Chem. Ed.* **2001**, *78*, 64.
- [29] Hitce, J.; Trost, B. M. *J. Am. Chem. Soc.* **2009**, *131*, 4572-4573.

- [30] Dockendorff, C.; Sahli, S.; Olsen, M.; Milhau, L.; Lautens, M. *J. Am. Chem. Soc.* **2005**, *127*, 15028-15029.
- [31] Chi, Y.; Guo, N. A.; Kopf, A.; Gellman, S. H. *J. Am. Chem. Soc.* **2008**, *130*, 5608-5609.

CHAPTER THREE

SILYL GLYOXIMIDES AS ASYMMETRIC CONJUNCTIVE REAGENTS THROUGH LONG-RANGE STEREOINDUCTION

3.1. Introduction

Remote stereocontrol, the ability to control stereoselectivity at sites greater than 3 carbon centers away from the stereoinducing group, has been a topic of significant interest since it mimics the high levels of control and selectivity usually reserved for enzyme-catalyzed reactions. Since the concept of remote stereocontrol was originally developed by Breslow over 30 years ago,¹ few effective methodologies for such stereocontrol have been developed for acyclic substrates.² While controlling acyclic stereochemistry at proximal sites (1,2 or 1,3 relationships) is well-established, the ability to affect stereocontrol at remote sites remains quite challenging. While successful examples of remote stereocontrol in 1,4 and 1,5 relationships have been developed in recent years,² these methodologies are typically highly substrate dependent and not widely applicable. Furthermore, examples of employing remote stereocontrol in the vinylogous Michael reaction is rare in the literature with only a few examples reported as of a review on the topic in 2011.³ In this Chapter, the utility of silyl glyoximides as a new class of asymmetric conjunctive reagents in the vinylation-initiated vinylogous Michael

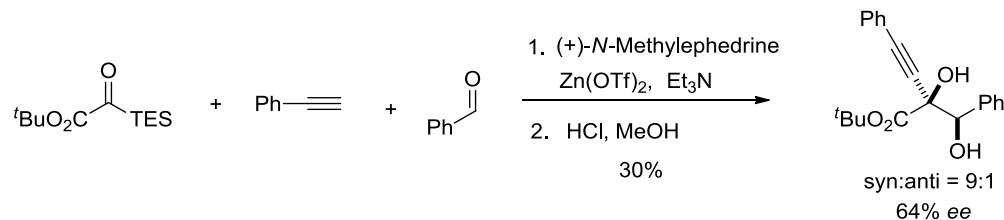
cascade of silyl glyoximides, nitroalkenes and vinylmagnesium bromide is reported. The disclosed methodology affords enolsilanes with complete regio- and diastereoselectivity. This disclosed methodology exploits a rare opportunity to utilize a 1,7 stereochemical relationship to provide complete asymmetric induction in the vinylogous Michael reaction. A discussion of investigations into the attempted secondary derivitizations of these stereodefined enolsilanes is also presented.

3.2. Background

3.2.1. Inducing Asymmetry in Silyl Glyoxylate Couplings

Inducing asymmetry in silyl glyoxylate couplings has been a topic of significant interest in our group since the inception of the reagent. In the first coupling reported by Nicewicz and Johnson,⁴ a preliminary result was described that employed Carreira's method⁵ for the enantioselective addition of terminal alkynes to aldehydes in the reported silyl glyoxylate coupling as illustrated in Scheme 3.1. Although useful levels of enantioselectivity were not observed, the result did provide evidence that inducing asymmetry in silyl glyoxylate couplings was possible. Since then, three examples of

Scheme 3-1. Asymmetric Induction in the Alkynylation of Silyl Glyoxylates Cascade



asymmetric silyl glyoxylate couplings have been developed as seen in Scheme 3.2. The first method that provided useful levels of selectivity was developed by Linghu and

Satterfield.⁶ This coupling provides the desired glycolate aldol product **1** in a 65% yield with 15:1 diastereoselection. This result demonstrates that chiral auxiliaries attached to the ester of the silyl glyoxylate can afford impressive levels of selectivity. Regrettably, this method proved to be highly substrate dependent and was not able to be developed to include a wider substrate scope. The second methodology provided a highly general method for the formation of functionalized Claisen condensation products due to a 1,4-stereochemical induction.⁷ This methodology provides for the efficient transmission of the β -lactone stereochemistry to the emerging fully substituted stereocenter with >20:1 diastereoselection for most examples. To date, this methodology remains the most widely applicable asymmetric coupling in silyl glyoxylate chemistry. The final asymmetric three-component coupling of silyl glyoxylates, an enolate addition/[1,2]-Brook rearrangement/Michael addition cascade is still in the developmental stage.⁸ The diastereoselectivity observed in this coupling further corroborates the finding by Linghu and coworkers that chiral auxiliaries on the ester portion of the silyl glyoxylate can be effective at asymmetric induction.

compound **2**. Kobayashi rationalized the high level of diastereoselectivity with the transition states proposed in Figure 3-1. The Kobayashi group assumed that the oxazolidinone ring was perpendicular to plane of the dienolsilane such that the isopropyl substituent would block the upper face of the substrate as depicted in structure **2**. With the facial selectivity of the nucleophile explained, Kobayashi employed a Newman project **3** to rationalize the approach of the aldehyde electrophile. Since the initial report, this 1,7-remote asymmetric induction has been used by the group in several total syntheses.¹⁰ To date, this methodology remains the only example of successful 1,7-remote asymmetric induction.

Scheme 3-3. Vinylogous Mukaiyama Aldol Reaction with Vinylketene Silyl *N,O*-Acetals

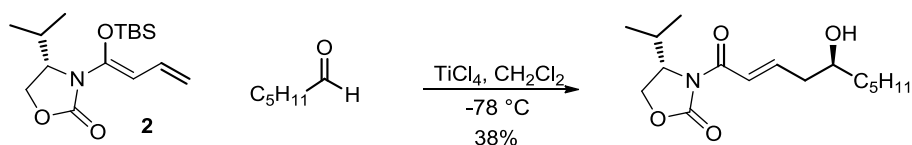
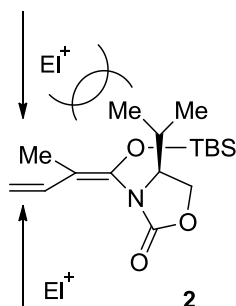
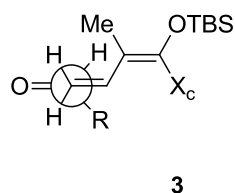


Figure 3-1. Proposed Transition State for the 1,7-Remote Asymmetric Induction of Vinylketene Silyl *N,O*-Acetals

Explanation for Facial Selectivity



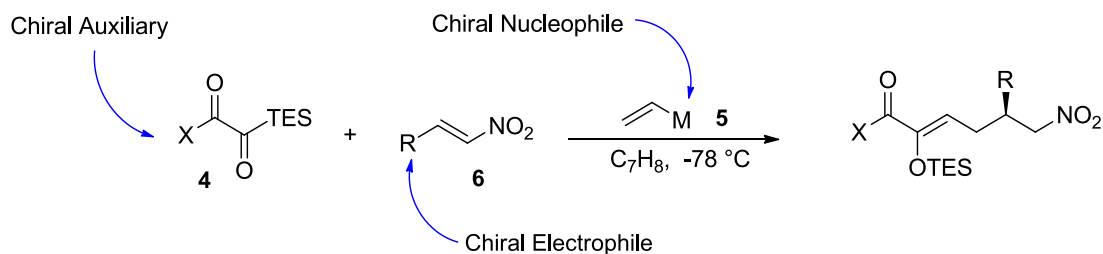
Newman Project for Preferred Aldehyde Approach



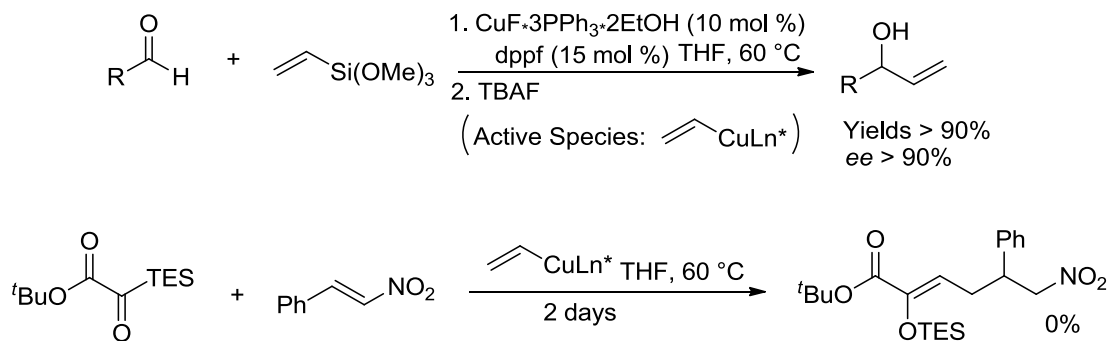
3.2.3. Origin of the Title Reaction and Initial Experiments

Based on the precedent for asymmetric silyl glyoxylate couplings summarized Section 3.2.1., we investigated the potential for inducing asymmetry in the three-component coupling reaction of silyl glyoxylates, nitroalkenes and vinylmagnesium bromide reported in Chapter 1. As illustrated in Scheme 3-4, the conceptual framework of the reported silyl glyoxylate chemistry provides for variation at three positions to provide asymmetry: a chiral auxiliary on the silyl glyoxylate **4**, a chiral nucleophile **5**, and a chiral electrophile **6**. Since chiral nitroalkenes are highly specialized substrates that are rarely reported in the literature, the two other variations were investigated. Initial studies with a chiral nucleophile based on the Shibasaki's enantioselective vinylation of aldehydes¹² provided only recovered starting material as illustrated in Scheme 3-5. Since chiral auxiliaries have shown promise in previous couplings, the application of chiral auxiliaries in the vinylogous Michael three-component coupling was investigated.

Scheme 3-4. Conceptual Framework for Asymmetry in the Vinylogous Michael Cascade



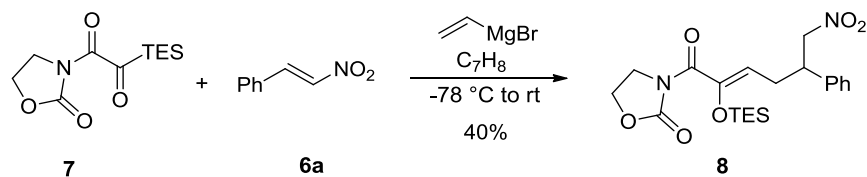
Scheme 3-5. Shibasaki's Synthesis of Allylic Alcohols and Attempted Application in the Silyl Glyoxylate Three-Component Coupling



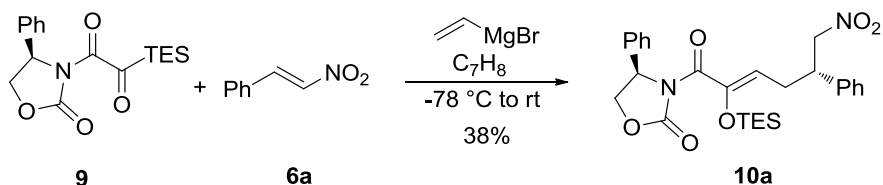
In conjunction with ynamide oxidation studies in their group, Hsung and coworkers synthesized a novel class of reagents known as silyl glyoximides.¹¹ The Hsung group generously provided us with several silyl glyoximide samples to investigate into the potential of these reagents as umpolung pronucleophiles.

Initial studies with the unsubstituted silyl glyoximide **7** demonstrated that these reagents can function as capable conjunctive reagents in the same manner as silyl glyoxylates as illustrated in Scheme 3.6 by providing a 40% isolated yield of **8** when each reagent is utilized in equal amounts. The stereodefined phenyl substituted silyl glyoximide **9** was then subjected to the reaction manifold as illustrated in Scheme 3-7 to determine whether the stereodefined imido acyl silane would react similarly and provide the desired asymmetric induction. Employing equivalent amounts of each reagent provided the desired γ -adduct **10a** in a 38% isolated yield as one diastereomer.

Scheme 3-6. Initial Silyl Glyoximide Three-Component Coupling



Scheme 3-7. Application of Imido Acyl silane **9** to the Three-Component Reaction Manifold



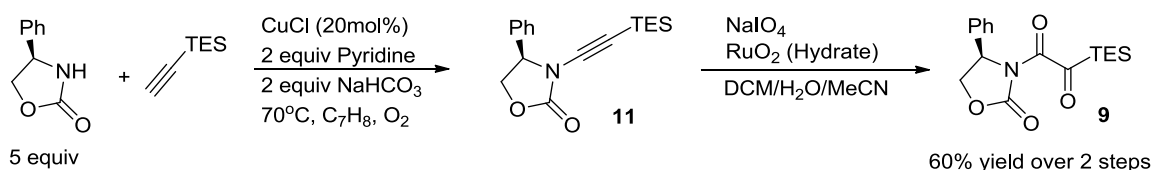
This initial silyl glyoximide result provided some useful information on the reactivity of the imido acyl silane. Unlike in silyl glyoxylate couplings where silyl glyoxylate oligomerization is the main byproduct; the main byproduct for the imido acyl silane coupling is the quenched metallodienolate species. The reaction was monitored by TLC every 10 °C while allowing the reaction to warm to room temperature. The three-component coupling product spot began to appear around -10 °C meaning that the vinylogous Michael reaction began to occur when the reaction reaches that temperature. Since the silyl glyoximide coupling is not susceptible to oligomerization, it is likely that reaction optimization can allow for no excess of the precious silyl glyoximide as opposed to the 50% excess required for the silyl glyoxylate couplings disclosed in Chapters 1 and 2.

3.3. Results and Discussion

3.3.1. Synthesis of Silyl Glyoximide **9**

Silyl glyoximide **9** was synthesized by the Hsung group in order to highlight the utility of their ynamide oxidation methodology.¹¹ The requisite ynamide **11** worked very well in the oxidation methodology providing a yield of 83% as illustrated in Scheme 3-8. However, the ynamide synthesis from the requisite oxazolidinone and alkyne was regrettably inefficient providing only a 23% yield under the aerobic oxidation conditions.¹¹ Since the silyl glyoximide would need to be readily accessible to be a useful coupling partner in the three-component coupling methodology, we sought to raise the yield of this step. Employing Stahl's conditions for the aerobic oxidation of terminal alkynes provided the desired ynamide **11** in a 74% yield. This optimization allowed for the desired silyl glyoximide product **9** to be isolated in a 60% overall yield over two steps as opposed to a 19% yield over two steps. With a reliable synthesis of the imido acyl silane in hand, the optimal conditions of the three-component coupling were investigated.

Scheme 3-8. Optimized Synthesis of Silyl Glyoximide **9**

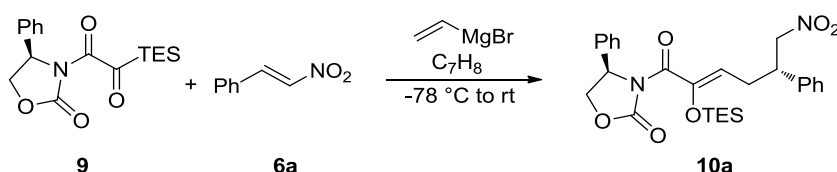


3.3.2. Optimization of the Reaction Parameters

Optimization studies began with a brief solvent screen. Of the solvents examined (toluene, THF, CH₂Cl₂, Et₂O), toluene was deemed the best solvent for the reaction since it provided the highest levels of nitroalkene consumption. The stoichiometry of the three-

component coupling was then varied to determine the optimal equivalents of each reagent. Increasing the equivalents of the nitroalkene secondary electrophile **6a** to 1.5 had a drastic effect on the yield as seen in entry 2. While 50% excess of the secondary electrophile provided almost twice the yield of the initial trial, increasing the equivalence to 100% (entry 3) provided negligible benefit.

Table 3-1. Stoichiometry Screen for the Silyl Glyoximide Three-Component Coupling



entry	9 (equiv)	6a (equiv)	vinylmagnesium bromide (equiv)	yield ^b
1	1	1	1	47%
2	1	1.5	1.5	76%
3	1.5	2	1.5	77%

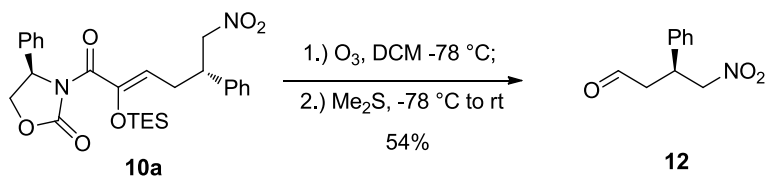
^aAll reactions were conducted $[9]_0 = 0.1\text{ M}$ with the reaction warmed to room temperature immediately after the addition was complete. ^bYields determined by 1H NMR spectroscopy compared to an internal standard of mesitylene.

3.3.3. Solving the Stereochemistry of Enolsilane **10a**

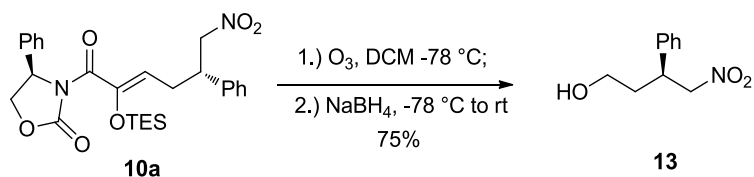
Since the three-component coupling product **10a** was isolated as a liquid, x-ray crystallography would not be possible. Instead, conversion to a compound of known absolute stereochemistry was required to identify the stereoisomer of the product. The optical rotations for both enantiomers of 4-nitro-3-phenyl butanal **12** are known, so we sought to convert γ -adduct **10a** to this compound by cleaving the olefin by ozonolysis as illustrated in Scheme 3-9.¹³ The ozonolysis provided 4-nitro-3-phenyl butanal as anticipated in a 54% yield. The optical rotation of this compound was taken and found to match the reported rotation for the (*S*)-enantiomer. To confirm that these results **10a** was

converted 4-nitro-3-phenylbutan-1-ol **13** by reductive ozonolysis in a 75% yield as depicted in Scheme 3-10.¹⁴ SFC analysis of this derivative showed a 96:4 enantiomeric ratio for the product which agrees well with the NMR analysis of the diastereoselectivity of the original three-component coupling. With the selectivity and the identity of the major diastereomer unambiguously assigned, we then investigated the scope of the reaction.

Scheme 3-9. Ozonolysis of **10a**



Scheme 3-10. Reductive Ozonolysis of **10a**

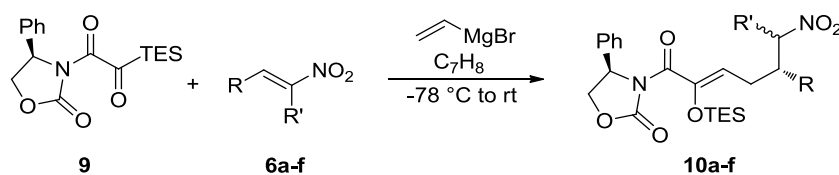


3.3.4. Reaction Scope

With the optimized conditions in hand for the imido acyl silane three-component coupling, a preliminary scope of amenable nitroalkene electrophilic partners was investigated. The results presented in Table 3.2 show that a wide variety of functionality is well tolerated by the reaction manifold. Aryl, heteroaryl, alkenyl and alkyl examples all provided very good yields ranging from 69-78% (entries 1-4). Nitroalkenes that were incompatible with previous silyl glyoxylate couplings such as α -methyl- β -nitrostyrene **6e** (entry 5) and ethyl 2-nitrovinyl ether **6f** (entry 6) provided the desired γ -adducts in 47%

and 70% yields respectively. The impressive level of functionality tolerated by this three-component coupling is a function of the lack of oligomerization byproducts which leaves the transient secondary nucleophile free to engage the secondary electrophile. This lack of oligomerization may be due to several factors including the added steric bulk of the chiral auxiliary, the altered electronics of the secondary nucleophile and the presumably delayed [1,2]-Brook rearrangement.

Table 3-2. Nitroalkene Substrate Scope for the Three-Component Coupling



entry	product	R	R'	yield (%)	d.r.
1	10a	Ph	H	78	>20:1
2	10b	2-furyl	H	77	>20:1
3	10c	(<i>E</i>)-styryl	H	67	>20:1
4	10d	<i>i</i> -Pr	H	71	>20:1
5	10e	Ph	Me	47	>20:1
6	10f	OEt	H	70	>20:1

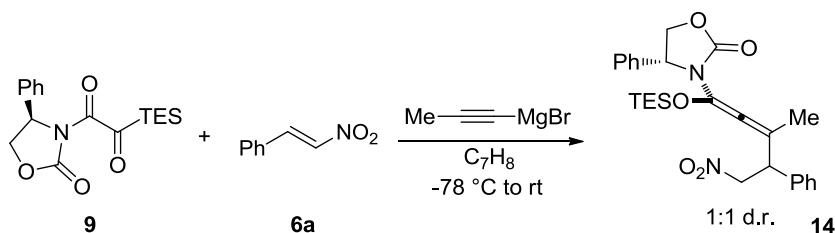
^aAll reactions were conducted $[9]_0 = 0.1\text{ M}$ with the reaction warmed to room temperature immediately after the addition was complete and stirred for 1.5 hrs. ^bIsolated Yield. See section 3.7 for additional experimental details.

Future studies will include augmenting the scope with additional nitroalkene substrates to provide a more complete understanding of the types of substrates that are compatible in the reaction manifold. Based on the highly varied levels of functionality inherent in the six substrates screened, significant diversification at the electrophilic partner is anticipated. Adding substitution to the nucleophilic partner will also be

investigated. Since oligomerization is unfavored in this coupling, it is possible that more functionalized vinyl Grignard reagents can be utilized.

To determine whether this excellent diastereoselectivity had wider applicability in other vinylogous Michael cascades, 1-propynylmagnesium bromide was employed in the reaction manifold. Although the reaction did provide the desired silyloxyallene **14** as illustrated in Scheme 3-11, the product was formed in a 1:1 diastereomeric ratio. The lack of asymmetric induction implies that a different mechanism is at work in this coupling compared to the vinylmagnesium bromide coupling.

Scheme 3-11. Silyl Glyoximide Coupling Employing 1-Propynylmagnesium Bromide



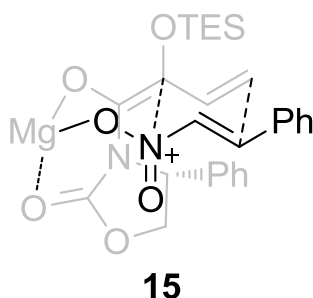
3.3.5. Proposed Transition State

Since the alkynyl nucleophile did not impart asymmetric induction to the reaction manifold, we can conclude that the transition state proposed for the alkynylation initiated coupling reported in Chapter 2 is not operative in the current three-component coupling. This suggests that the dicoordination of the nitro group to the presumed (*Z*)-metallodienolate is not occurring in the transition state, however the complete selectivity observed in the reaction requires that the approach of the nitroalkene to the (*Z*)-metallodienolate be highly ordered. Any ordered transition state for this type of coupling likely still relies on the chelating potential of the nitro group to the magnesium cation of

the (*Z*)-dienolate. For this reason, we propose a monodentate coordination of the nitro group to the nucleophilic partner.

Previous studies have invoked both the mono and dicoordination of the nitro group depending on the exact conditions of the reaction.¹⁵ In this instance, it is possible that the added steric bulk of the oxazolidinone disfavors the dicoordinate orientation. Proceeding with this hypothesis, the following transition state **15**, illustrated in Figure 3-2, is proposed.

Figure 3-2. Proposed *trans* Decalin-Like Transition State for the Silyl Glyoximide Coupling



While organized transition states with more than six members are unusual; there is significant precedent for 10-membered decalin-like transition state structures when multiple electronic interactions are possible.¹⁶ The proposed decalin-like transition state hinges on the electronic attraction between the positively charged nitrogen atom of the nitro group and the accumulation of negative charge at the α -position of the (*Z*)-metallodienolate. This electronic interaction in conjunction with the monocoordination of the nitro group oxygen to the magnesium cation provides the necessary framework for the fused 6,6 ring system. The (*Z*)-geometry of the metallodienolate would force the decalin transition state into a *trans* orientation. This proposed transition state allows the R

substituent of the nitroalkene to adopt the favored *pseudo*-equatorial position which corroborates the feasibility of this proposed transition state. Future studies will include the incorporation of other types of Michael acceptors such as α,α -dicyanoolefins and malonates. Based on the diastereoselectivity observed in these three-component couplings, the importance of coordination of the electrophile to the (*Z*)-metallodienolate can be determined. This methodology may also benefit from a quantum mechanical evaluation of the intermediates and transition states using the density functional theory (DFT) approach at the level of B3LYP/6-311G(d).

3.4. Secondary Transformation to Asymmetric Cyclopentanol Derivatives

As enumerated in Chapter 1, the ε -nitro silyl enol ether moiety is well poised to undergo Henry cyclization by functioning as a latent nitroketone species. This type of transformation was well suited for the enolsilanes synthesized in Chapter 1 and a modified procedure enabled access to cyclopentenols from silyloxyallenes in Chapter 2. The enolsilanes provided by the current methodology would allow access to similar cyclopentane derivatives with high levels of enantiopurity.

As noted in Chapter 2, the cyclopentanols provided by the original vinylogous Michael adducts accessed in Chapter 1 provide limited opportunity to functionalize the C4 and C5 positions of the cyclopentanol thereby restricting the utility of the substrates. Since the stereodefined ε -nitro silyl enol ethers provided by the disclosed methodology will provide the same functional drawback, we chose to investigate a novel Henry cyclization cascade which would arrive at the same cyclopentenols accessed in Chapter 2 from the ε -nitro silyl enol ethers. To accomplish this transformation, the oxidation state of the δ -position of the enolsilane would have to be increased to the olefin as illustrated

in Scheme 3-12. We envisioned this oxidation state alteration/Henry cyclization cascade occurring by the strategy outlined in Figure 3-3. The proposed alternative Henry cyclization would require the attachment of a leaving group X to substrate **10** by utilizing the inherent nucleophilicity of the silyl enol ether moiety. Once **16** is formed the Henry cyclization should proceed without incident to provide intermediate **17** in a similar manner to the methodology disclosed in Chapter 1. At this point, elimination of X as a leaving group will provide the desired stereodefined cyclopentenol **18**. Halogenation of the silyl enol ether moiety would likely be the most direct route to the desired α -functionalization.

Scheme 3-12. Comparison of the Reported Henry Cyclization to the Proposed Cyclization

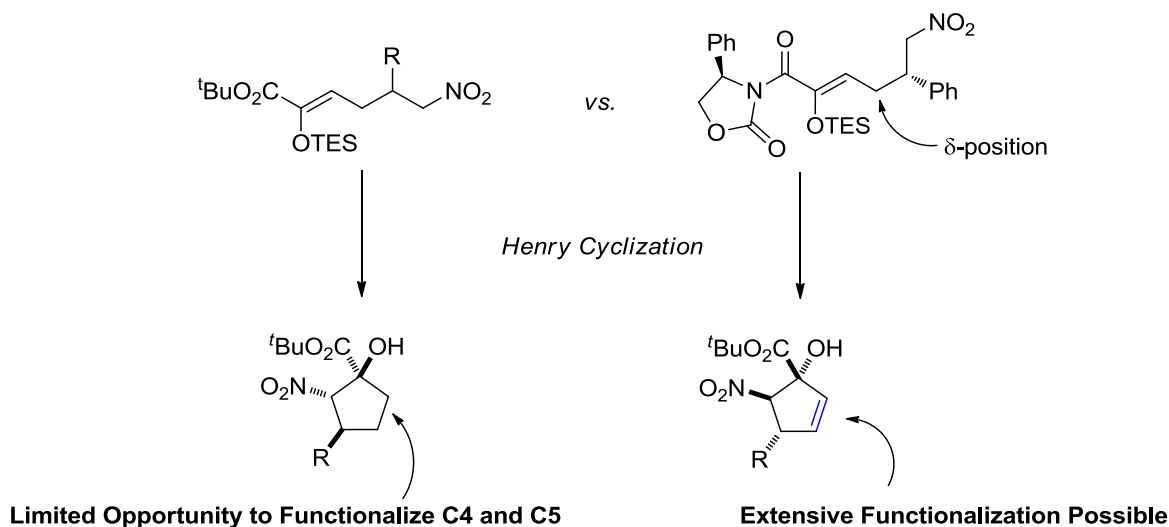
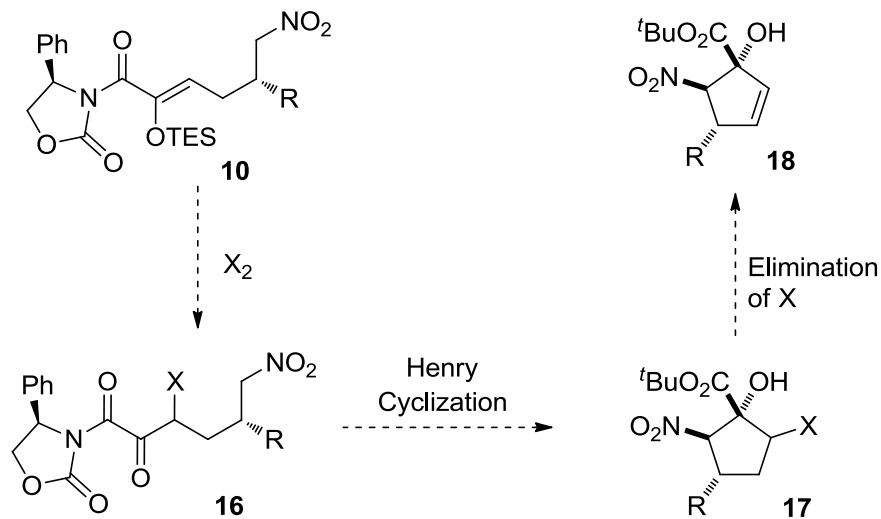


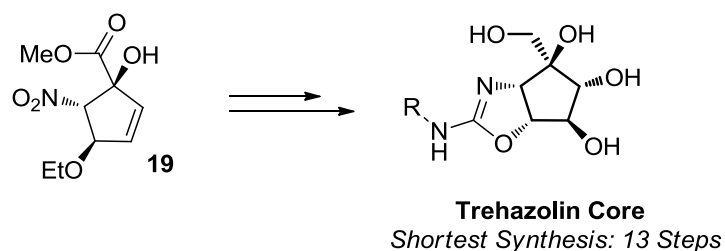
Figure 3-3. Strategy for the Synthesis of Cyclopentenols from Enolsilanes



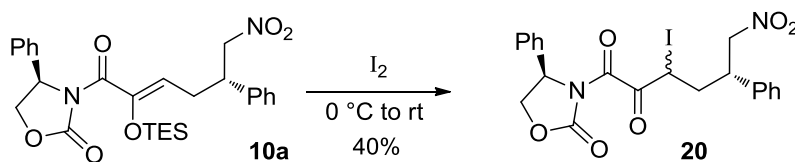
3.4.1 Asymmetric Cyclopentanol Synthesis

The heteroatom substituted enolsilane **10f** was utilized in these studies due to the structural similarities the cyclized adduct **19** would have with the aminocyclitol natural product (+)-trehazolin as illustrated in Figure 3-4.¹⁷ Investigations commenced with the attempted halogenations with bromine and iodine sources. A variety of conditions for these transformations (Br_2 , I_2 , NBS, NIS, ICl) provided either the acyclic α -haloketone or a complex product mixture. The iodoketone of **10a** was readily accessible from treatment with I_2 providing the halogenated product **20** in a 40% yield as shown in Scheme 3-13. Subsequent treatment with a variety of amine and alkoxide bases provided complex product mixtures with no desired product isolated.

Figure 3-4. Structural Similarities between Cyclopentenol **19** and the Core Structure of (+)-Trehazolin



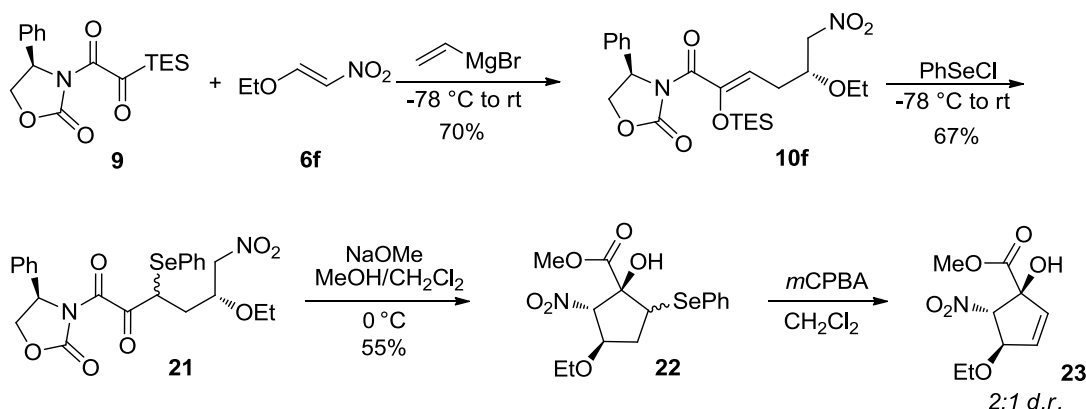
Scheme 3-13. Iodination of Enolsilane **10a**



With the halogenation route proving to be problematic, experiments utilizing selenium chemistry were initiated. Treating **10f** with phenylselenium chloride provided the desired selenide **21** in a 67% yield as illustrated in Scheme 3-14. Treatment of the selenide **21** with NaOH provided the cyclized selenide **22** in a 57% yield and a 3:1 diastereomeric ratio. At this point it was unknown whether the poor diastereoselection was a function of the stereogenic organoselenide or a cyclization event with poor diastereoselectivity. Treatment of the cyclized product **22** with *m*CPBA at room temperature provided the desired elimination of the selenoxide species to provide cyclopentenol **23**. Regrettably, cyclopentenol **23** was isolated with a non-synthetically useful 2:1 diastereomeric ratio. The diastereoselectivity may be able to be enhanced by re-exposing the cyclopentenol to basic methanol conditions. The two preceding chapters illustrated that the diastereoselection of the Henry cyclization can be enhanced upon re-

exposure to basic conditions at 0 °C. Future studies will investigate this potential solution to provide for the highly diastereoselective rapid assembly of complex, highly oxygenated cyclopentane derivatives.

Scheme 3-14. Synthesis of Cyclopentenol **23** Utilizing Organoselenium Chemistry



3.5. Conclusion

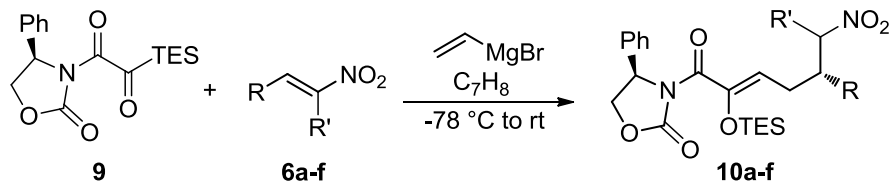
Preliminary studies for a novel reactivity pattern for silyl glyoximides, vinylmagnesium bromide, and nitroalkenes to provide for the highly diastereoselective synthesis of (*Z*)-enolsilanes is disclosed. The three-component coupling provides good to very good yields for nitroalkene substrates with a wide range of functionality including aryl, heteroaryl, alkenyl, alkyl, ether substitution at the β -site and either hydrogen or methyl substitution at the α -site of the nitroalkene. A possible *trans* decalin-like transition state is proposed as a plausible explanation for the excellent long-range stereochemical induction observed in this coupling. Lastly, preliminary studies on novel Henry cyclization reactions to diastereomerically and enantiomerically pure cyclopentane derivatives were recounted. Future studies will include the expansion of the substrate

scope and further investigations into potential valuable secondary derivations of the enolsilane products.

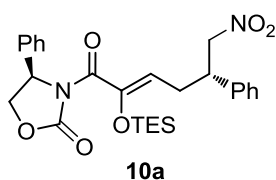
3.6 Experimental Details

Materials and Methods: General. Infrared (IR) spectra were obtained using a Nicolet 560-E.S.P. infrared spectrometer. Proton and carbon nuclear magnetic resonance spectra (^1H and ^{13}C NMR) were recorded on either a Bruker model Avance 500 (^1H at 500 MHz and ^{13}C NMR at 125 MHz), or a Bruker model Avance 400 (^1H NMR at 400 MHz and ^{13}C NMR at 100 MHz) spectrometer with solvent resonance as the internal standard (^1H NMR: CDCl_3 at 7.26 ppm; ^{13}C NMR: CDCl_3 at 77.0 ppm). ^1H NMR data are reported as follows: chemical shift, multiplicity (s = singlet, br s = broad singlet, d = doublet, t = triplet, q = quartet, sept = septet, m = multiplet), coupling constants (Hz), and integration. Analytical thin layer chromatography (TLC) was performed on Whatman 0.25 mm silica gel 60 plates. Visualization was accomplished with UV light and aqueous ceric ammonium molybdate solution followed by heating. Purification of the reaction products was carried out by flash chromatography using Sorbent Technologies silica gel 60 (32-63 μm). All reactions were carried out under an atmosphere of nitrogen in oven-dried glassware with magnetic stirring. Yield refers to isolated yield of analytically pure material. Yields are reported for a specific experiment and as a result may differ slightly from those found in the tables, which are averages of at least two experiments. Dichloromethane, tetrahydrofuran, and toluene were dried by passage through a column of neutral alumina under nitrogen prior to use. Nitroalkenes **6a**, **6b**, **6c**, **6d**, **6e** are commercially available from Sigma-Aldrich. Nitroalkene **6f**^[18] was prepared according to the literature procedure.

General Procedure for the Asymmetric Synthesis of Enolsilanes (10a-10f)



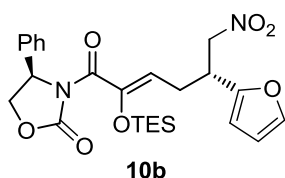
The triethylsilyl glyoximate^[11] **9** and nitroalkene **6a-e** were added to an oven-dried vial. The vial was then purged with N₂ and toluene (0.1 M) was added. The resulting solution was cooled to -78 °C using an acetone/dry ice bath and vinylmagnesium bromide was added dropwise to the solution. Once the addition was complete the reaction was allowed to warm to room temperature and stirred for 1 h then diluted with diethyl ether (5 mL), and quenched with saturated ammonium chloride (5 mL). The resulting mixture was stirred for 10 min. The layers were separated, and the aqueous layer was extracted with ethyl acetate (3 x 10 mL). The organic extracts were combined, washed with brine (5 mL), dried with magnesium sulfate, and concentrated *in vacuo*. The crude mixture was purified by flash chromatography (15% EtOAc/hexanes) to afford products **10a-f**.



(R)-3-((S,E)-6-nitro-5-phenyl-2-((triethylsilyl)oxy)hex-2-enyl)-4-phenyloxazolidin-2-one (10a): The title compound was prepared according to the general procedure using **9** (30.0 mg,

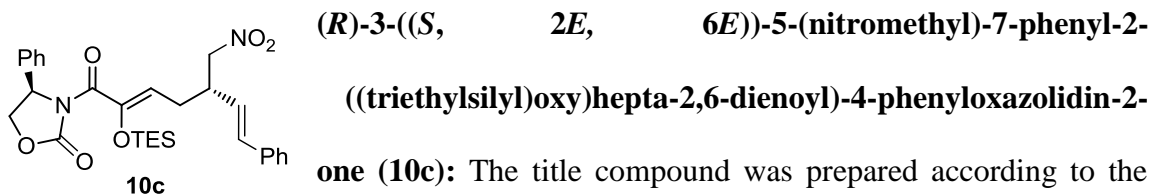
0.090 mmol, 1.0 equiv), nitroalkene **6a** (20.1 mg, 0.1349 mmol, 1.5 equiv), and vinylmagnesium bromide (0.12 mL, 0.1169 mmol, 1.2 equiv). Once the addition was complete the reaction was allowed to warm to room temperature and stirred for 1 h then quenched. The crude mixture was purified by flash chromatography (15% EtOAc/hexanes) to afford 34.5 mg (75%) of the product as a yellow oil. Analytical data

for **10a**: **IR** (thin film, cm^{-1}): 3436, 3064, 3032, 2957, 2913, 2877, 1785, 1692, 1644, 1552, 1381, 1320, 1204, 1157; **^1H NMR** (400 MHz, CDCl_3): δ 7.41-7.24 (m, 10H), 5.51-5.47 (m, 2H), 4.75-4.63 (m, 3H), 4.26 (dd, $J = 8.4, 7.2$ Hz, 1H), 3.70-3.62 (m, 1H), 2.71-2.55 (m, 2H), 0.97 (dd, $J = 8, 7.6$ Hz, 9H), 0.67 (q, $J = 8$ Hz, 6H); **^{13}C NMR** (100 MHz, CDCl_3): δ 165.9, 153.0, 144.6, 139.3, 137.2, 129.1, 129.0, 128.9, 127.7, 127.3, 126.4, 117.9, 79.5, 69.8, 58.5, 43.5, 29.6, 6.5, 5.2 ; **TLC** (20% EtOAc/hexanes) R_f 0.36. **LRMS** (ESI) Calcd. for $\text{C}_{27}\text{H}_{34}\text{N}_2\text{O}_6\text{SiNa}$: 533.21. Found: 533.1.

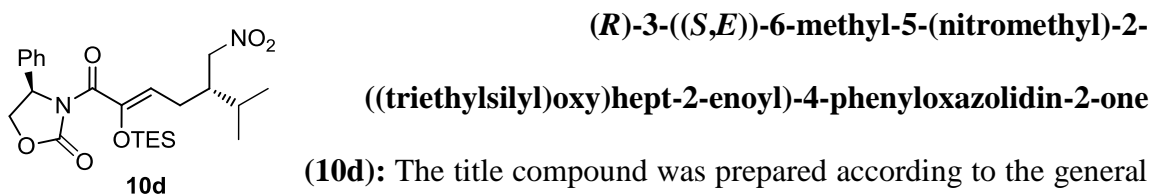


(R)-3-((R,E)-5-(furan-2-yl)-6-nitro-2-((triethylsilyl)oxy)hex-2-enoyl)-4-phenyloxazolidin-2-one (10b): The title compound was prepared according to the general procedure using **9** (30.0

mg, 0.090 mmol, 1.0 equiv), nitroalkene **6a** (19.0 mg, 0.1349 mmol, 1.5 equiv), and vinylmagnesium bromide (0.14 mL, 0.1349 mmol, 1.5 equiv). Once the addition was complete the reaction was allowed to warm to room temperature and stirred for 1 h then quenched. The crude mixture was purified by flash chromatography (15% EtOAc/hexanes) to afford 34.5 mg (77%) of the product isolated as an orange oil. Analytical Data for **10b**: **IR** (thin film, cm^{-1}): 2957, 2877, 2360, 2341, 1787, 1693, 1555, 1379, 1321, 1204, 746, 700; **^1H NMR** (600 MHz, CDCl_3): δ 7.37-7.30 (m, 7H), 6.32 (d, , $J = 1.8$ Hz, 1H), 6.31(d, , $J = 1.8$ Hz, 1H), 6.15-6.14 (m, 1H), 5.50-5.45 (m, 3H), 4.72-4.71 (m, 1H), 4.26-4.23 (m, 1H), 2.62-2.61 (m, 2H), 0.92-0.89 (m, 9H), 0.63-0.59 (m, 6H); **^{13}C NMR** (125 MHz, CDCl_3): δ 166.0, 153.2, 152.2, 144.9, 142.3, 137.0, 129.2, 129.1, 126.5, 117.7, 110.4, 107.1, 69.9, 58.5, 37.2, 27.1, 6.6, 5.1; **TLC** (30% EtOAc/hexanes) R_f 0.44.



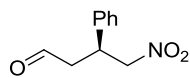
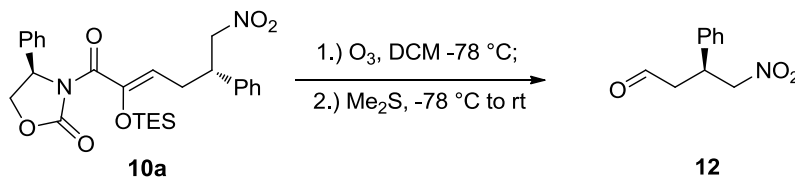
general procedure using **9** (30.0 mg, 0.090 mmol, 1.0 equiv), nitroalkene **6a** (23.6 mg, 0.1349 mmol, 1.5 equiv), and vinylmagnesium bromide (0.14 mL, 0.1349 mmol, 1.5 equiv). Once the addition was complete the reaction was allowed to warm to room temperature and stirred for 1 h then quenched. The crude mixture was purified by flash chromatography (15% EtOAc/hexanes) to afford 34.5 mg (69%) of the product as a yellow oil. Analytical Data for **10c**: **IR** (thin film, cm^{-1}) 2957, 2877, 1786, 1693, 1551, 1381, 1320, 1204, 1064, 1003, 747, 699; **^1H NMR** (600 MHz, CDCl_3): 7.37-7.25 (m, 10H), 6.98 (d, $J = 16.2$ Hz, 1H), 6.09-6.08 (m, 1H), 5.60-5.57 (m, 1H), 5.48-5.42 (m, 1H), 4.71 (t, $J = 3.0$ Hz, 1H), 4.53-4.52 (m, 1H), 4.52 (d, $J = 9.0$ Hz, 1H), 4.26-4.24 (m, 1H), 2.45-2.34 (m, 1H), 2.46-2.42 (m, 1H), 0.90-0.89 (m, 9H), 0.63-0.59 (m, 6H); **^{13}C NMR** (125 MHz, CDCl_3): δ 166.1, 153.2, 144.7, 137.1, 136.3, 133.3, 129.2, 129.1, 128.6, 127.9, 127.1, 126.5, 118.1, 79.0, 69.9, 58.6, 41.7, 28.4, 6.7, 5.1; **TLC** (30% EtOAc/hexanes) R_f 0.47.



procedure using **9** (30.0 mg, 0.090 mmol, 1.0 equiv), nitroalkene **6d** (15.5 mg, 0.1349 mmol, 1.5 equiv), and vinylmagnesium bromide (0.14 mL, 0.1349 mmol, 1.5 equiv). Once the addition was complete the reaction was allowed to warm to room temperature

and stirred for 1.5 hr then quenched. The crude mixture was purified by flash chromatography (15% EtOAc/hexanes) to afford 34.5 mg (71%) of the product as a pale yellow oil. Analytical Data for **10d**: **IR** (thin film, cm^{-1}): 2459, 2877, 2360, 1788, 1693, 1550, 1383, 1205, 1004, 745, 700; **^1H NMR** (600 MHz, CDCl_3): δ 7.40-7.33 (m, 5H), 5.60-5.58 (m, 1H), 5.50-5.47 (m, 1H), 4.36-4.34 (m, 1H), 4.31-4.25 (m, 3H), 2.39-2.15 (m, 3H), 1.88-1.68 (m, 1H), 0.95-0.88 (m, 15H), 0.62-0.58 (m, 6H); **^{13}C NMR** (125 MHz, CDCl_3): δ 166.1, 153.3, 144.7, 137.0, 129.2, 129.1, 126.5, 120.3, 69.9, 58.7, 41.7, 28.4, 6.7, 5.1; **TLC** (30% EtOAc/hexanes) R_f 0.59.

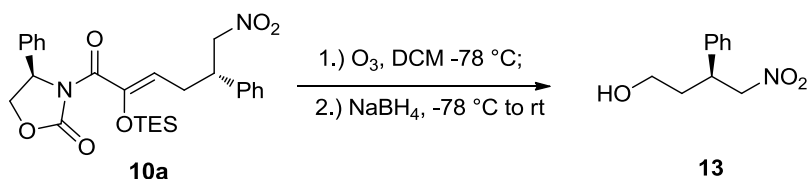
Procedure for the Preparation of (S)-4-nitro-3-phenylbutanal (12):



(S)-4-nitro-3-phenylbutanal (12): A 20-mL scintillation vial was charged with **10a** (35 mg, 0.069 mmol, 1.0 equiv) and CH_2Cl_2 (1.0 mL, 0.07 M). Ozone was bubbled through the solution at -78°C until the solution turned a light blue. The reaction was then purged with N_2 for 15 minutes until the color dissipated. Dimethyl sulfide (0.08 mg, 0.135 mmol, 5.0 equiv) was added and the reaction was warmed to room temperature. Once the reaction was complete the solution was diluted with CH_2Cl_2 (5 mL) and H_2O (5 mL). The layers were separated and the aqueous layer was extracted with methylene chloride (3 x 5 mL). The combined organic extracts were washed with brine (5 mL), dried with sodium sulfate, and concentrated *in vacuo*. The crude mixture

was purified by flash chromatography (30% EtOAc/hexanes) to provide 13.4 mg (52%) of the product as a colorless oil. ^1H NMR spectral data matched those reported for the title compound **12**.^[13] $[\alpha]_{\text{D}} -24$ (c 0.71, (CHCl_3))

Procedure for the Preparation of (S)-4-nitro-3-phenylbutan-1-ol (13):

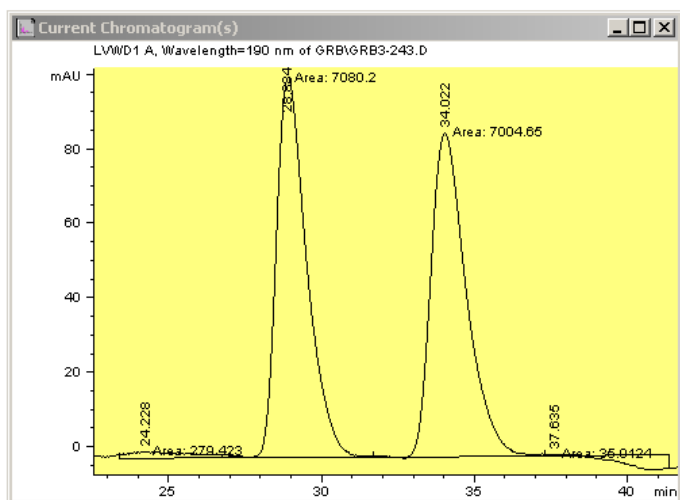


(S)-4-nitro-3-phenylbutan-1-ol (13): A 20-mL scintillation vial was charged with **10a** (14 mg, 0.027 mmol, 1.0 equiv) and CH_2Cl_2 (1.0 mL, 0.03 M). Ozone was bubbled through the solution at $-78\text{ }^\circ\text{C}$ until the solution turned a light blue. The reaction was then purged with N_2 for 15 minutes until the color dissipated. NaBH_4 (3.11 mg, 0.082 mmol, 3.0 equiv) was added and the reaction was warmed to room temperature. Once the reaction was complete the solution was diluted with CH_2Cl_2 (5 mL) and H_2O (5 mL). The layers were separated and the aqueous layer was extracted with methylene chloride (3 x 5 mL). The combined organic extracts were washed with brine (5 mL), dried with sodium sulfate, and concentrated *in vacuo*. The crude mixture was purified by flash chromatography (30% EtOAc/hexanes) to provide 4 mg (75%) of the product as a colorless oil. ^1H NMR spectral data matched those reported for the title compound **13**.^[14] SFC analysis showed a 96:4 er for the product.

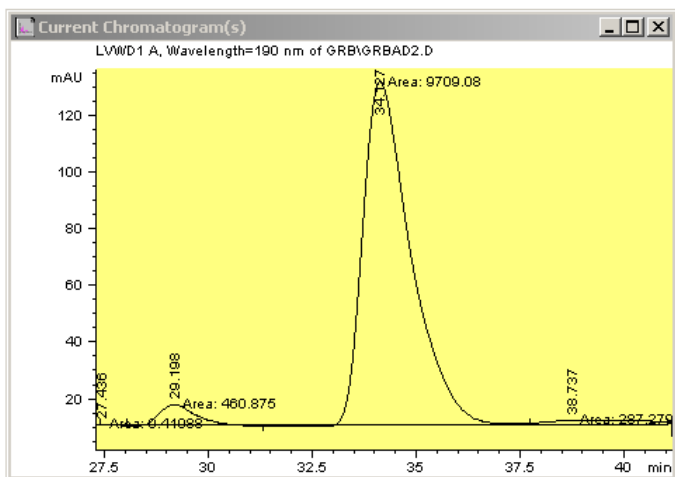
SFC Analytic Data for the (S)-4-nitro-3-phenylbutan-1-ol **13**:

CSP-SFC analysis of 4-nitro-3-phenylbutan-1-ol **13** showed that the major (S)-enantiomer was formed in a 92% enantiomeric excess. (Chiralpak AD column 5% MeOH, 1mL/min, 150 psi, 37 °C 190 nm t_r - (S)-enantiomer: 34.1 min, t_r - (R)-enantiomer: 29.2 min; CSP-SFC traces for the racemic and enantioriched products are attached (*vide infra*).

Racemic Sample:



Enantioenriched Sample:



3.7 References

- [1] Breslow, R. *Acc. Chem. Res.* **1980**, *13*, 170-177.
- [2] (a) Mitchell, H. J.; Nelson, A.; Warren, S. *J. Chem. Soc., Perkin Trans.* **1999**, *1*, 1899- 1914. (b) Mikami, K; Shimizu, M.; Zhang, H.-C.; Maryanoff, B. E. *Tetrahedron* **2001**, *57* 2917-2951.
- [3] Casiraghi, G.; Battistini, L.; Curti, C.; Rassu, G.; Zanardi, F. *Chem. Rev.* **2011**, *111*, 3076-3154.
- [4] Nicewicz, D. A.; Johnson J. S. *J. Am. Chem. Soc.* **2005**, *127*, 6170-6171.
- [5] Anand, N. K.; Carreira, E. M. *J. Am. Chem. Soc.* **2001**, *123*, 9687-9688.
- [6] Linghu, X.; Satterfield, A. D. Unpublished results.
- [7] Greszler, S. N.; Malinowski, J. T.; Johnson, J. S. *J. Am. Chem. Soc.* **2010**, *132*, 17393- 17395.
- [8] Schmitt, D. C. Unpublished results.
- [9] Shirokawa, S.-I.; Kamiyama, M.; Nakamura, T.; Okada, M.; Nakazaki, A.; Hosokawa, S.; Kobayashi, S. *J. Am. Chem. Soc.* **2004**, *126*, 13604-13605.
- [10] (a) Nakamura, T.; Shirokawa, S.-I.; Hosokawa, S.; Nakazaki, A.; Kobayashi, S. *Org. Lett.* **2006**, *8*, 677-679. (b) Shirokawa, S.-I.; Shinoyama, M.; Ooi, I.; Hosokawa, S.; Nakazaki, A.; Kobayashi, S. *Org. Lett.* **2007**, *9*, 849-852. (c) Shinoyama, M.; Shirokawa, S.-I.; Nakazaki, A.; Kobayashi, S. *Org. Lett.* **2009**, *11*, 1277-1280.
- [11] Al-Rashid, Z. F.; Johnson, W. L.; Hsung, R. P.; Wei, Y.; Yao, P.-Y.; Liu, R.; Zhao, K. *J. Org. Chem.* **2008**, *73*, 8780-8784.
- [12] Tomita, D.; Wada, R.; Kanai, M.; Shibasaki, M. *J. Am. Chem. Soc.* **2005**, *127*, 4138- 4139.
- [13] Gotoh, H.; Ishikawa, H.; Hayashi, Y. *Org. Lett.* **2007**, *9*, 5307-5309.
- [14] Palomo, C.; Landa, A.; Mielgo, A.; Oiarbide, M.; Puente, A.; Vera, S. *Angew. Chem. Int. Ed.* **2007**, *46*, 8431-8435.
- [15] (a) Lecea, B.; Arrieta, A.; Morao, I.; Cossío, F. P. *Chem. Eur. J.* **1997**, *3*, 20-28. (b) Hara, K.; Tosaki, S.-Y.; Gnanadesikan, V.; Morimoto, H.; Harada, S.; Sugita, M.; Yamagiwa, N.; Matsunaga, S.; Shibasaki, M. *Tetrahedron* **2009**, *65*, 5030-5036. (c) Ito, H.; Ito, T. *Chem. Lett.* **1985**, 1251. (d) Diel, B. N.; Hope,

- H. *Inorg. Chem.* **1986**, 25, 4448. (e) Kovacs, T.; Speier, G.; Reglier, M.; Giorgi, M.; Vertes, A.; Vanko, G. *Chem Commun.* **2000**, 469. (f) Simonsen, O. *Acta Crystallogr., Sect B: Struct. Crystallogr. Cryst. Chem.* **1973**, 29, 2600.
- [16] (a) McNutly, J.; Mo, R. *Chem. Commun.* **1998**, 933-934. (b) Robertson, J.; Hall, M. J.; Green, S. P. *Org. Biomol. Chem.* **2003**, 1, 3635-3638. (c) Bildi, L. E.; Assaf, Z.; Bres, F. C., Veschambre, H., Thery, V.; Bolte, J.; Lemaire, M. *ChemCatChem* **2009**, 1, 463-471. (d) Xiao, H.; Chai, Z.; Zheng, C.-W.; Yang, Y.-Q.; Liu, W.; Zhang, J.-K.; Zhao, G. *Angew. Chem. Int. Ed.* **2010**, 49, 4467-4470.
- [17] Boiron, A.; Zillig, P.; Faber, D.; Geise, B. *J. Org. Chem.* **1998**, 63, 5877-5882.
- [18] Kogan, T. P.; Gaeta, F. C. A. *Synthesis* **1988**, 706-707.